

# LARGE-SCALE STRUCTURE BEYOND THE POWER SPECTRUM

Marcel Schmittfull

Berkeley Center for Cosmological Physics (BCCP)

arxiv:1411.6595 (PRD 91, 043530)

arxiv:1508.06972

In collaboration with

Tobias Baldauf, Uros Seljak

Yu Feng, Florian Beutler, Blake Sherwin, Man Yat Chu

Berkeley BCCP Seminar, Sep 8 2015

# OVERVIEW

- Introduction
- Part I: Simple bispectrum estimators
- Part II: Eulerian reconstructions and N-point statistics

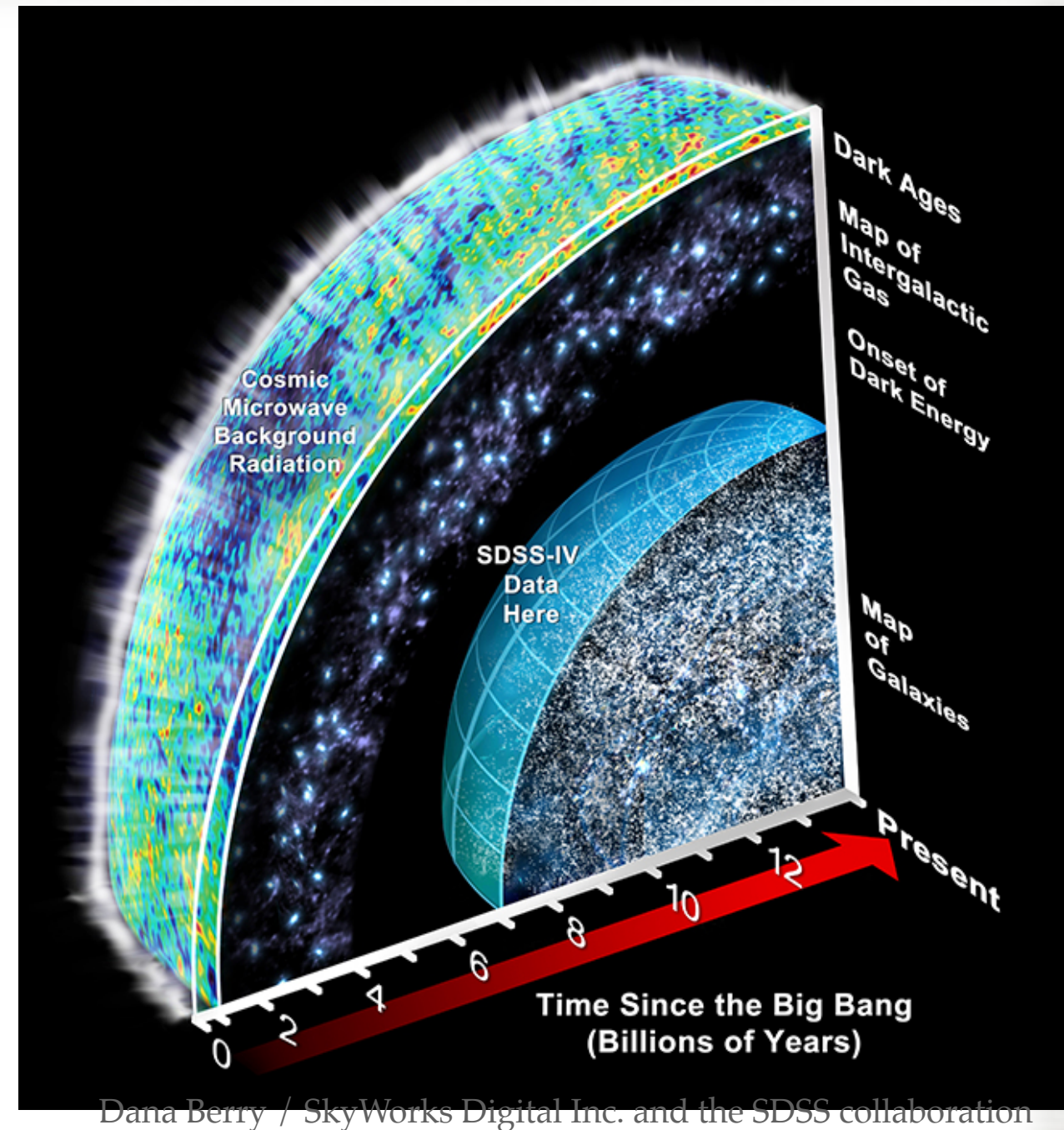


# INTRODUCTION



# MAIN COSMOLOGICAL PROBES

- ▶ Young universe (*380,000 yrs after big bang*)
  - ◆ [Gravity waves]
  - ◆ Cosmic Microwave Background (CMB)
- ▶ 'Recent' universe (*billions yrs after big bang*)
  - ◆ Large-scale structure (LSS)
    - ◆ 21cm,  $\text{Ly}\alpha$ , CMB lensing, **galaxy clustering**, weak lensing
  - ◆ Supernovae
- ▶ All observations can be described with LCDM cosmological model  
(start with inflation, then expand with CDM and cosmological constant dark energy)

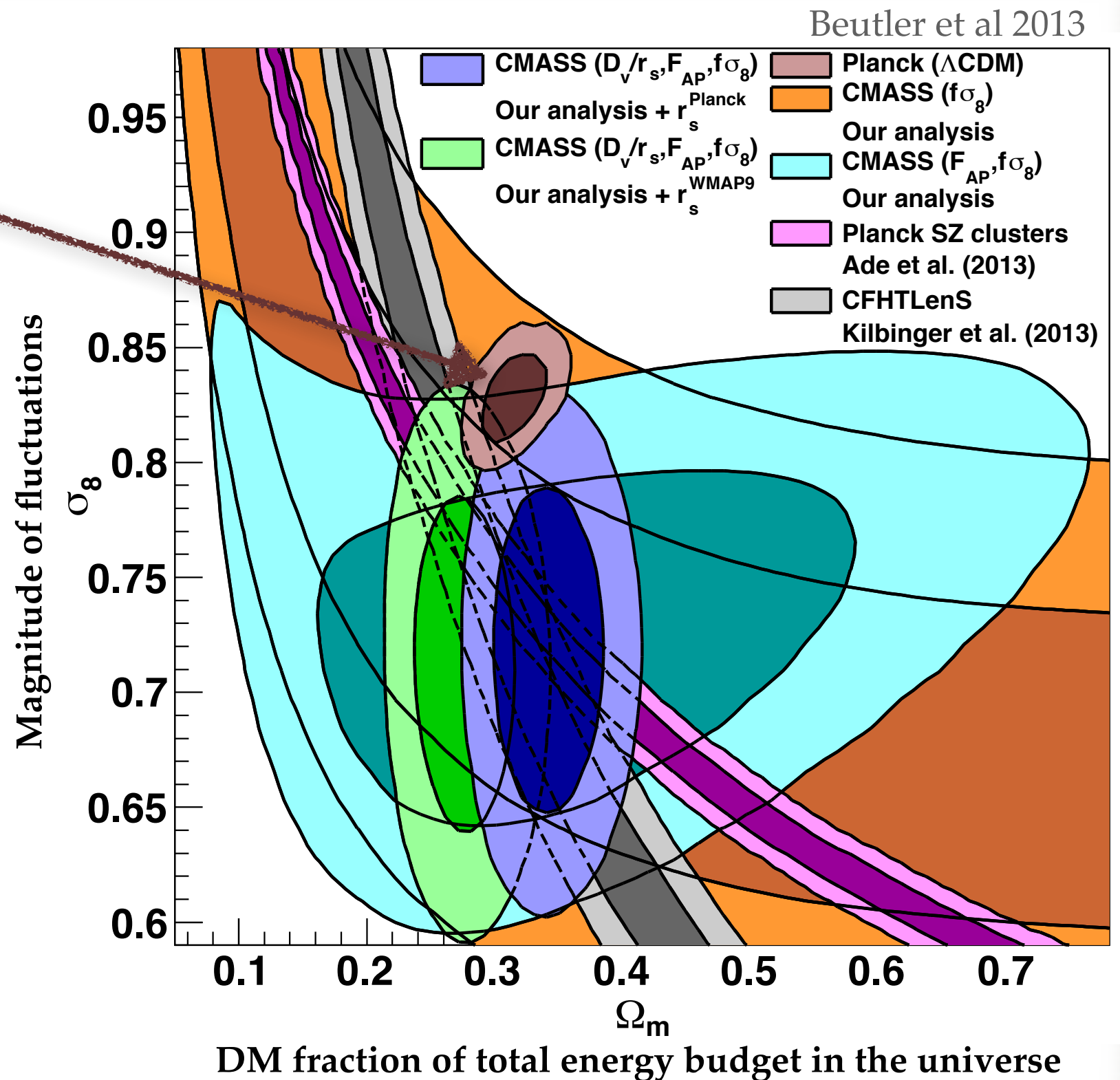




# MAIN COSMOLOGICAL PROBES

► Constraints on 6-parameter  
LCDM model:

- ◆ CMB is most powerful



# MAIN COSMOLOGICAL PROBES

► Constraints on 6-parameter  
LCDM model:

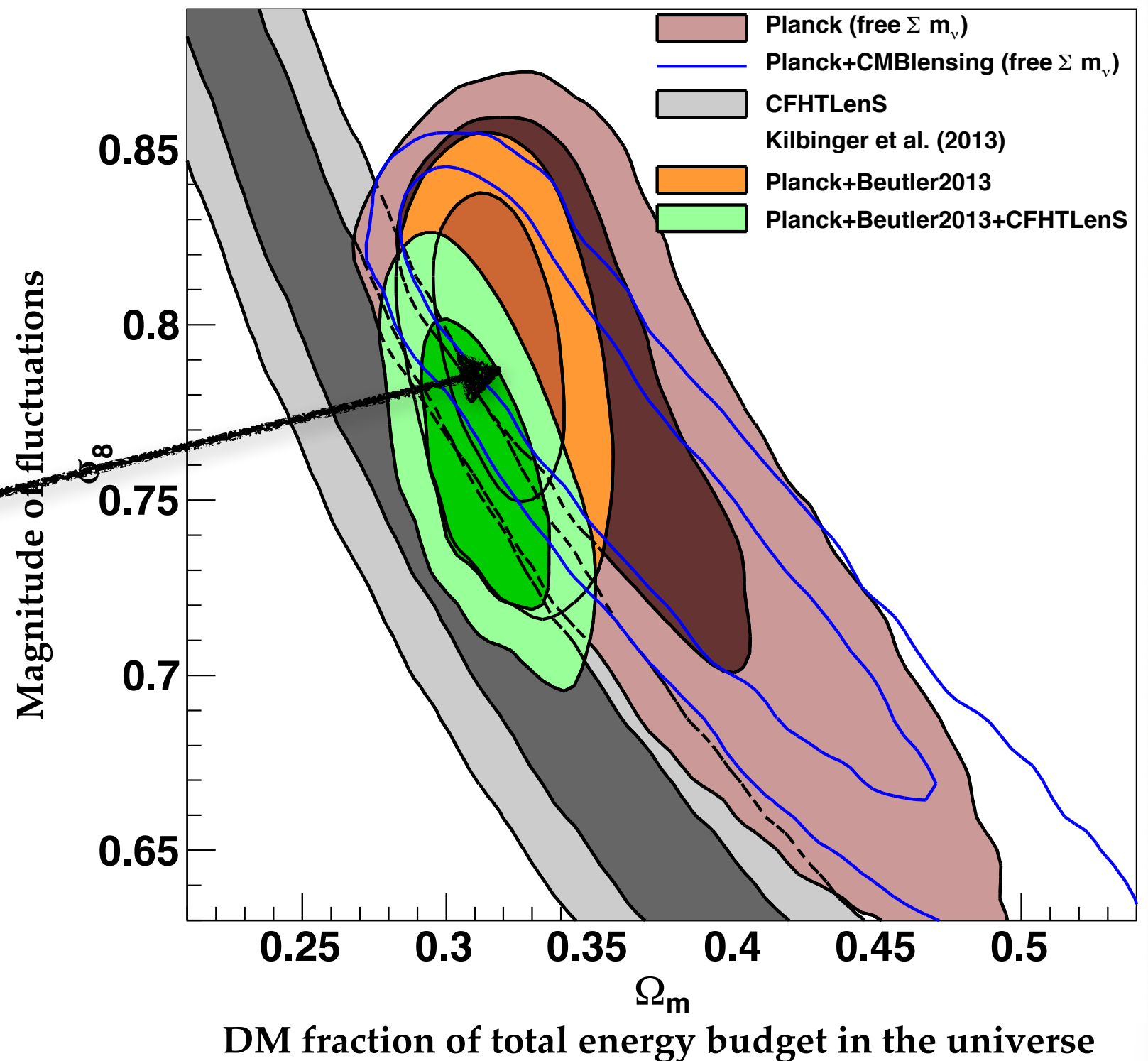
- ◆ CMB is most powerful

► Free neutrino mass  $\Sigma m_\nu$

- ◆ Constraints degrade  
because  $\Sigma m_\nu$  and  $\sigma_8$   
degenerate in CMB

- ◆ LSS helps

Beutler et al 2013





# MAIN COSMOLOGICAL PROBES

Beutler et al 2013

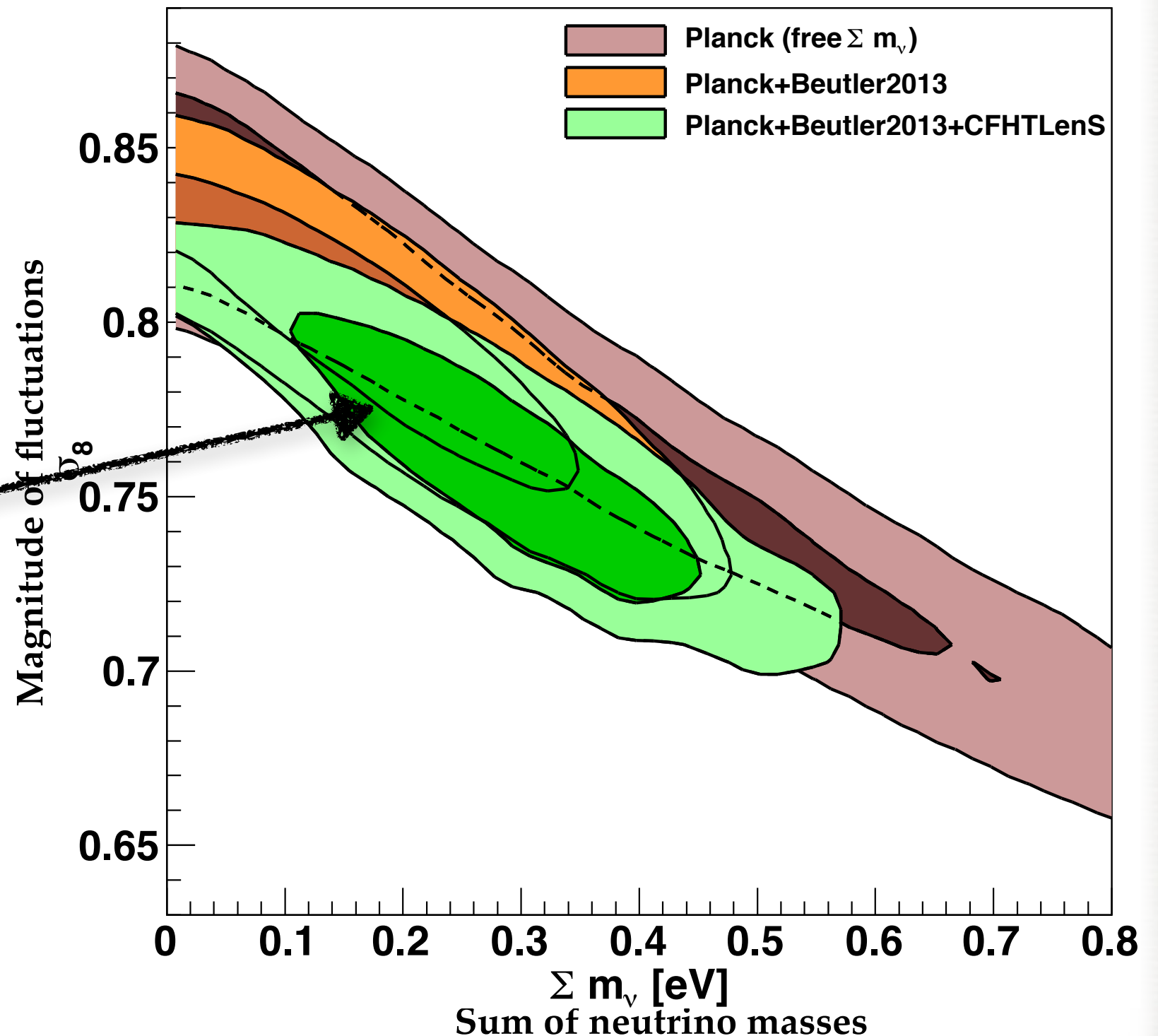
## ► Constraints on 6-parameter

$\Lambda$ CDM model:

- ◆ CMB is most powerful

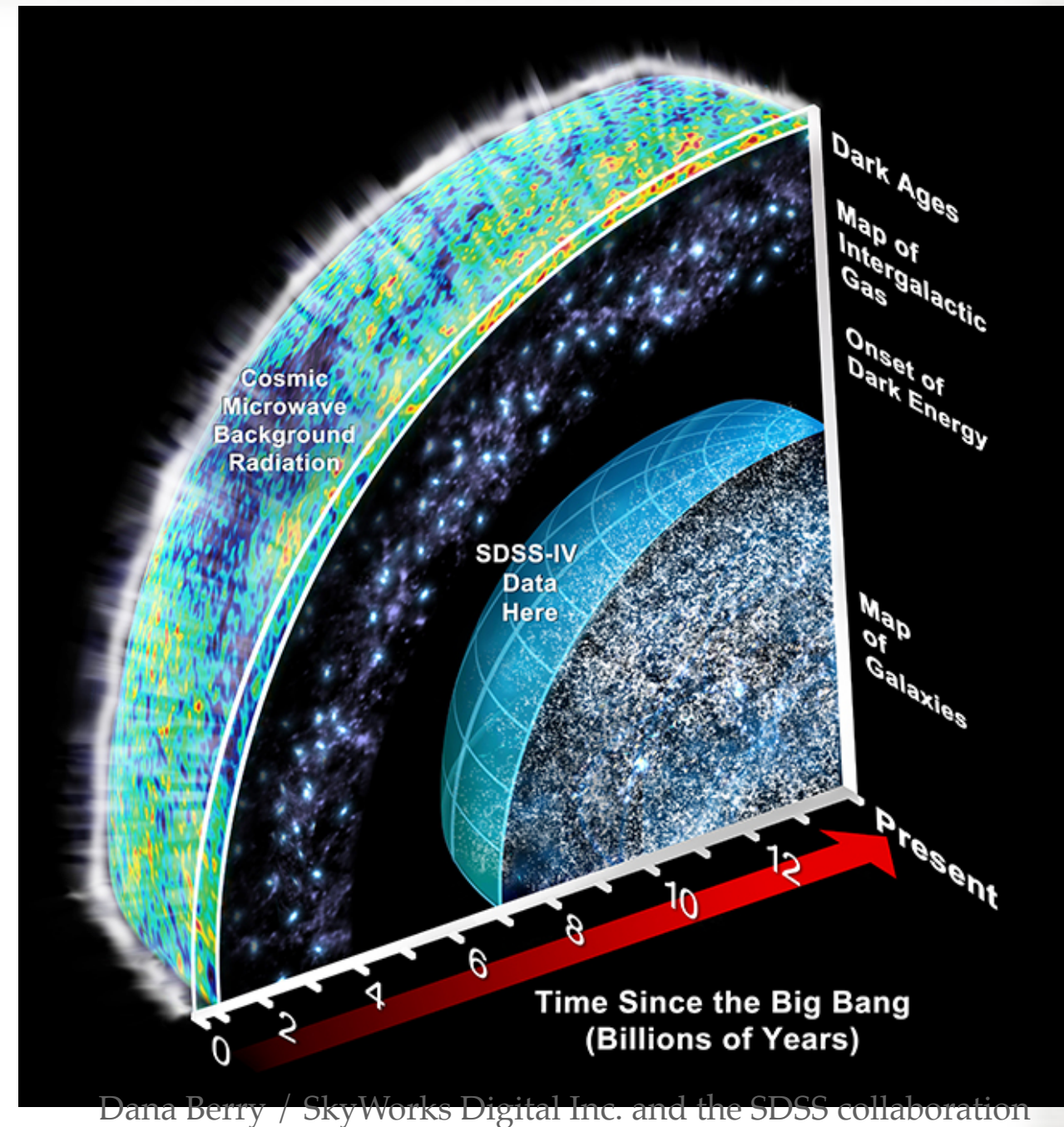
## ► Free neutrino mass $\Sigma m_\nu$

- ◆ Constraints degrade because  $\Sigma m_\nu$  and  $\sigma_8$  degenerate in CMB
- ◆ LSS helps



# MAIN COSMOLOGICAL PROBES

- ▶ Constraints on 6-parameter  $\Lambda$ CDM model:
  - ◆ CMB is most powerful
- ▶ Free neutrino mass  $\Sigma m_\nu$ 
  - ◆ Constraints degrade because  $\Sigma m_\nu$  and  $\sigma_8$  degenerate in CMB
  - ◆ LSS helpful
- ▶ Other model extensions (curvature, time-varying dark energy, mod. grav. etc)
  - ◆ LSS crucial
- ▶ Generally, should not just compare constraining power: LSS checks cosmological model as a whole (low  $z$  vs high  $z$  from CMB)



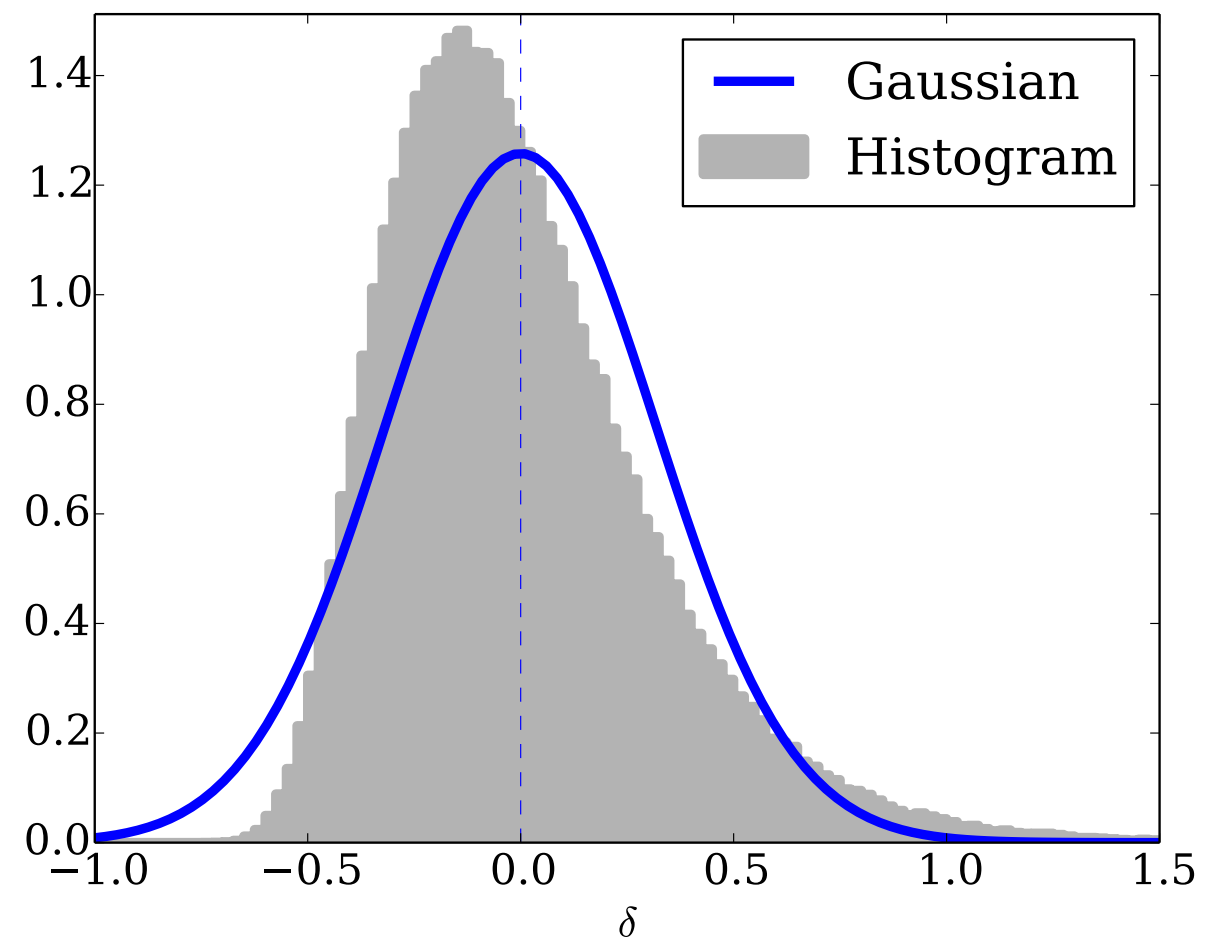
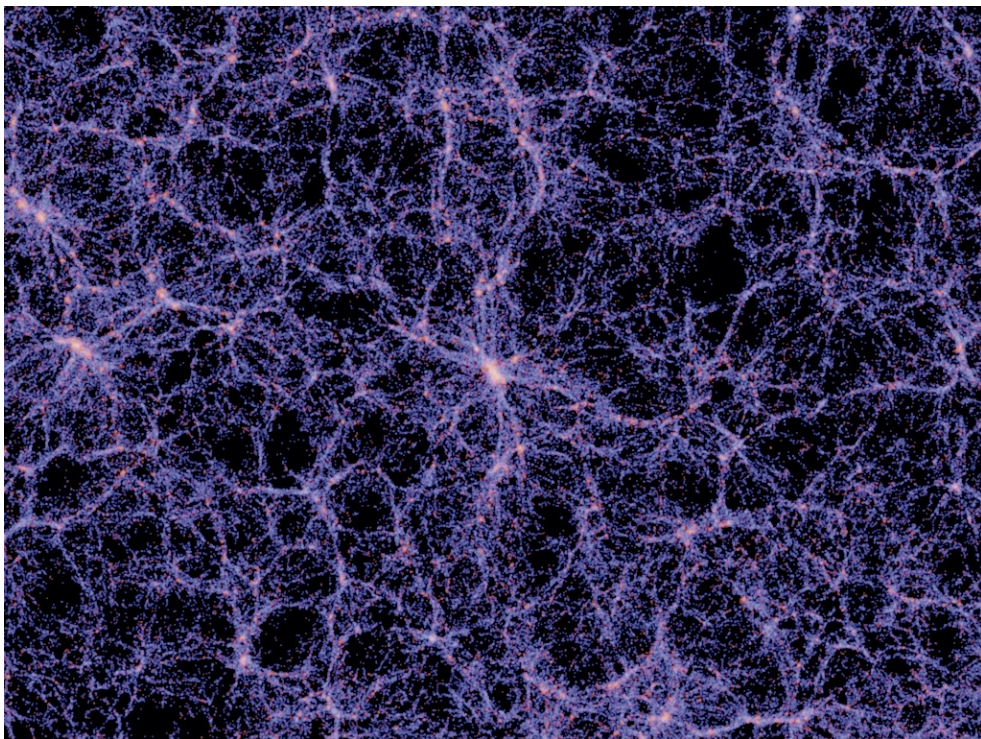


# STATISTICAL PROPERTIES OF LSS



# DARK MATTER DENSITY

- Equations of motion for **DM** are **non-linear**, containing products of Gaussian first-order perturbations (e.g. continuity equation  $\partial_\eta \delta + \nabla[(1 + \delta)\mathbf{v}] = 0$ )
  - DM density is not Gaussian (even in absence of primordial non-Gaussianity):





# NON-GAUSSIANITY FROM GRAVITY

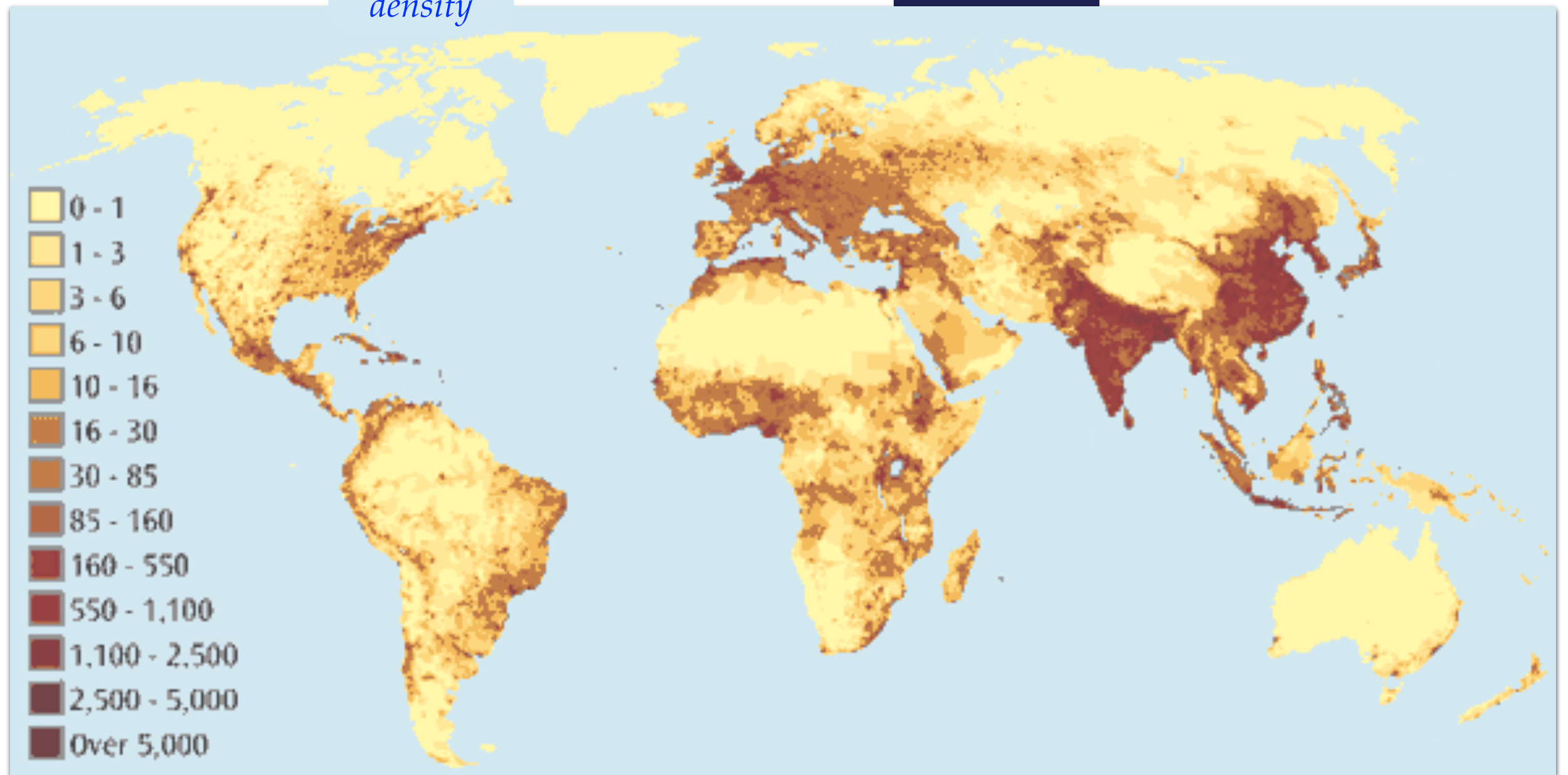
► Another complication:

- Distribution of **dark matter** is different from that of **galaxies**      ⇒ “Galaxy bias”

# NON-GAUSSIANITY FROM GRAVITY

## ► Another complication:

- Distribution of *human population density* is different from that of *galaxies* *night* → “Galaxy bias”

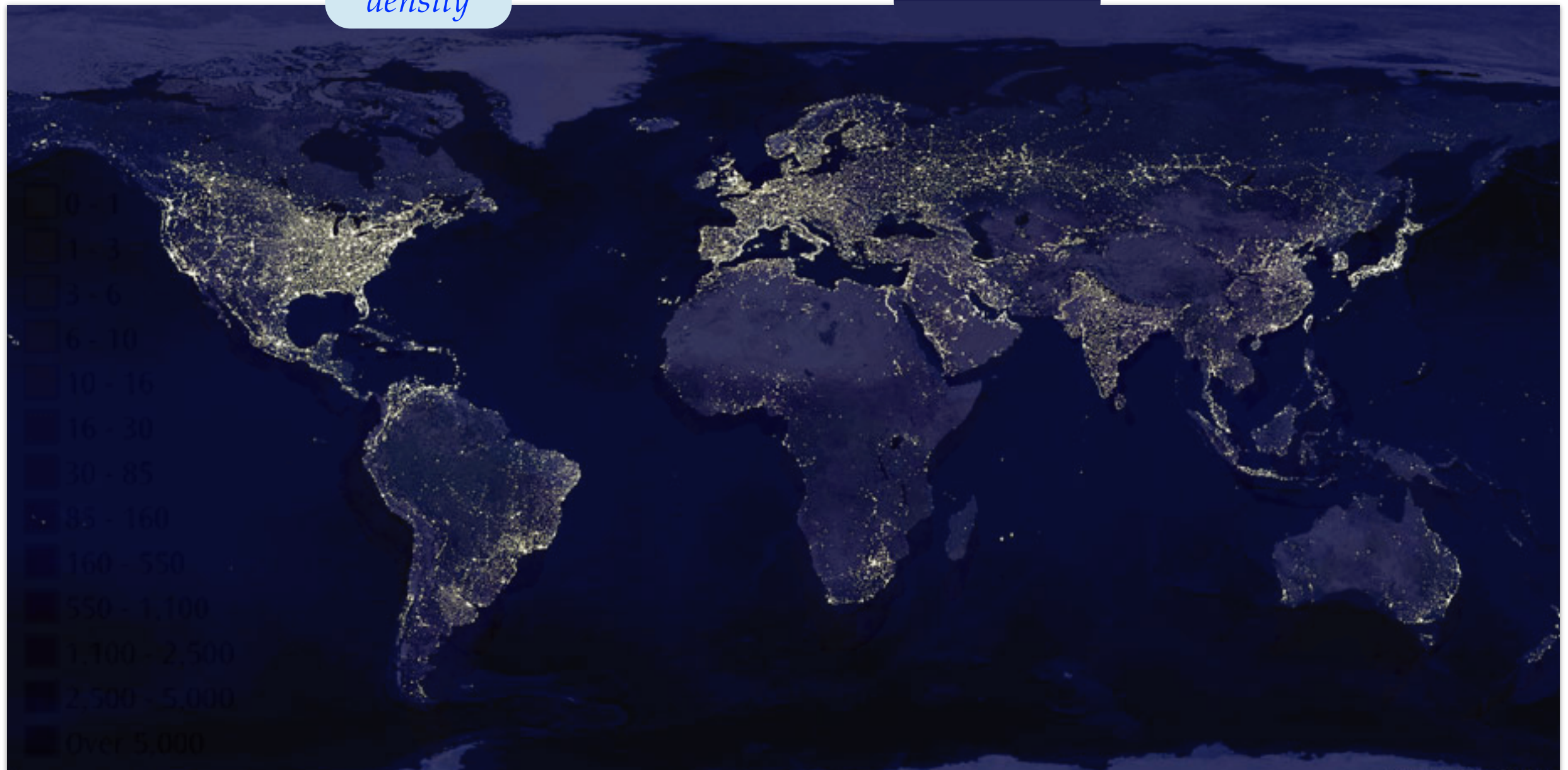




# NON-GAUSSIANITY FROM GRAVITY

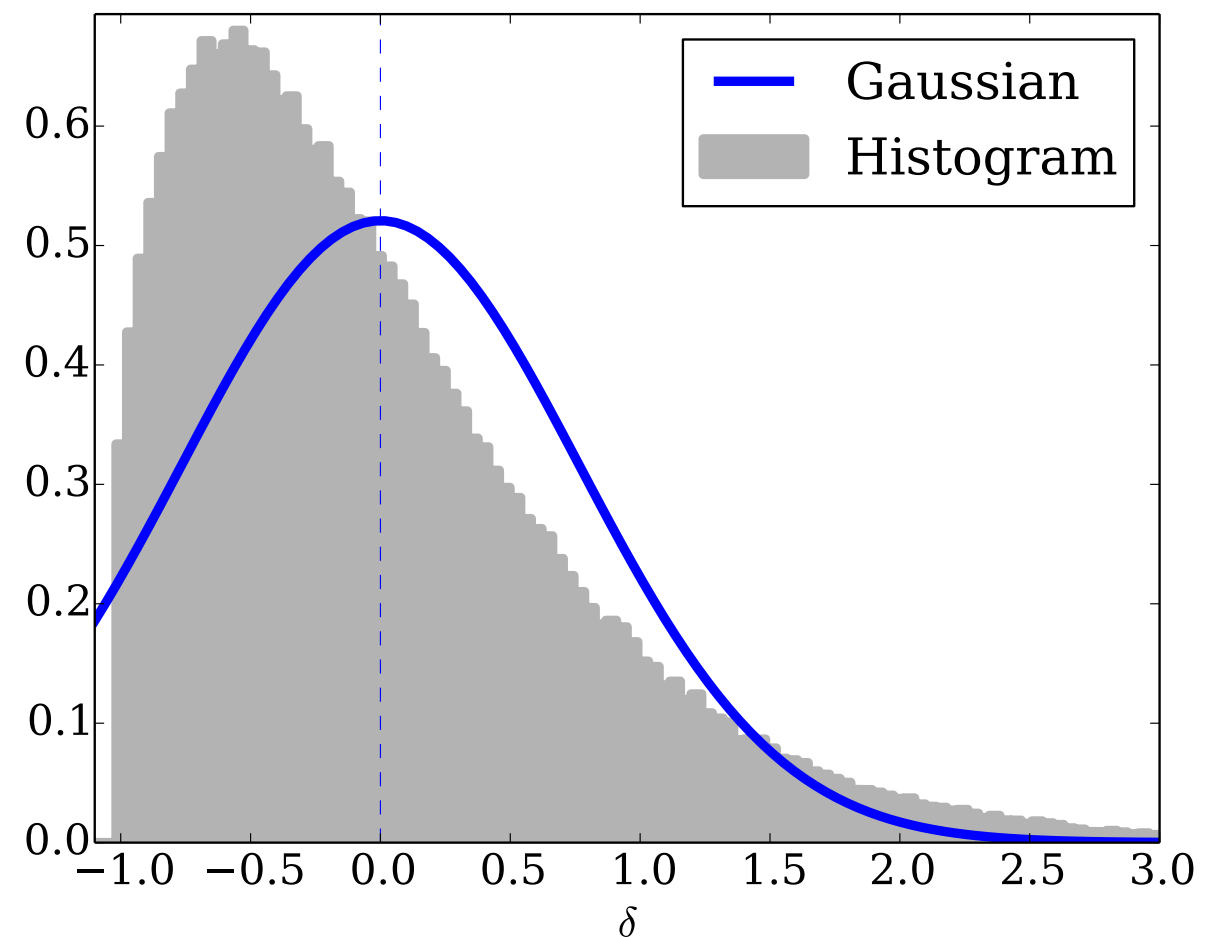
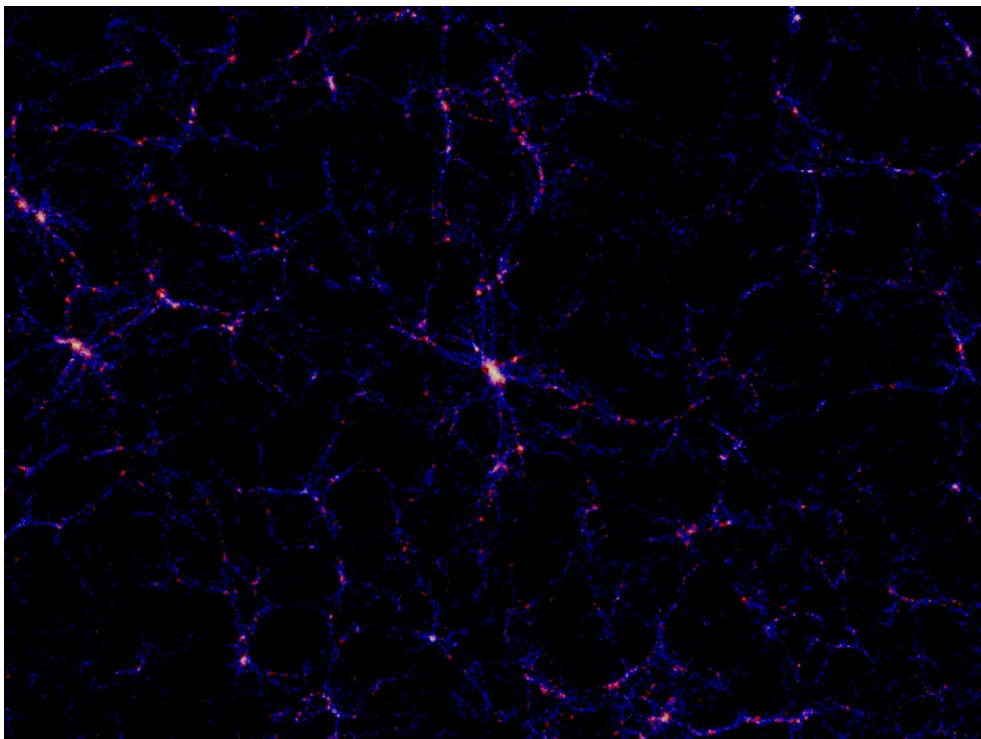
## ► Another complication:

- Distribution of *human population density* is different from that of *galaxies* night night ⇒ “Galaxy bias”



# GALAXY DENSITY

- Galaxies are biased tracer of DM
- Bias relation has additional non-linearities  $\delta_g(\mathbf{x}) \sim b_1 \delta_m(\mathbf{x}) + b_2 \delta_m^2(\mathbf{x}) + b_{s^2} s_m^2(\mathbf{x})$ 
  - pdf of galaxy density is even more non-Gaussian than that for DM:





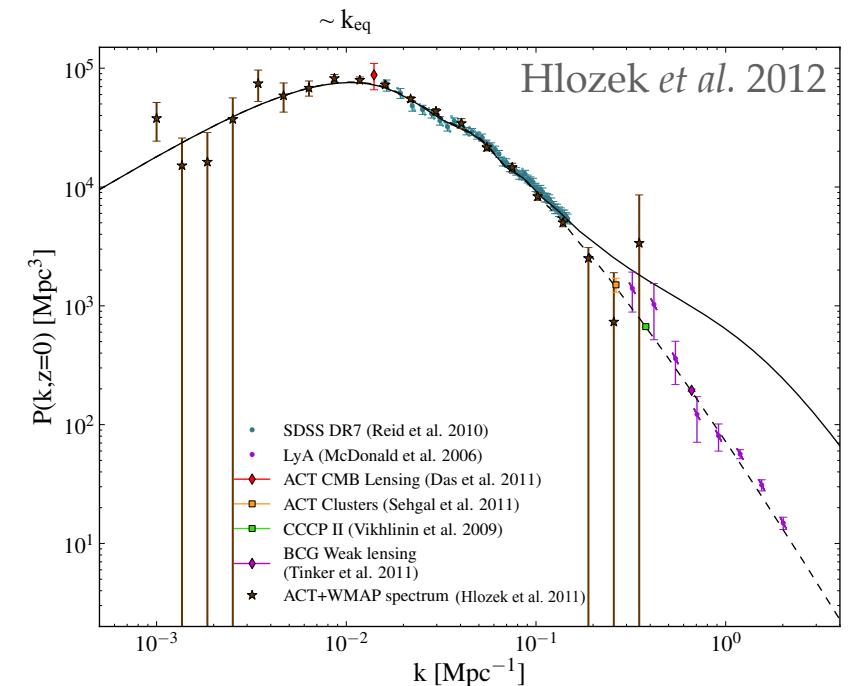
# QUANTIFYING THE PDF

# POWER AND BISPECTRUM

- Gaussian field is completely specified by its **power spectrum**  $P_\delta$

(2-point correlation function in Fourier space)

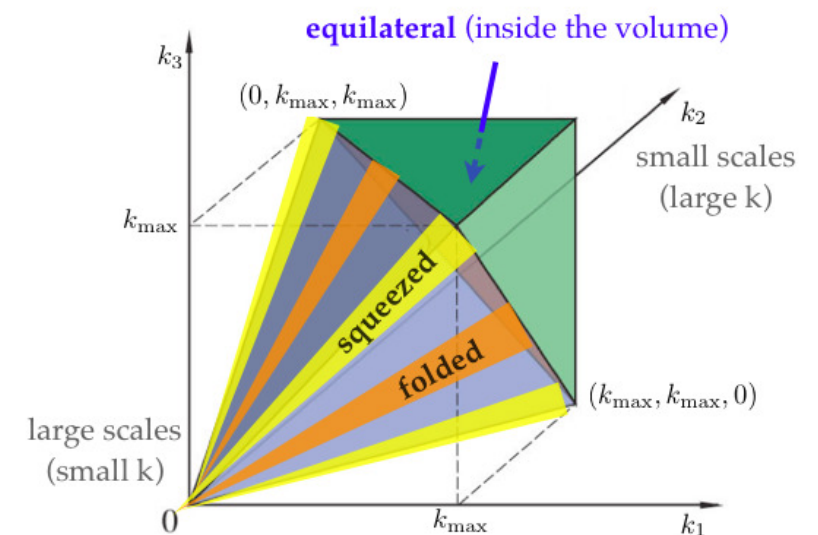
$$\langle \delta(\mathbf{k}_1) \delta(\mathbf{k}_2) \rangle = (2\pi)^3 \delta_D(\mathbf{k}_1 + \mathbf{k}_2) P_\delta(k_1)$$



- Primary diagnostic for **non-Gaussianity** is the **bispectrum**  $B_\delta$

(3-point correlation function in Fourier space: given 2 over-densities, specifies probability of having a third overdensity)

$$\begin{aligned} \langle \delta(\mathbf{k}_1) \delta(\mathbf{k}_2) \delta(\mathbf{k}_3) \rangle \\ = (2\pi)^3 \delta_D(\mathbf{k}_1 + \mathbf{k}_2 + \mathbf{k}_3) B_\delta(k_1, k_2, k_3) \end{aligned}$$



*bispectrum drawn on space of triangle configurations*



# MOTIVATION FOR MEASURING BISPECTRUM

► *Late universe*: Break parameter degeneracies, e.g. between  $b_1$  and  $\sigma_8$ :

- Power spectrum:  $P_{hh} \propto b_1^2 \sigma_8^2$
- Bispectrum:  $B_{hhh} \propto \sim b_1^3 \sigma_8^4 + \sim b_1^2 b_2 \sigma_8^4 + \dots$
- Lots of upcoming LSS experiments that could benefit, e.g. eBOSS, DESI, EUCLID, WFIRST, LSST, ...

Fry 1994  
Verde *et al.* 1997-2002  
Scoccimarro *et al.* 1998  
Sefusatti *et al.* 2006  
Gil-Marín *et al.* 2014

► *Early universe*: Constrain primordial non-Gaussianity

- CMB close to cosmic variance limit, so need LSS
- $f_{NL}^{loc}$ : Bispectrum complementary to  $P(k)$  and less affected by low- $k$  systematics
- $f_{NL}^{eq}$ : No signal in  $P(k) \rightarrow$  need bispectrum
- e.g. SPHEREX (proposed satellite)

Doré *et al.* 2014

# MOTIVATION FOR MEASURING BISPECTRUM

► *Late universe*: Break parameter degeneracies, e.g. between  $b_1$  and  $\sigma_8$ :

- Power spectrum:  $P_{hh} \propto b_1^2 \sigma_8^2$
- Bispectrum:  $B_{hhh} \propto \sim b_1^3 \sigma_8^4 + \sim b_1^2 b_2 \sigma_8^4 + \dots$
- Lots of upcoming LSS experiments that could benefit, e.g. eBOSS, DESI, EUCLID, WFIRST, LSST, ...

Fry 1994  
Verde *et al.* 1997-2002  
Scoccimarro *et al.* 1998  
Sefusatti *et al.* 2006  
Gil-Marín *et al.* 2014

► *Early universe*: Constrain primordial non-Gaussianity

- CMB close to cosmic variance limit, so need LSS
- $f_{NL}^{loc}$ : Bispectrum complementary to  $P(k)$  and less affected by low- $k$  systematics
- $f_{NL}^{eq}$ : No signal in  $P(k) \rightarrow$  need bispectrum
- e.g. SPHEREX (proposed satellite)

Doré *et al.* 2014

But: Beyond 2-point plagued by **increased complexity** of analysis  
(covariances, window function, fiber collisions, computational cost  $\sim N^6$ ;  
non-linear DM, bias, redshift-space distortions, galaxy-halo connection, ...)



# SIMPLE BISPECTRUM ESTIMATORS

# THEORY DM BISPECTRUM

## ► Non-linear DM density (2<sup>nd</sup> order SPT)

$\delta_m$ : *nonlinear* DM density

$\delta_0$ : linear DM density

$\Psi_0$ : linear displacement  $\equiv -\frac{i\mathbf{k}}{k^2}\delta_0(\mathbf{k})$

$s_0$ : linear tidal tensor

$$\delta_m(\mathbf{x}) = \underbrace{\delta_0(\mathbf{x})}_{\text{linear}} + \underbrace{\frac{17}{21}\delta_0^2(\mathbf{x})}_{\text{nonlinear growth}} + \underbrace{\Psi_0(\mathbf{x}) \cdot \nabla \delta_0(\mathbf{x})}_{\text{shift}} + \underbrace{\frac{4}{21}s_0^2(\mathbf{x})}_{\text{tidal}}$$

$$\Rightarrow \langle \delta_m(\mathbf{k}_1)\delta_m(\mathbf{k}_2)\delta_m(\mathbf{k}_3) \rangle \sim 2P_{\text{mm}}^{\text{lin}}(k_1)P_{\text{mm}}^{\text{lin}}(k_2)F_2(\mathbf{k}_1, \mathbf{k}_2) + 2 \text{ perms in } k_1, k_2, k_3$$

where

$$F_2(\mathbf{k}_1, \mathbf{k}_2) = \underbrace{\frac{17}{21}}_{\text{nonlinear growth}} + \underbrace{\frac{1}{2} \left( \frac{k_1}{k_2} + \frac{k_2}{k_1} \right) \hat{\mathbf{k}}_1 \cdot \hat{\mathbf{k}}_2}_{\text{shift}} + \underbrace{\frac{4}{21} \frac{3}{2} \left( (\hat{\mathbf{k}}_1 \cdot \hat{\mathbf{k}}_2)^2 - \frac{1}{3} \right)}_{\text{tidal}}$$



# THEORY HALO BISPECTRUM

## ► Non-linear halo bias

$\delta_m$ : *nonlinear* DM density

$\delta_h$ : halo density

$s_m$ : DM tidal tensor

$$\delta_h(\mathbf{x}) = b_1 \delta_m(\mathbf{x}) + b_2 [\delta_m^2(\mathbf{x}) - \langle \delta_m^2(\mathbf{x}) \rangle] + \frac{2}{3} b_{s^2} [s_m^2(\mathbf{x}) - \langle s_m^2(\mathbf{x}) \rangle]$$

$$\Rightarrow \langle \delta_h(\mathbf{k}_1) \delta_h(\mathbf{k}_2) \delta_h(\mathbf{k}_3) \rangle \\ \sim 2P_{\text{mm}}^{\text{lin}}(k_1) P_{\text{mm}}^{\text{lin}}(k_2) \left[ b_1^3 F_2(\mathbf{k}_1, \mathbf{k}_2) + b_1^2 b_2 + \frac{2}{3} b_1^2 b_{s^2} P_2(\hat{\mathbf{k}}_1 \cdot \hat{\mathbf{k}}_2) \right] + 2 \text{ perms}$$

# THEORY HALO BISPECTRUM

## ► Non-linear halo bias

$\delta_m$ : nonlinear DM density

$\delta_h$ : halo density

$s_m$ : DM tidal tensor

$$\delta_h(\mathbf{x}) = b_1 \delta_m(\mathbf{x}) + b_2 [\delta_m^2(\mathbf{x}) - \langle \delta_m^2(\mathbf{x}) \rangle] + \frac{2}{3} b_{s^2} [s_m^2(\mathbf{x}) - \langle s_m^2(\mathbf{x}) \rangle]$$

$$\Rightarrow \langle \delta_h(\mathbf{k}_1) \delta_h(\mathbf{k}_2) \delta_h(\mathbf{k}_3) \rangle \\ \sim 2P_{\text{mm}}^{\text{lin}}(k_1) P_{\text{mm}}^{\text{lin}}(k_2) \left[ b_1^3 F_2(\mathbf{k}_1, \mathbf{k}_2) + b_1^2 b_2 + \frac{2}{3} b_1^2 b_{s^2} P_2(\hat{\mathbf{k}}_1 \cdot \hat{\mathbf{k}}_2) \right] + 2 \text{ perms}$$

## ► Decompose in Legendre polys $P_l$ with $l = 0, 1, 2$

$$B_{\text{hhh}}^{(l=0)} = \left( \frac{34}{21} b_1^3 + 2b_1^2 b_2 \right) P_{\text{mm}}^{\text{lin}}(k_1) P_{\text{mm}}^{\text{lin}}(k_2) + 2 \text{ perms},$$

$$B_{\text{hhh}}^{(l=1)} = b_1^3 \left( \frac{k_1}{k_2} + \frac{k_2}{k_1} \right) P_{\text{mm}}^{\text{lin}}(k_1) P_{\text{mm}}^{\text{lin}}(k_2) P_1(\hat{\mathbf{k}}_1 \cdot \hat{\mathbf{k}}_2) + 2 \text{ perms},$$

$$B_{\text{hhh}}^{(l=2)} = \left( \frac{8}{21} b_1^3 + \frac{4}{3} b_1^2 b_{s^2} \right) P_{\text{mm}}^{\text{lin}}(k_1) P_{\text{mm}}^{\text{lin}}(k_2) P_2(\hat{\mathbf{k}}_1 \cdot \hat{\mathbf{k}}_2) + 2 \text{ perms}.$$



# BISPECTRUM ESTIMATION

- **Goal:** Given **DM/halo density**  $\delta$ , estimate *coefficients* of all bispectrum contributions  
 ⇒ these depend on bias and cosmological parameters that we aim to extract

- **Method:** Maximum likelihood estimators for the coefficient of contribution  $B^{\text{contri}}$

$$\hat{\text{coeff}}(B^{\text{contri}}|\delta) \propto \int_{\mathbf{k}, \mathbf{q}} \underbrace{B^{\text{contri}}(\mathbf{q}, \mathbf{k} - \mathbf{q}, -\mathbf{k})}_{\text{theory template}} \underbrace{\frac{\delta(\mathbf{q})\delta(\mathbf{k} - \mathbf{q})\delta(-\mathbf{k})}{P_\delta(q)P_\delta(|\mathbf{k} - \mathbf{q}|)P_\delta(k)}}_{\text{inv. - variance weighted data}}$$

- **Example:**  $B^{\text{contri}} = P(k_1)P(k_2)$

MS, Baldauf, Seljak, [1411.6595](#)

$$\Rightarrow \hat{\text{coeff}} \propto \int dk \frac{k^2}{P(k)} \hat{P}_{\delta^2, \delta}(k)$$

relies on separability of LSS bispectrum

$$\begin{aligned} \hat{P}_{\delta^2, \delta}(k) &\sim \sum_{\mathbf{k}, |\mathbf{k}|=k} [\delta^2](\mathbf{k})\delta(-\mathbf{k}) \\ &= \langle \delta^2 | \delta \rangle = \text{cross-spectrum of } \delta^2(\mathbf{x}) \text{ and } \delta \end{aligned}$$

# GET ALL BISPECTRUM CONTRIS FROM 3 CROSS-SPECTRA

MS, Baldauf, Seljak, [1411.6595](#)

**$l=0$   
growth**

$$\hat{P}_{\delta^2, \delta}(k) \sim \sum_{\mathbf{k}, |\mathbf{k}|=k} \overset{\text{squared density}}{[\delta^2](\mathbf{k})} \times \overset{\text{density}}{\delta(-\mathbf{k})}$$

- nonlinear DM growth  $\delta^2$
- quadratic bias  $b_2$

**$l=1$   
shift**

$$\hat{P}_{-\Psi^i \partial_i \delta, \delta}(k) \sim \sum_{\mathbf{k}, |\mathbf{k}|=k} \overset{\text{displacement dot density gradient}}{[-\Psi^i \partial_i \delta](\mathbf{k})} \times \overset{\text{density}}{\delta(-\mathbf{k})}$$

- nonlinear DM shift  
 $\Psi(\mathbf{x}) \cdot \nabla \delta(\mathbf{x})$

$$\Psi^i(\mathbf{k}) \equiv -\frac{ik^i}{k^2} \delta(\mathbf{k})$$

**$l=2$   
tidal**

$$\hat{P}_{s^2, \delta}(k) \sim \sum_{\mathbf{k}, |\mathbf{k}|=k} \overset{\text{tidal tensor}}{[s^2](\mathbf{k})} \times \overset{\text{density}}{\delta(-\mathbf{k})}$$

- nonlinear DM tidal term
- tidal tensor bias  $b_{s^2}$

$$s^2(\mathbf{x}) \equiv \frac{3}{2} s_{ij}(\mathbf{x}) s_{ij}(\mathbf{x})$$

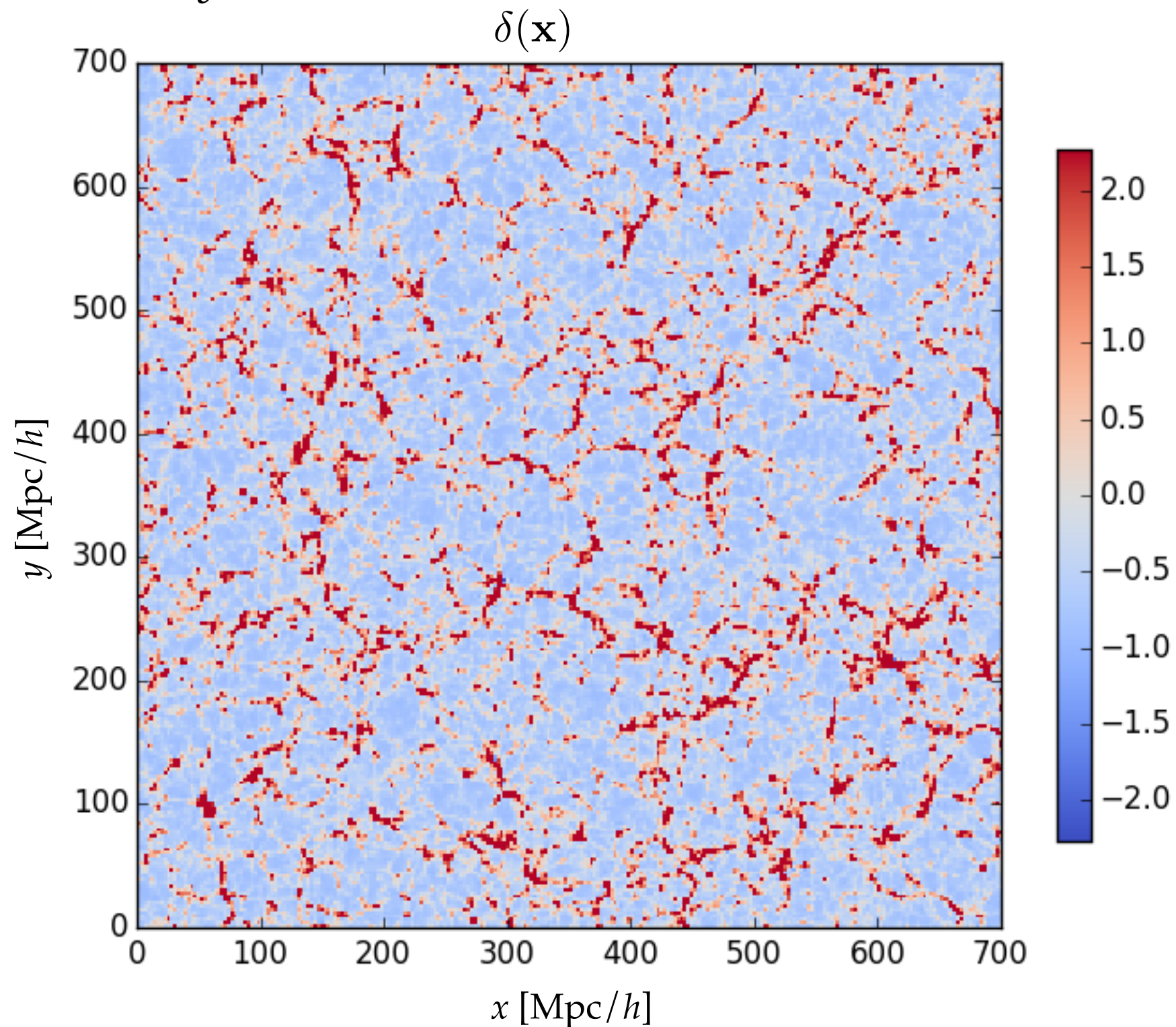
$$s_{ij}(\mathbf{k}) = \left( \frac{k_i k_j}{k^2} - \frac{1}{3} \delta_{ij}^{(K)} \right) \delta(\mathbf{k})$$



# IN PICTURES

MS, Baldauf, Seljak, [1411.6595](#)

## ► 1. Start with density

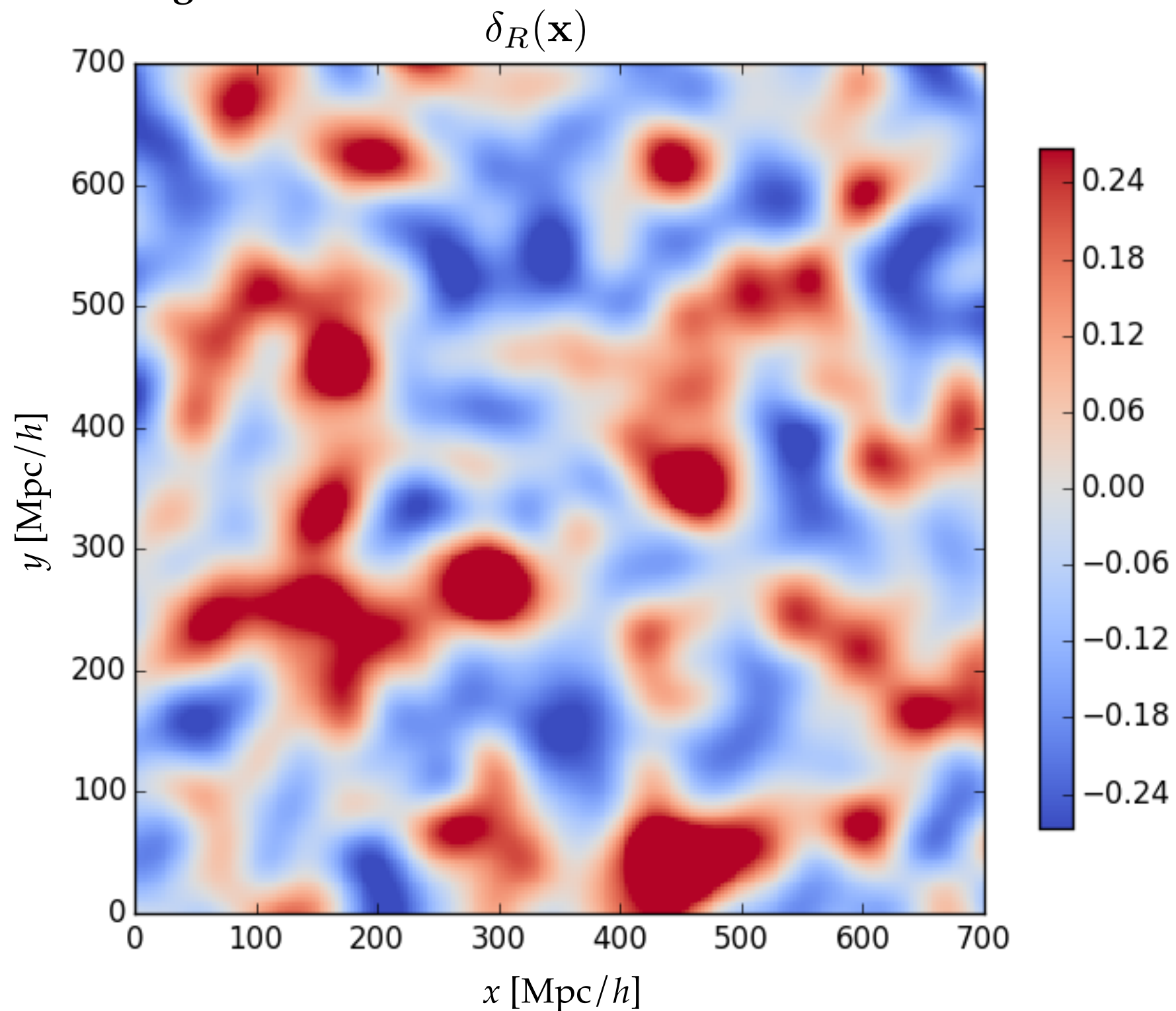


# IN PICTURES

MS, Baldauf, Seljak, [1411.6595](#)

## ► 2. Apply smoothing

(here Gaussian with  $R=20 \text{ Mpc}/h$ )

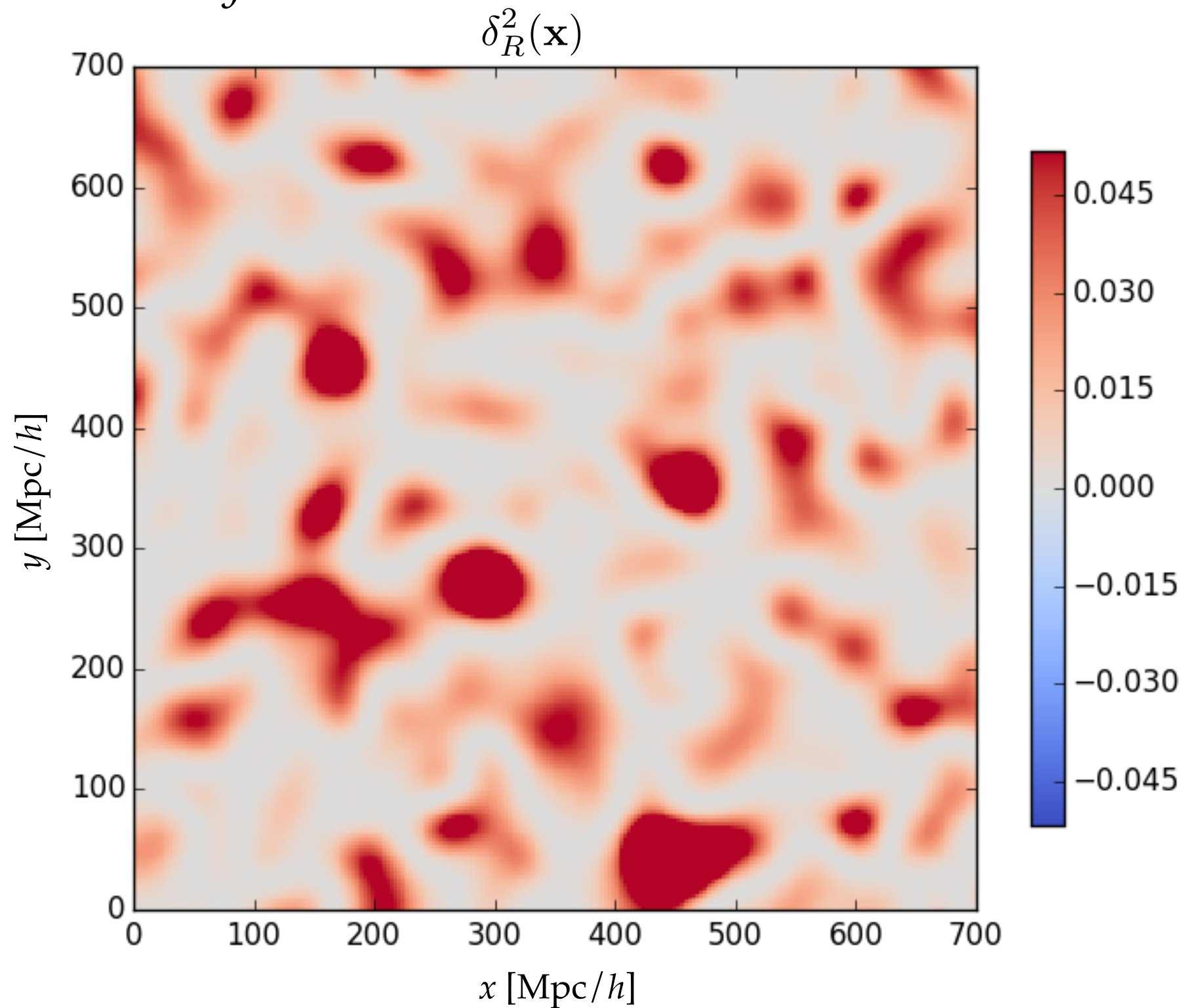




# IN PICTURES

MS, Baldauf, Seljak, [1411.6595](#)

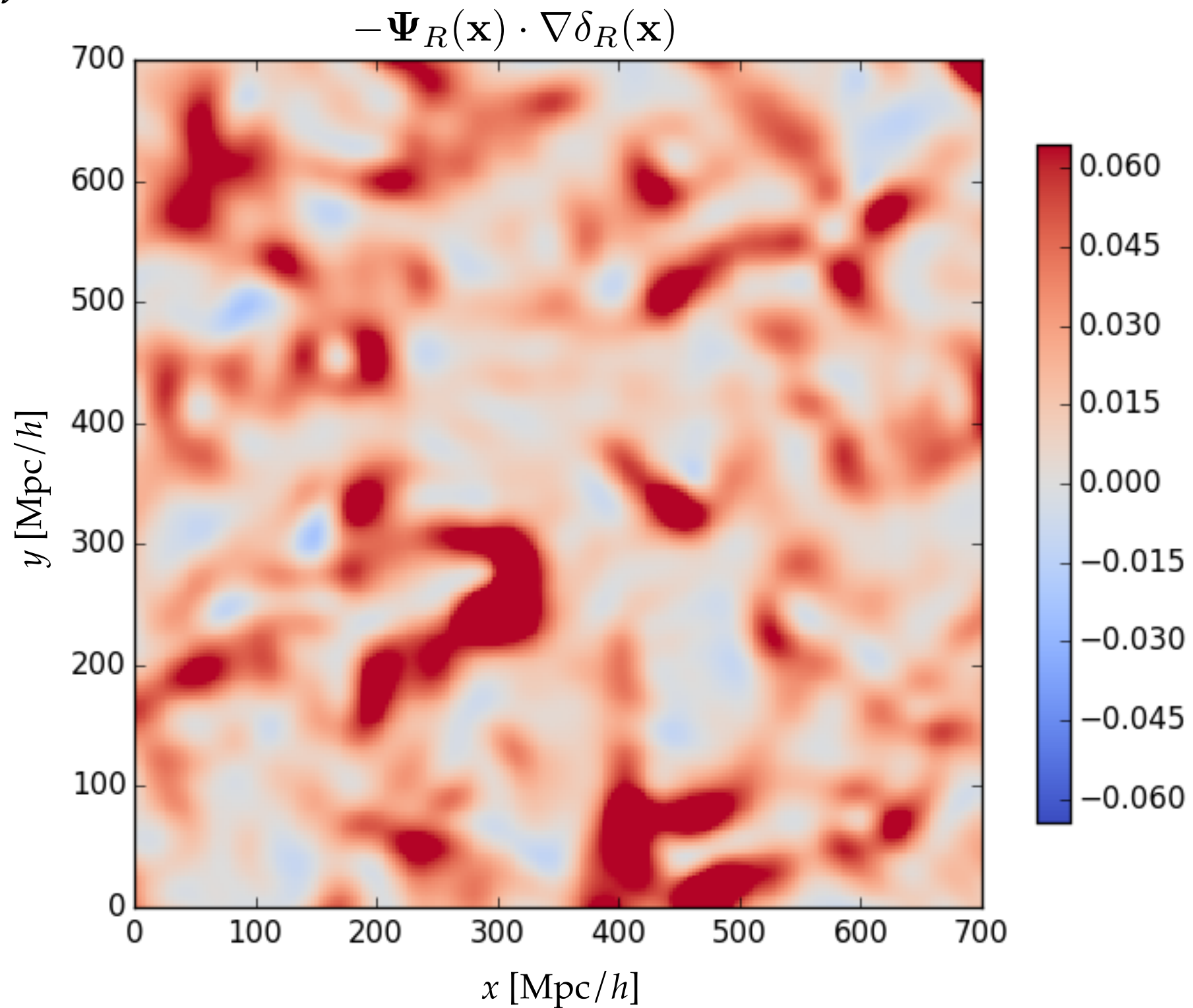
## ► 3. Get squared density



# IN PICTURES

MS, Baldauf, Seljak, [1411.6595](#)

## ► 4. *Get shift term*

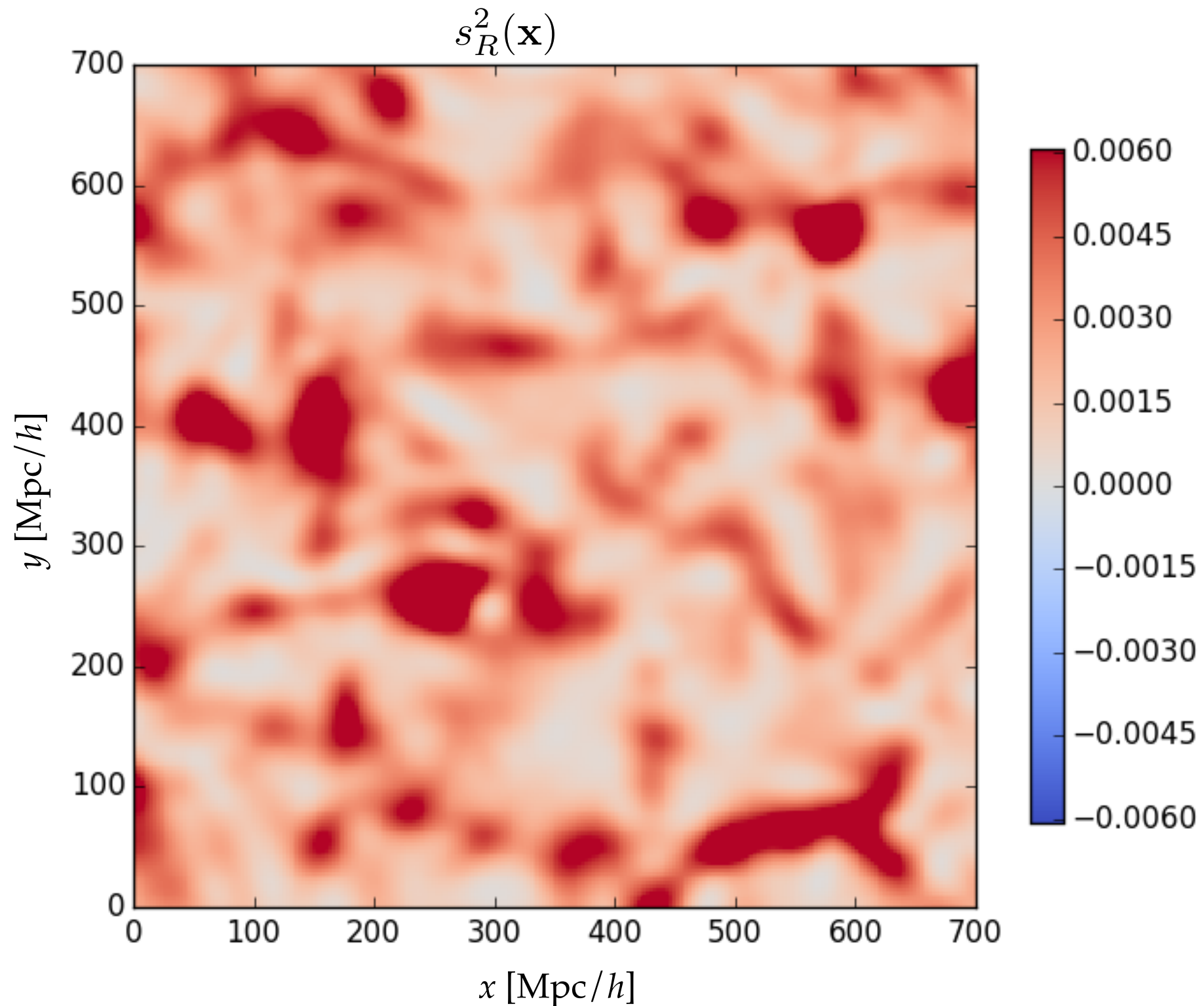




# IN PICTURES

MS, Baldauf, Seljak, [1411.6595](#)

## ► 5. *Get tidal term*



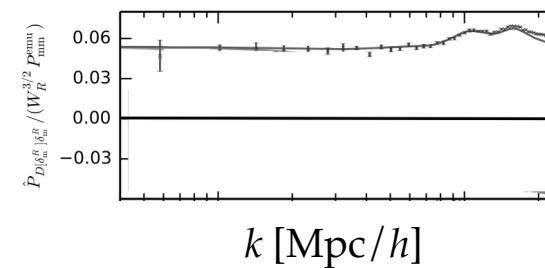
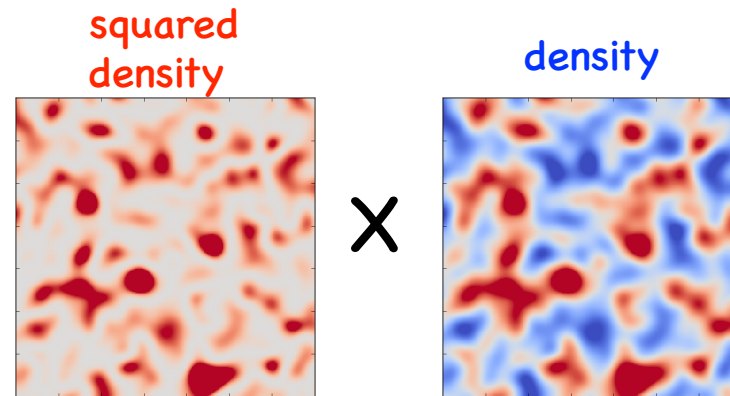
# IN PICTURES

MS, Baldauf, Seljak, [1411.6595](#)

## ► 6. Cross-correlate

**$l=0$   
growth**

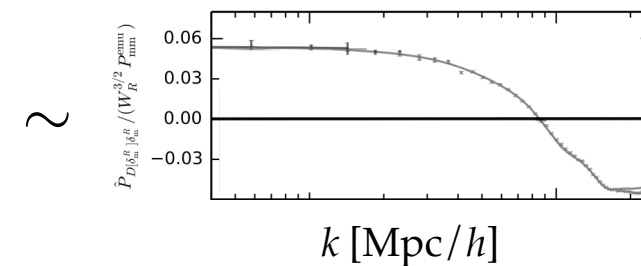
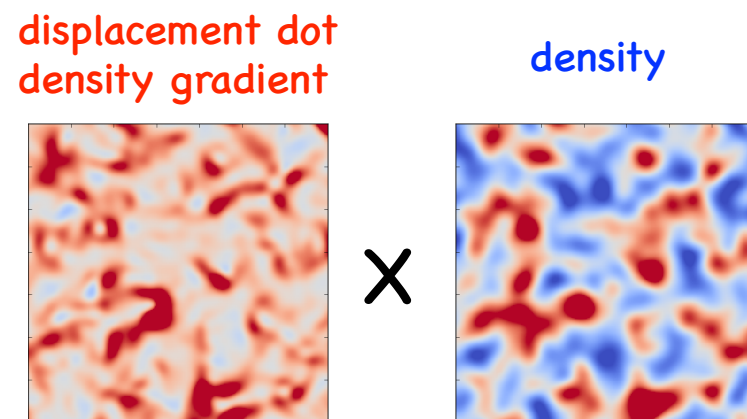
$$\hat{P}_{\delta^2, \delta}(k) \sim$$



- nonlinear DM growth  $\delta^2$
- quadratic bias  $b_2$

**$l=1$   
shift**

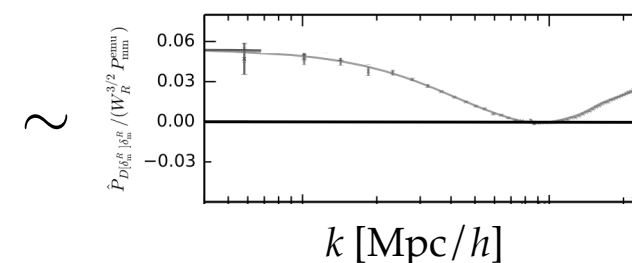
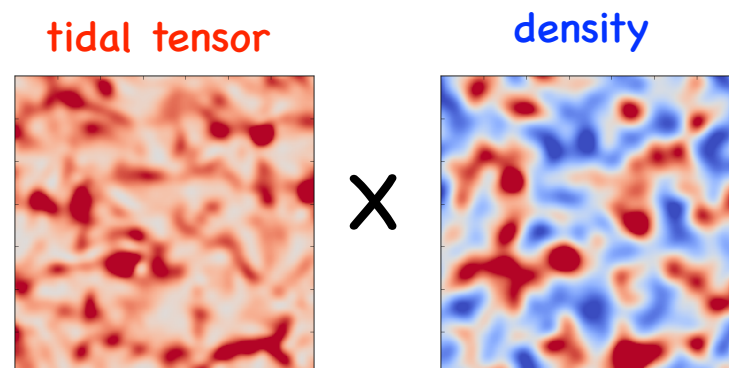
$$\hat{P}_{-\Psi^i \partial_i \delta, \delta}(k) \sim$$



- nonlinear DM shift  $\Psi(\mathbf{x}) \cdot \nabla \delta(\mathbf{x})$

**$l=2$   
tidal**

$$\hat{P}_{s^2, \delta}(k) \sim$$



- nonlinear DM tidal term
- tidal tensor bias




# PRIMORDIAL NON-GAUSSIANITY

MS, Baldauf, Seljak, [1411.6595](#)

► Optimal  $f_{\text{NL}}^{\text{loc}}$  estimator from DM bispectrum:

$$\hat{f}_{\text{NL}}^{\text{loc}} = \frac{24\pi L^3}{N_{\text{loc}}} \int dk \frac{k^2 M^2(k)}{P_{\text{mm}}(k)} \hat{P}_{[\frac{\delta_{\text{m}}}{M}]^2, \frac{\delta_{\text{m}}}{M}}(k)$$


$$M(k, z) \equiv \frac{2}{3} \frac{k^2 T(k) D(z)}{\Omega_{\text{m}} H_0^2} \quad (\text{Poisson factor})$$

⇒ basically just  $\phi^2$  cross  $\phi$ , where  $\phi \sim \delta/k^2$

⇒ in principle same  $S/N$  as getting  $f_{\text{NL}}^{\text{loc}}$  from measurement of the entire LSS bispectrum

# THEORETICAL MODELING



# MODELING CROSS-SPECTRA

MS, Baldauf, Seljak, [1411.6595](#)

► Expectation value of cross-spectrum with *general* kernel  $D \in \{P_0, -F_2^1 P_1, P_2\}$

$$P_{D[\delta_a^R], \delta_b^R}(k) = W_R(k) \int \frac{d^3 q}{(2\pi)^3} W_R(q) W_R(|\mathbf{k} - \mathbf{q}|) D(\mathbf{q}, \mathbf{k} - \mathbf{q}) B_{\delta_a \delta_a \delta_b}(\mathbf{q}, \mathbf{k} - \mathbf{q}, -\mathbf{k})$$

*integrated  
bispectrum*

# MODELING CROSS-SPECTRA

MS, Baldauf, Seljak, 1411.6595

- Expectation value of cross-spectrum with *general* kernel  $D \in \{P_0, -F_2^1 P_1, P_2\}$

$$P_{D[\delta_a^R], \delta_b^R}(k) = W_R(k) \int \frac{d^3 q}{(2\pi)^3} W_R(q) W_R(|\mathbf{k} - \mathbf{q}|) D(\mathbf{q}, \mathbf{k} - \mathbf{q}) B_{\delta_a \delta_a \delta_b}(\mathbf{q}, \mathbf{k} - \mathbf{q}, -\mathbf{k})$$

*integrated bispectrum*

- Leading-order SPT for  $hhh$  cross-spectra

$$\begin{aligned} P_{D[\delta_h^R], \delta_h^R}(k) = & \left( \frac{34}{21} b_1^3 + 2b_1^2 b_2 \right) \left[ I_{DP_0}^R(k) + 2I_{DP_0}^{\text{bare}, R}(k) \right] \\ & + 2b_1^3 \left[ I_{D, F_2^1 P_1}^R(k) + 2I_{D, F_2^1 P_1}^{\text{bare}, R}(k) \right] \\ & + \left( \frac{8}{21} b_1^3 + \frac{4}{3} b_1^2 b_{s^2} \right) \left[ I_{DP_2}^R(k) + 2I_{DP_2}^{\text{bare}, R}(k) \right] \end{aligned}$$

$$I_{DE}^R(k) \equiv W_R(k) \int \frac{d^3 q}{(2\pi)^3} W_R(q) W_R(|\mathbf{k} - \mathbf{q}|) P_{\text{mm}}^{\text{lin}}(q) P_{\text{mm}}^{\text{lin}}(|\mathbf{k} - \mathbf{q}|) D(\mathbf{q}, \mathbf{k} - \mathbf{q}) E(\mathbf{q}, \mathbf{k} - \mathbf{q})$$

$$I_{DE}^{\text{bare}, R}(k) \equiv W_R(k) P_{\text{mm}}^{\text{lin}}(k) \int \frac{d^3 q}{(2\pi)^3} W_R(q) W_R(|\mathbf{k} - \mathbf{q}|) P_{\text{mm}}^{\text{lin}}(q) D(\mathbf{q}, \mathbf{k} - \mathbf{q}) E(\mathbf{q}, -\mathbf{k})$$



# MODELING CROSS-SPECTRA

MS, Baldauf, Seljak, 1411.6595

- Expectation value of cross-spectrum with *general* kernel  $D \in \{P_0, -F_2^1 P_1, P_2\}$

$$P_{D[\delta_a^R], \delta_b^R}(k) = W_R(k) \int \frac{d^3 q}{(2\pi)^3} W_R(q) W_R(|\mathbf{k} - \mathbf{q}|) D(\mathbf{q}, \mathbf{k} - \mathbf{q}) B_{\delta_a \delta_a \delta_b}(\mathbf{q}, \mathbf{k} - \mathbf{q}, -\mathbf{k})$$

*integrated bispectrum*

- Leading-order SPT for  $hhh$  cross-spectra

$$\begin{aligned} P_{D[\delta_h^R], \delta_h^R}(k) = & \left( \frac{34}{21} b_1^3 + 2b_1^2 b_2 \right) \left[ I_{DP_0}^R(k) + 2I_{DP_0}^{\text{bare}, R}(k) \right] \\ & + 2b_1^3 \left[ I_{D, F_2^1 P_1}^R(k) + 2I_{D, F_2^1 P_1}^{\text{bare}, R}(k) \right] \\ & + \left( \frac{8}{21} b_1^3 + \frac{4}{3} b_1^2 b_{s^2} \right) \left[ I_{DP_2}^R(k) + 2I_{DP_2}^{\text{bare}, R}(k) \right] \end{aligned}$$

$$I_{DE}^R(k) \equiv W_R(k) \int \frac{d^3 q}{(2\pi)^3} W_R(q) W_R(|\mathbf{k} - \mathbf{q}|) P_{\text{mm}}^{\text{lin}}(q) P_{\text{mm}}^{\text{lin}}(|\mathbf{k} - \mathbf{q}|) D(\mathbf{q}, \mathbf{k} - \mathbf{q}) E(\mathbf{q}, \mathbf{k} - \mathbf{q})$$

$$I_{DE}^{\text{bare}, R}(k) \equiv W_R(k) P_{\text{mm}}^{\text{lin}}(k) \int \frac{d^3 q}{(2\pi)^3} W_R(q) W_R(|\mathbf{k} - \mathbf{q}|) P_{\text{mm}}^{\text{lin}}(q) D(\mathbf{q}, \mathbf{k} - \mathbf{q}) E(\mathbf{q}, -\mathbf{k})$$

- Covariance between cross-spectra at the same  $k$

$$\text{cov}(\hat{P}_{D[\delta_a^R], \delta_b^R}(k), \hat{P}_{E[\delta_a^R], \delta_b^R}(k)) = \frac{2}{N_{\text{modes}}(k)} P_{bb}^R(k) I_{DE}^{P_{aa}^R P_{aa}^R}(k)$$

# SIMULATIONS & RESULTS



# SIMULATIONS

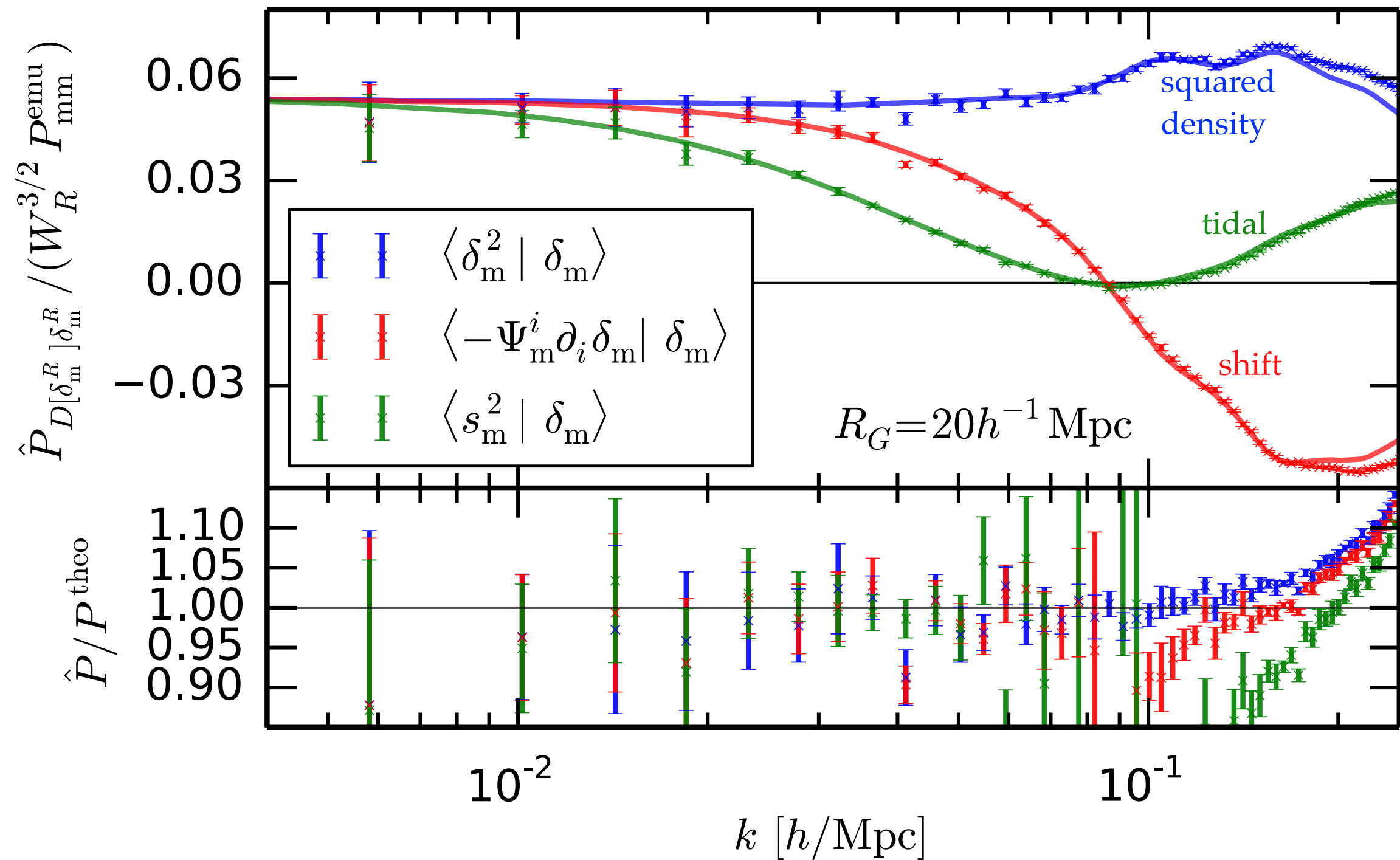
## ► **RunPB** sims from Martin White / Beth Reid

Reid *et al.* 1404.3742  
White *et al.* 1408.5435  
White astro-ph/0207185

- $L = 1380 \text{ Mpc}/h$
- $2048^3$  DM particles or FoF ( $b=0.168$ ) halos
- 10 realizations
- $z = 0.55$

# DM CROSS-SPECTRA

MS, Baldauf, Seljak, [1411.6595](#)

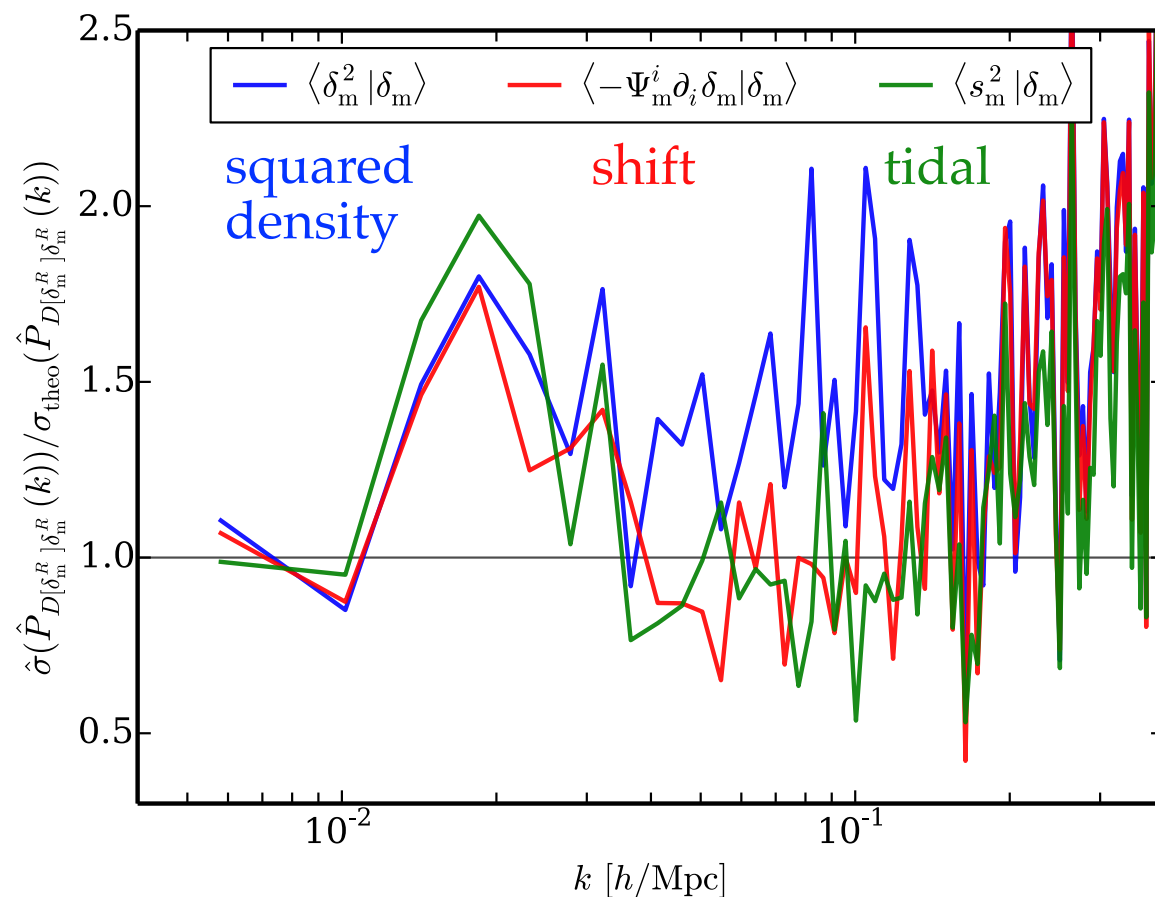




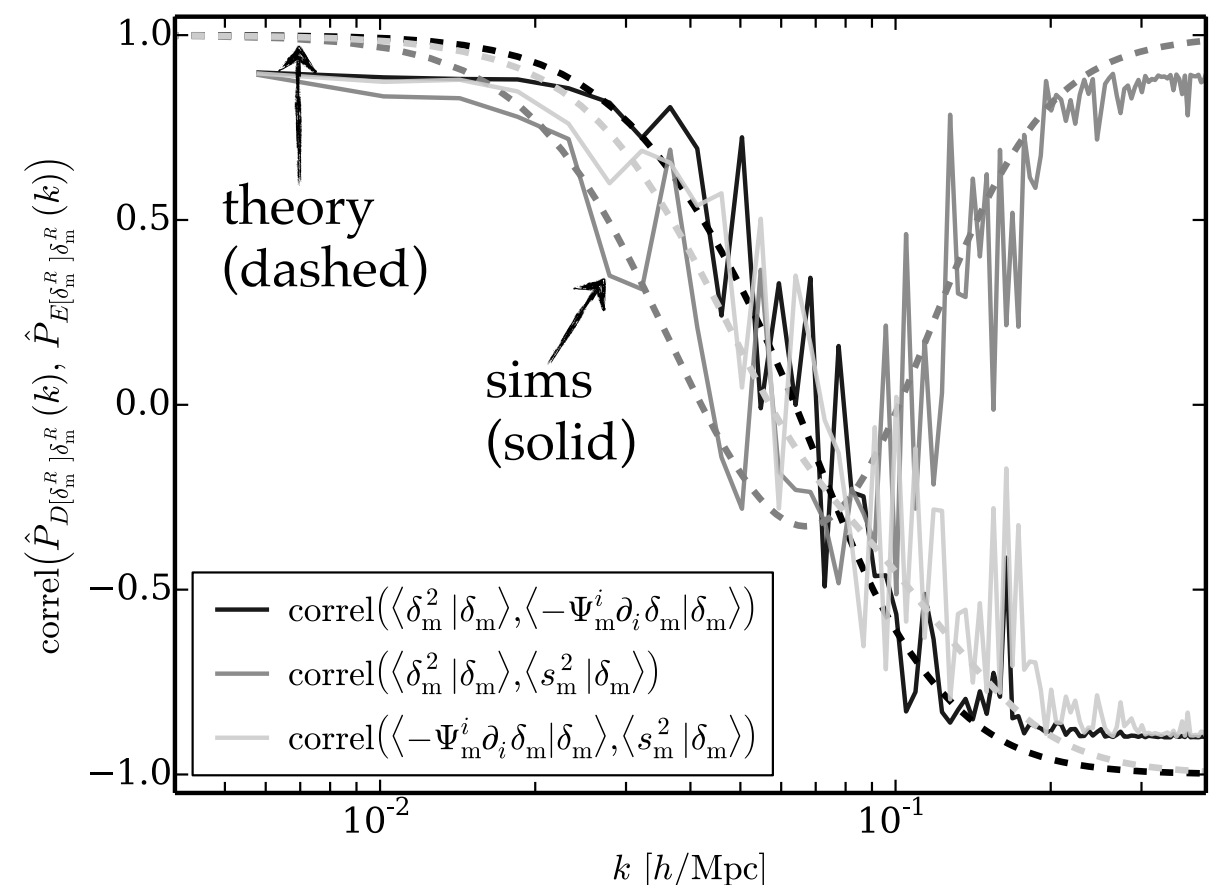
# DM CROSS-SPECTRA: COVARIANCE

MS, Baldauf, Seljak, 1411.6595

*Standard deviations* of individual cross-spectra (sims divided by theory)



*Correlations* between different cross-spectra at the same  $k$



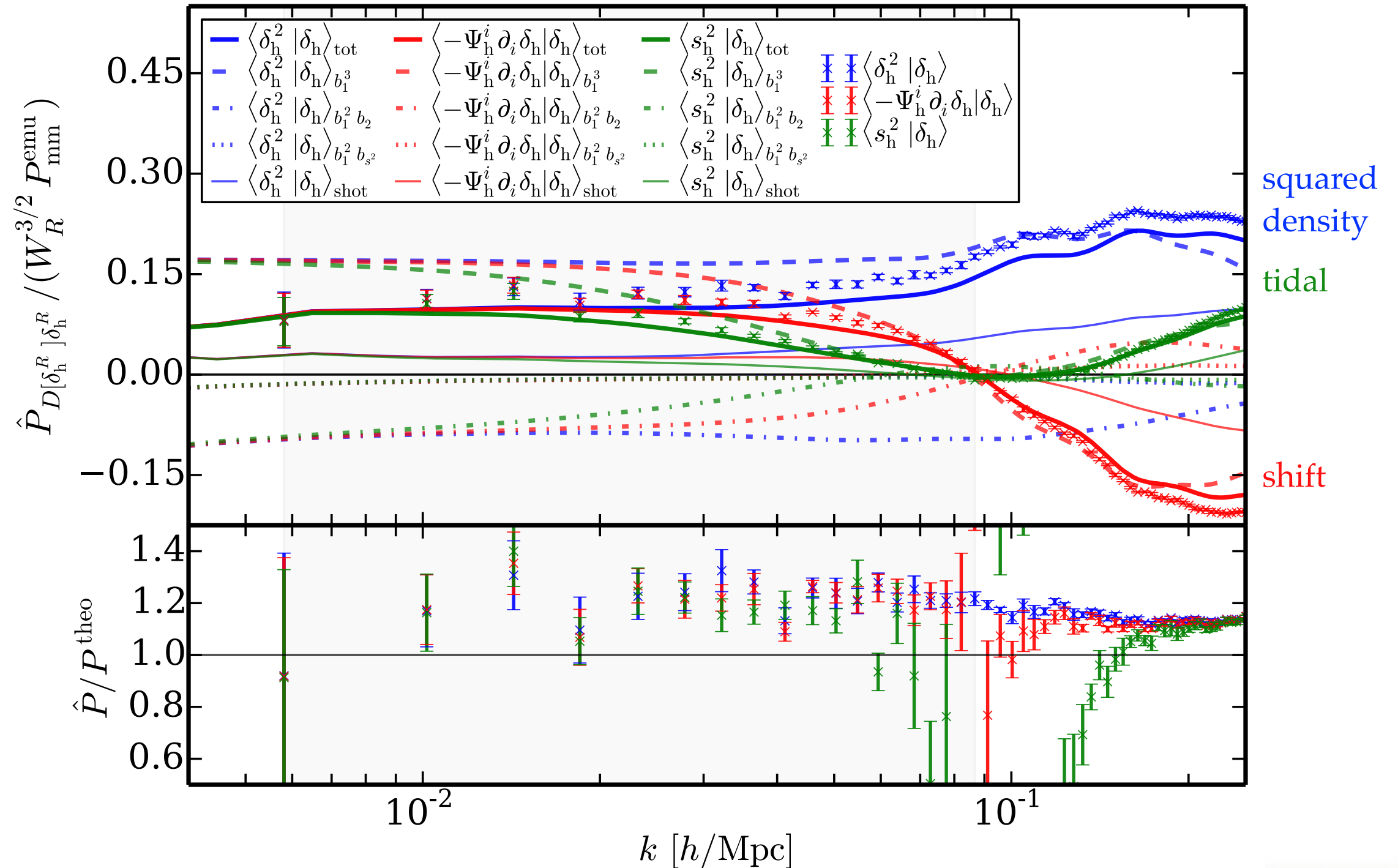
Perfectly (anti-)correlated at low  $k$  and high  $k$ , but uncorrelated at intermediate  $k$

# HALO CROSS-SPECTRA

MS, Baldauf, Seljak, [1411.6595](#)

Assuming Poisson shot noise

$$(4.51 \times 10^{12} - 1.35 \times 10^{13}) h^{-1} M_{\odot}, \chi^2/\text{d.o.f.} = 16.60, \Delta_1 = 0, b_1 = 1.47, b_2 = -0.37, b_{s^2} = -0.29$$



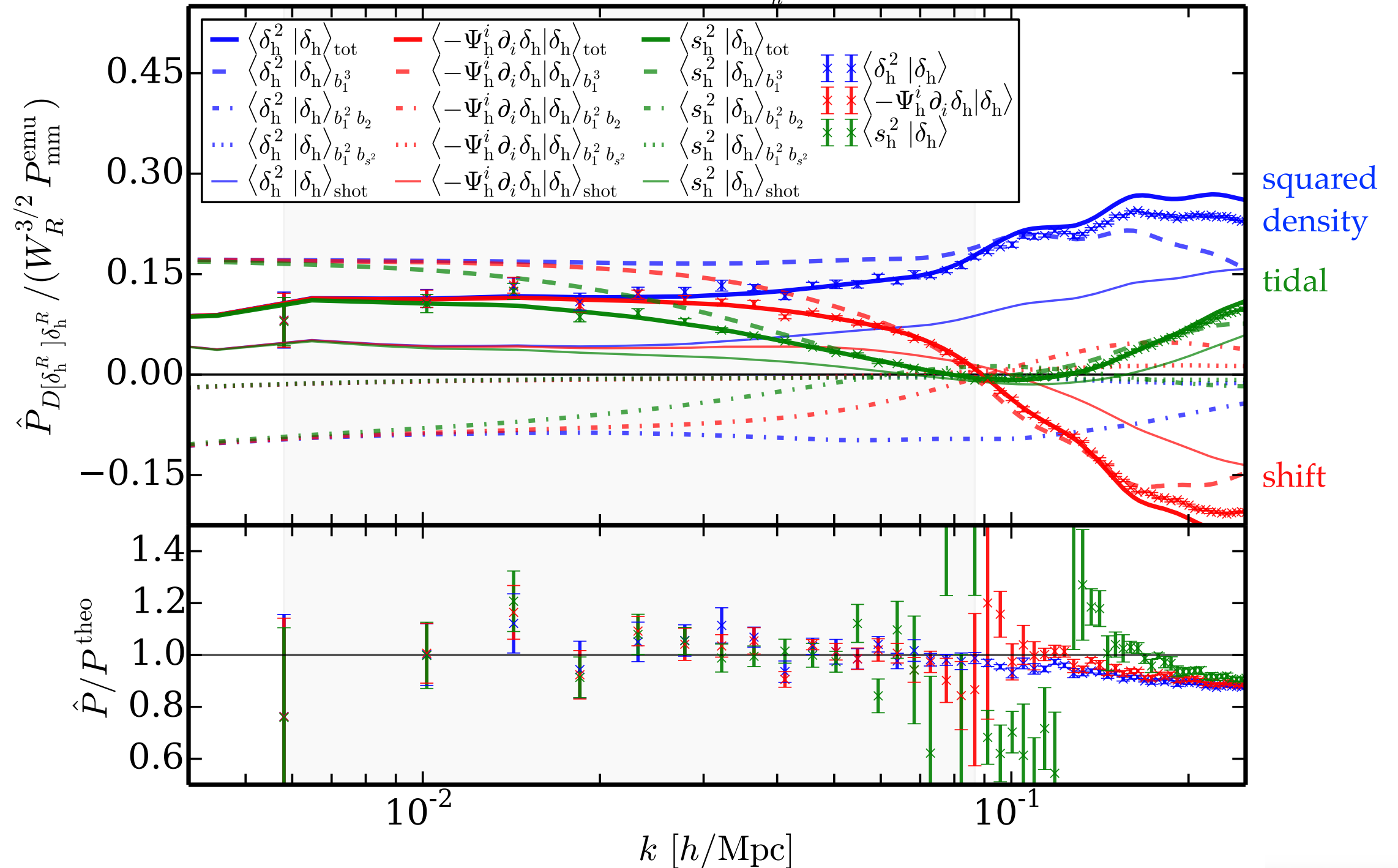


# HALO CROSS-SPECTRA

MS, Baldauf, Seljak, [1411.6595](#)

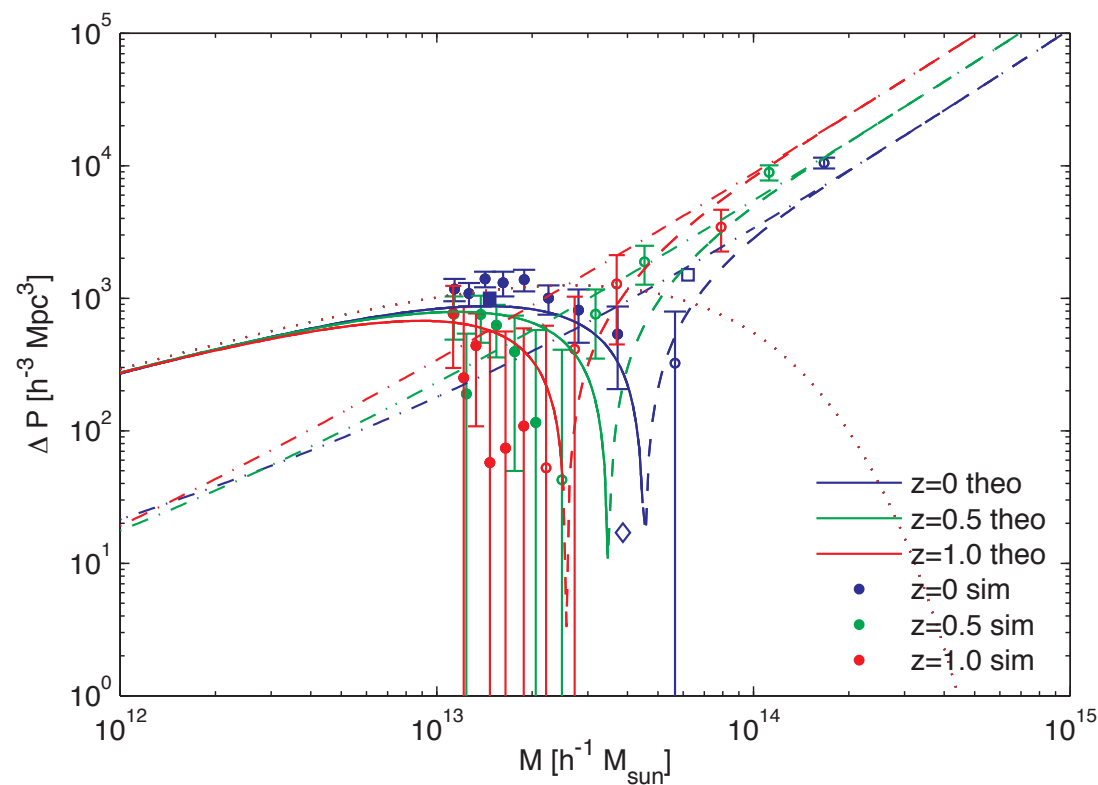
Corrected shot noise (rescaling Poisson prediction by free  $A_{\text{shot}}$ )

$$(4.51 \times 10^{12} - 1.35 \times 10^{13}) h^{-1} M_{\odot}, \chi^2/\text{d.o.f.} = 1.25, \Delta_1 = 1.25 \frac{\text{Gpc}^3}{h^3}, b_1 = 1.47, b_2 = -0.37, b_{s^2} = -0.29$$

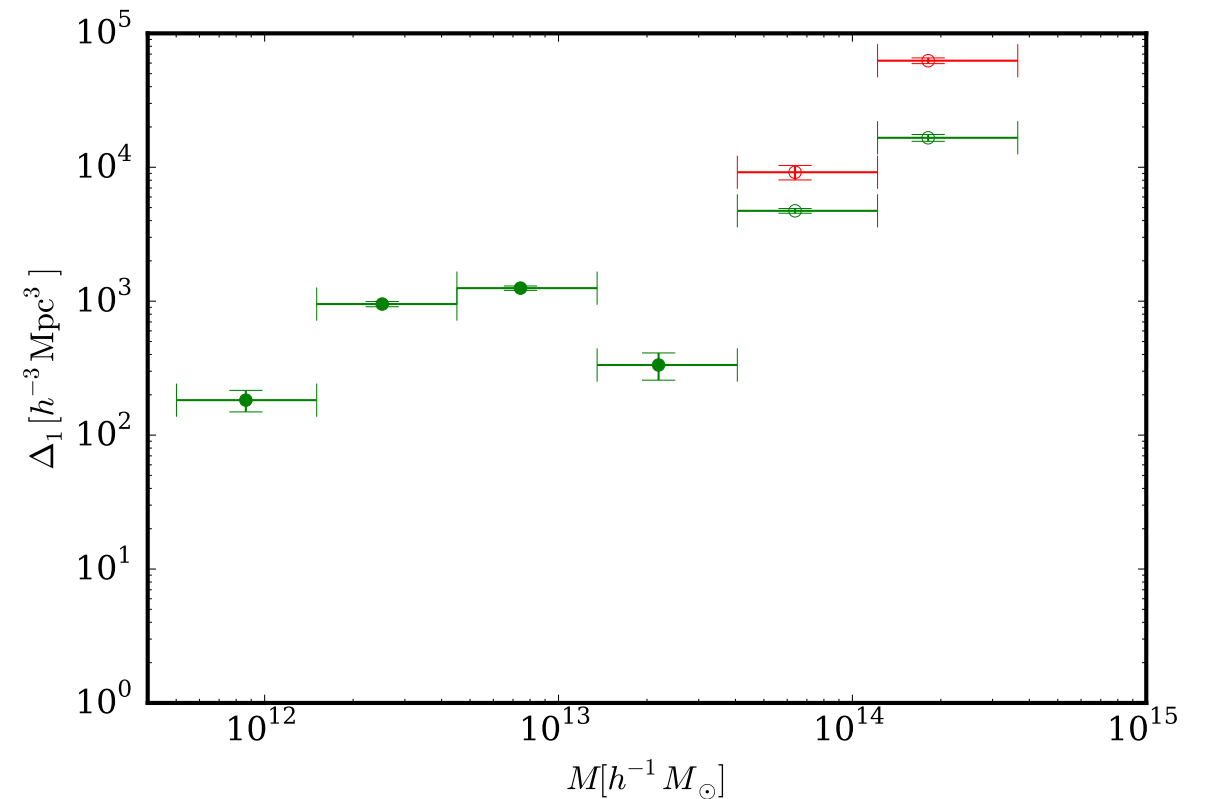


# MASS DEPENDENCE OF SHOT NOISE CORRECTION

Correction to  $1/n$  shot noise in  $P(k)$  (Baldauf *et al.* 1305.2917)



Correction to  $P(k)/n$  part of shot noise in **bispectrum**

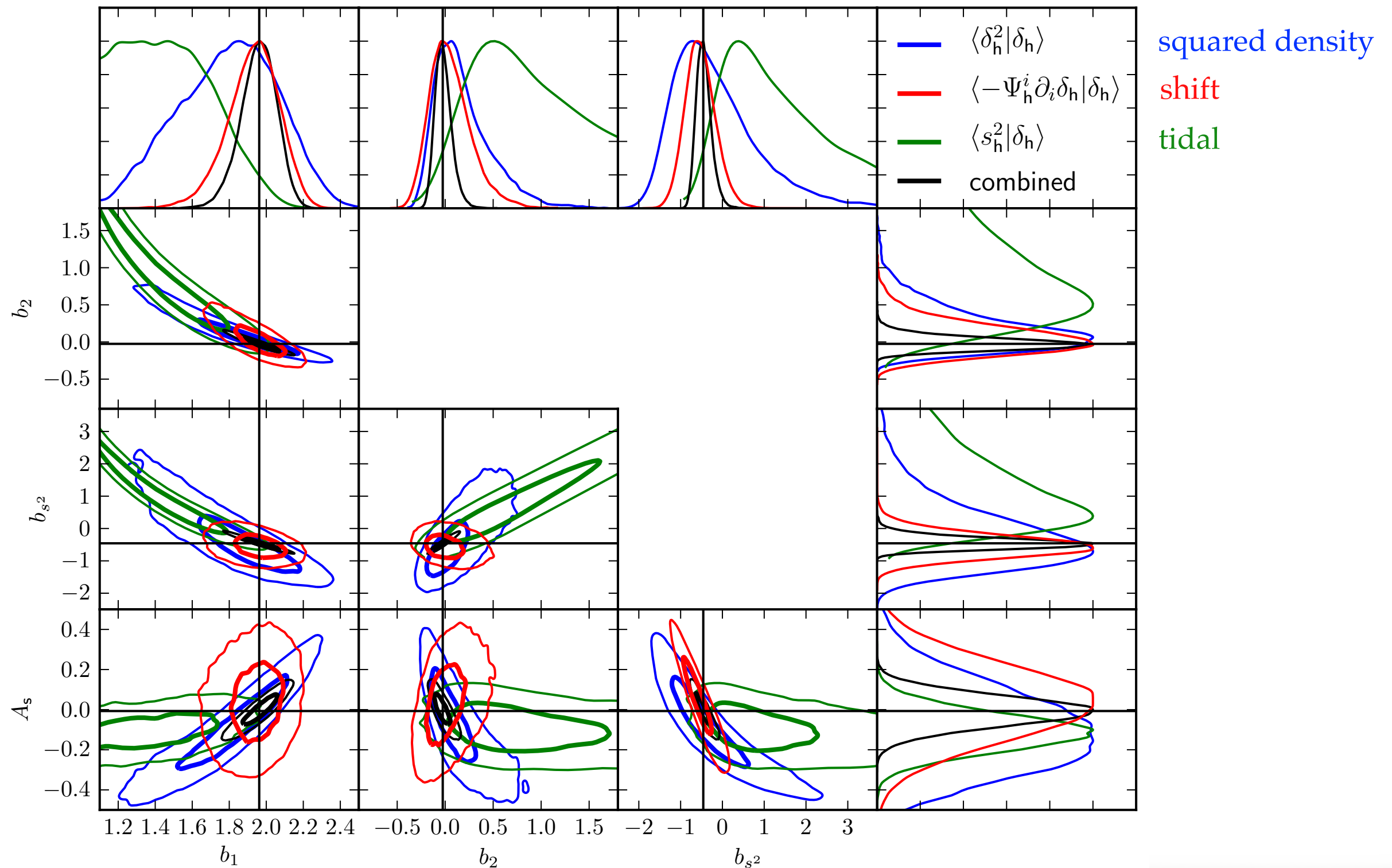




# BIAS CONSTRAINTS

MS, Baldauf, Seljak, [1411.6595](#)

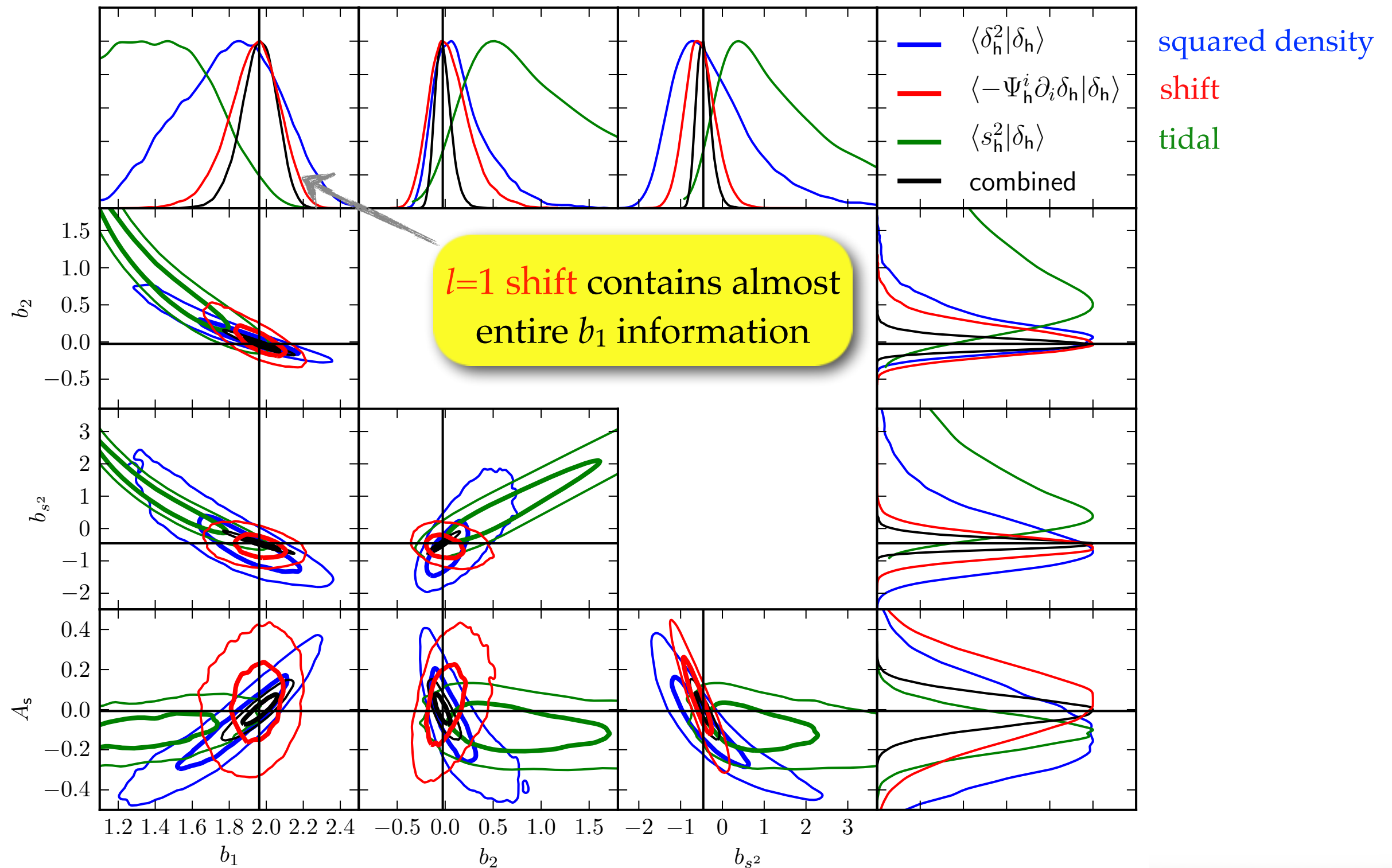
Fit  $b_1, b_2, b_{s^2}, A_{\text{shot}}$  from  $hhh$  cross-spectra (only 3-point, no 2-point)



# BIAS CONSTRAINTS

MS, Baldauf, Seljak, [1411.6595](#)

Fit  $b_1, b_2, b_{s^2}, A_{\text{shot}}$  from  $hhh$  cross-spectra (only 3-point, no 2-point)





CONCLUDING  
REMARKS  
(PART I)

# COMPARISON WITH TRADITIONAL BISPECTRUM ESTIMATION

MS, Baldauf, Seljak, [1411.6595](#)

## ► **Advantages** of cross-spectra over estimating bispectrum for individual triangles

- *Simple*
- *Nearly optimal* (contains entire bispectrum information)
- *Fast* (like power spectrum estimation)
- Depends on just single  $k$ , i.e. covariances are easy

Position-dependent power spectrum (Chiang++) is only sensitive to squeezed limit where grav. signal vanishes

## ► **Challenges**

- Redshift space distortions: messier but doable (ideas / tricks welcome!)
- Not optimal beyond tree level and beyond weakly non-Gaussian fields (could be improved with better theory or by combining with modal estimators that are sensitive to arbitrary bispectra)



# WHAT DO CMB PEOPLE DO?


## ► CMB bispectrum estimation

- 2001: individual triangles of COBE data ( $l_{\text{max}}=20$ ) Komatsu *et al.* 2001
- since 2003: **KSW**  $f_{\text{NL}}$  estimators for separable bispectrum templates (now standard) Komatsu+Spergel  
+Wandelt 2003
- **CMB lensing trispectrum:**
  - ⇒ never used individual quadrilaterals, but always max-likeli estimators for known trispectrum shape
  - ⇒ reconstructed lensing potential is  $\widehat{\nabla\phi} \propto T\nabla T$
  - ⇒ trispectrum = auto-power of this quadratic field
- ISW-lensing bispectrum: cross-spectrum of  $\hat{\phi} \sim T^2$  and  $T$  Lewis *et al.* 2011,  
Planck 2013 XIX (ISW)
- modal estimators (sensitive to arbitrary bispectra — reduce to our cross-spectra if halo bispectrum contributions are used as basis shapes) Fergusson+Shellard  
+Liguori 2009-2014,  
Planck 2013 XXIV (NG)



# WHAT DO CMB PEOPLE DO?

## ► CMB bispectrum estimation

- 2001: individual triangles  LSS methods at the level where CMB was 2001
- since 2003: **KSW**  $f_{\text{NL}}$  estimators for separable bispectrum templates (now standard) Komatsu+Spergel  
+Wandelt 2003
- **CMB lensing** trispectrum:
  - ⇒ never used individual quadrilaterals, but always max-likeli estimators for known trispectrum shape
  - ⇒ reconstructed lensing potential is  $\widehat{\nabla\phi} \propto T\nabla T$
  - ⇒ trispectrum = auto-power of this quadratic field
- ISW-lensing bispectrum: cross-spectrum of  $\hat{\phi} \sim T^2$  and  $T$  Lewis *et al.* 2011,  
Planck 2013 XIX (ISW)
- modal estimators (sensitive to arbitrary bispectra — reduce to our cross-spectra if halo bispectrum contributions are used as basis shapes) Fergusson+Shellard  
+Liguori 2009-2014,  
Planck 2013 XXIV (NG)

# WHAT DO CMB PEOPLE DO?

## ► CMB bispectrum estimation

- 2001: individual triang

LSS methods at the level where CMB was 2001

- since 2003: **KSW**  $f_{\text{NL}}$  estimators for separable bispectrum templates (now standard)

Komatsu+Spergel  
+Wandelt 2003

- **CMB lensing** trispectrum:
  - ⇒ never used individual quadr
  - ⇒ likeli estimators for known t
  - ⇒ reconstructed lensing potent
  - ⇒ trispectrum = auto-power of

- ISW-lensing bispectrum: cross-sp

- modal estimators (sensitive to arbitra
- cross-spectra if halo bispectrum contrib

Cross-spectrum method is *first step* to  
modernize this for LSS

but it's really only a first step:

our method is not yet ready for real data,

while traditional method has been applied to real data

(most recently by Gil-Marín *et al.* 2014)



# CONCLUSIONS (PART I)

MS, Baldauf, Seljak, [1411.6595](#)

- Explored new estimators to measure bispectrum parameters in a nearly optimal way using cross-spectra of 3 quadratic fields with the density

$$\begin{aligned}\hat{P}_{\delta^2, \delta}(k) &\sim \sum_{\mathbf{k}, |\mathbf{k}|=k} [\delta^2](\mathbf{k}) \delta(-\mathbf{k}), \\ \hat{P}_{-\Psi^i \partial_i \delta, \delta}(k) &\sim \sum_{\mathbf{k}, |\mathbf{k}|=k} [-\Psi^i \partial_i \delta](\mathbf{k}) \delta(-\mathbf{k}) \\ \hat{P}_{s^2, \delta}(k) &\sim \sum_{\mathbf{k}, |\mathbf{k}|=k} [s^2](\mathbf{k}) \delta(-\mathbf{k}).\end{aligned}$$

- Simulations agree with theory on large scales
- Linear halo bias  $b_1$  mostly determined by shift term cross density
- Shot noise requires non-Poissonian corrections
- *Future*: e.g. RSDs, model to higher  $k$ , apply to real data

# PART II

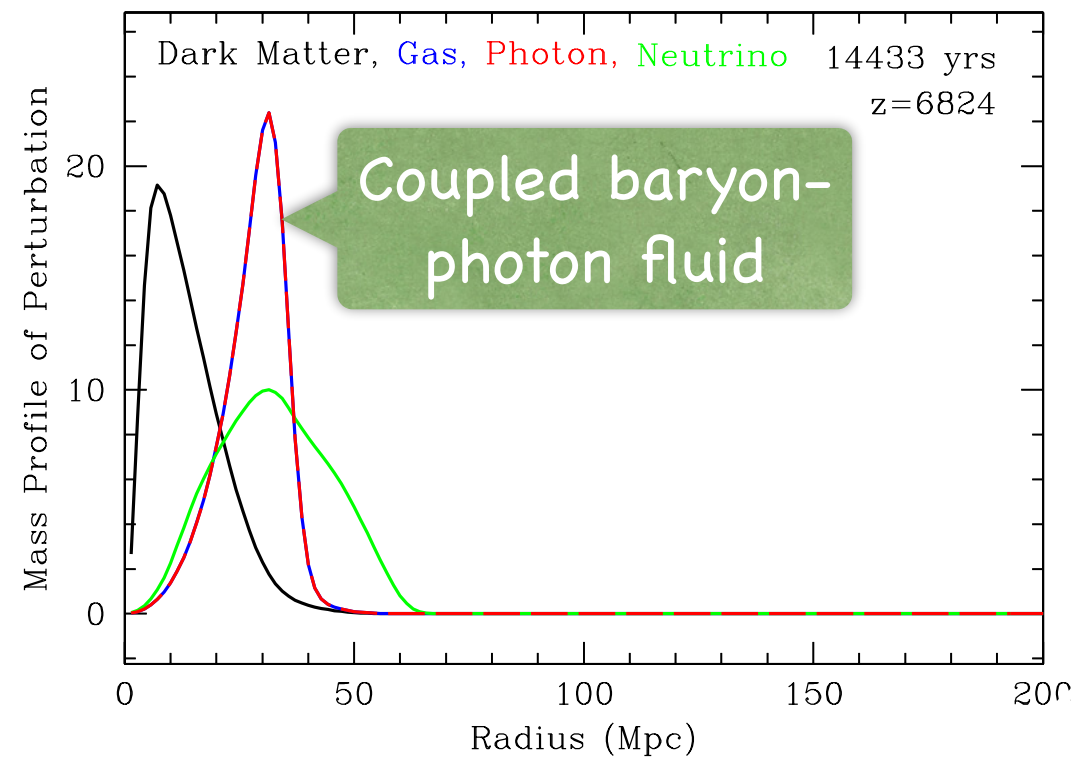
## EULERIAN BAO RECONSTRUCTIONS & N-POINT STATISTICS

ARXIV:1508.06972

W/ Y. FENG, F. BEUTLER, B. SHERWIN, M.Y. CHU

# BARYONIC ACOUSTIC OSCILLATIONS (BAO)

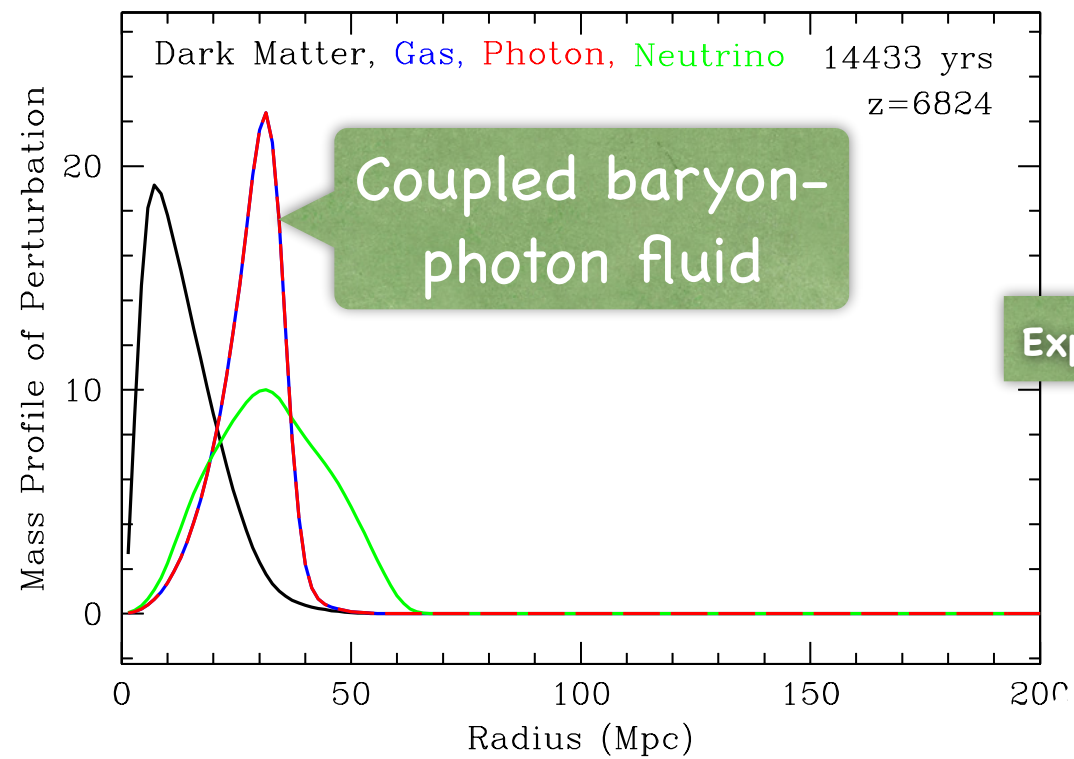
Eisenstein/Seo/White 2006



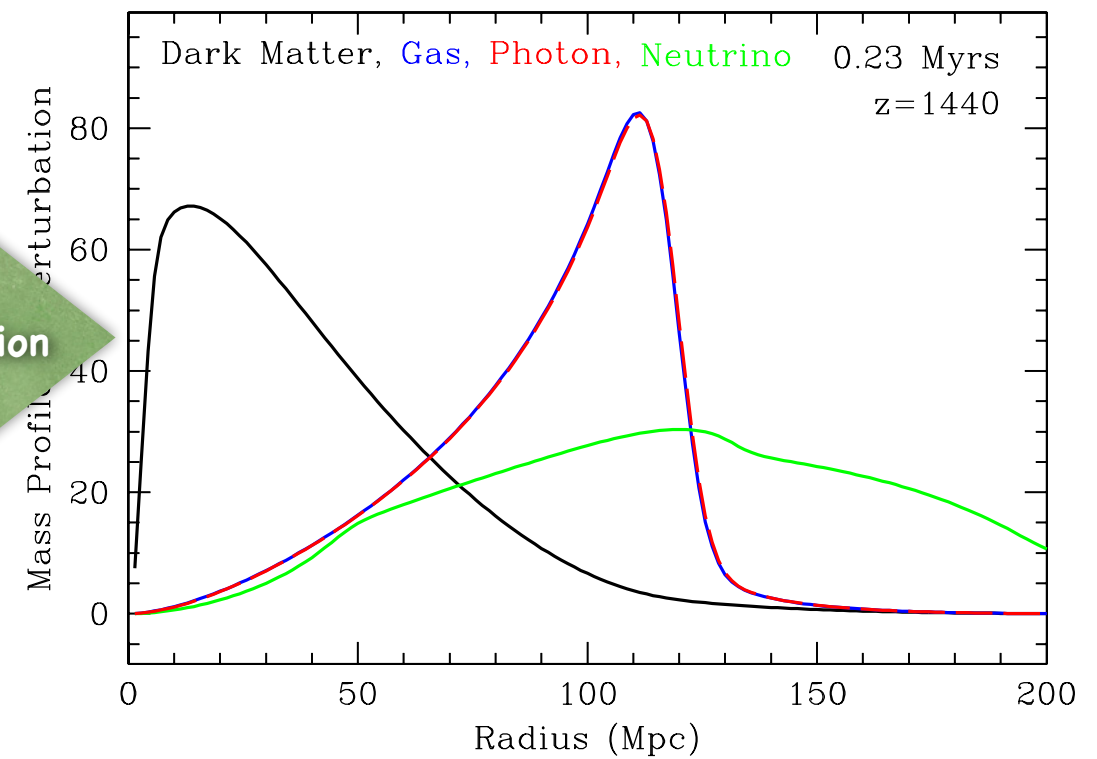


# BARYONIC ACOUSTIC OSCILLATIONS (BAO)

Eisenstein/Seo/White 2006

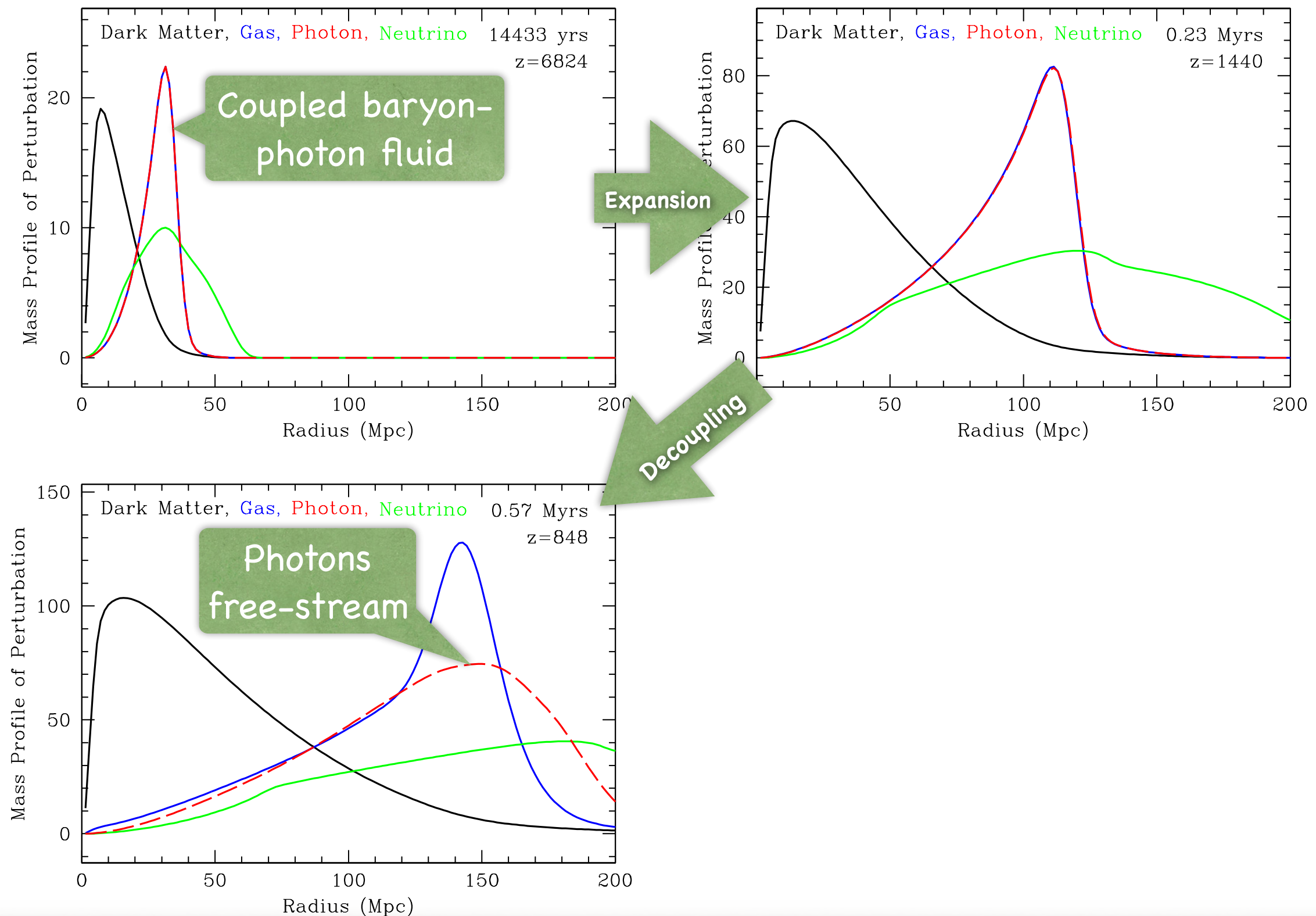


Expansion



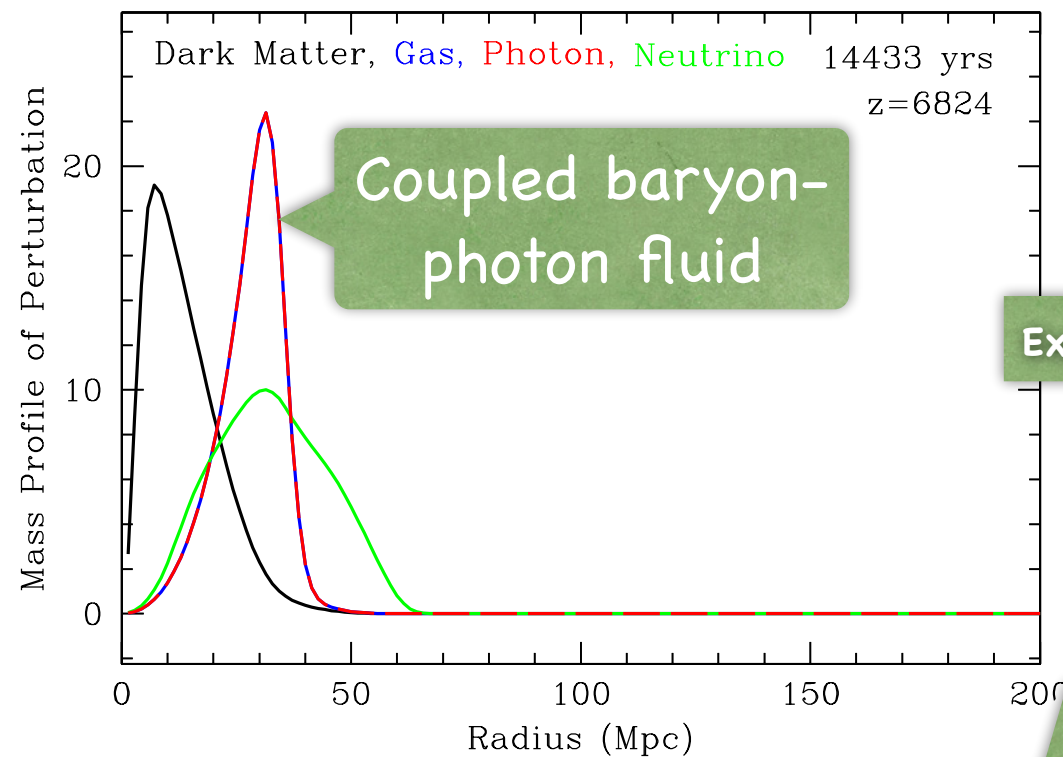
# BARYONIC ACOUSTIC OSCILLATIONS (BAO)

Eisenstein/Seo/White 2006

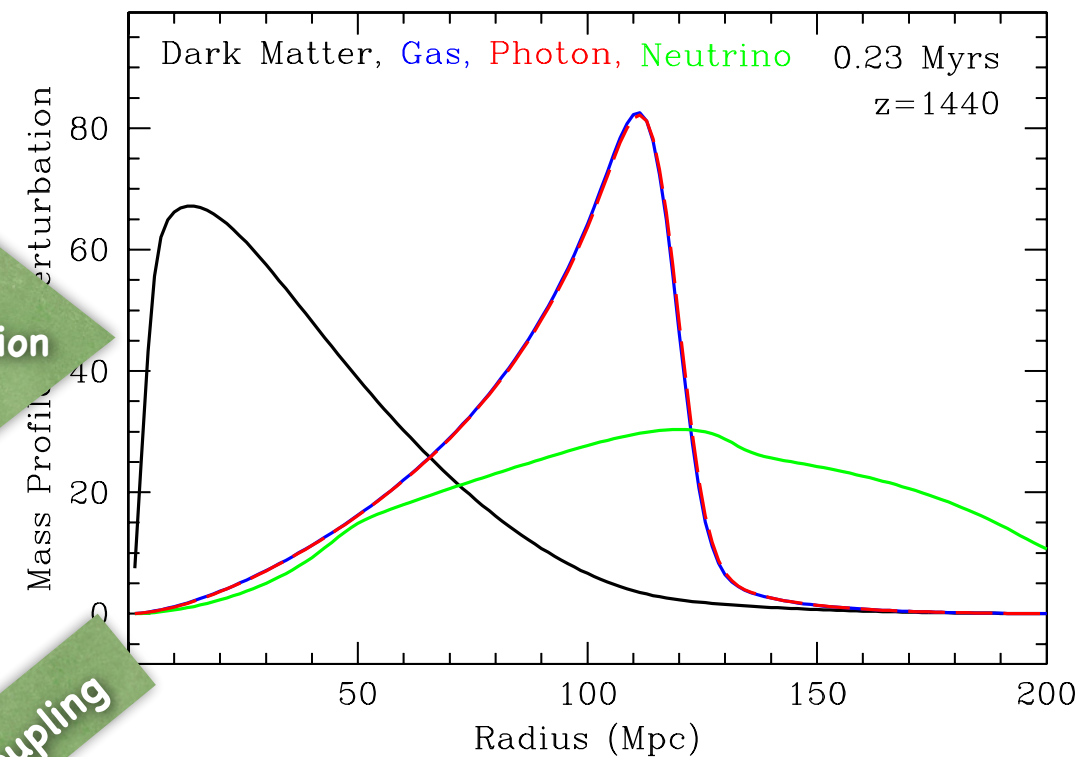


# BARYONIC ACOUSTIC OSCILLATIONS (BAO)

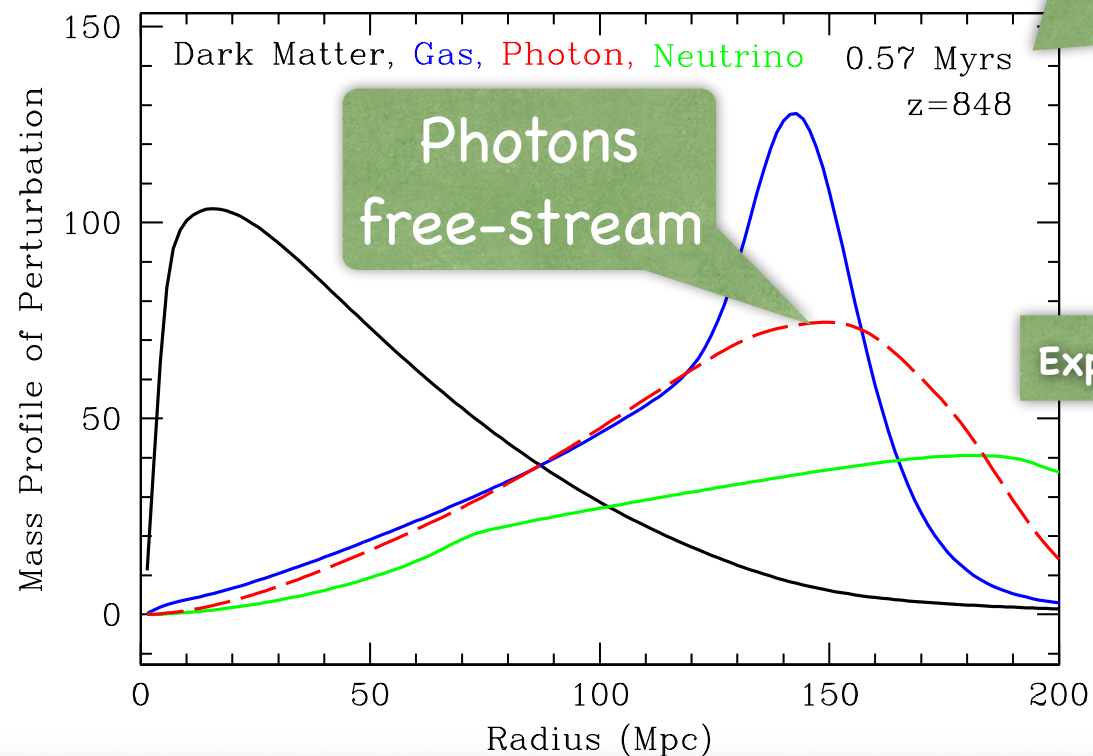
Eisenstein/Seo/White 2006



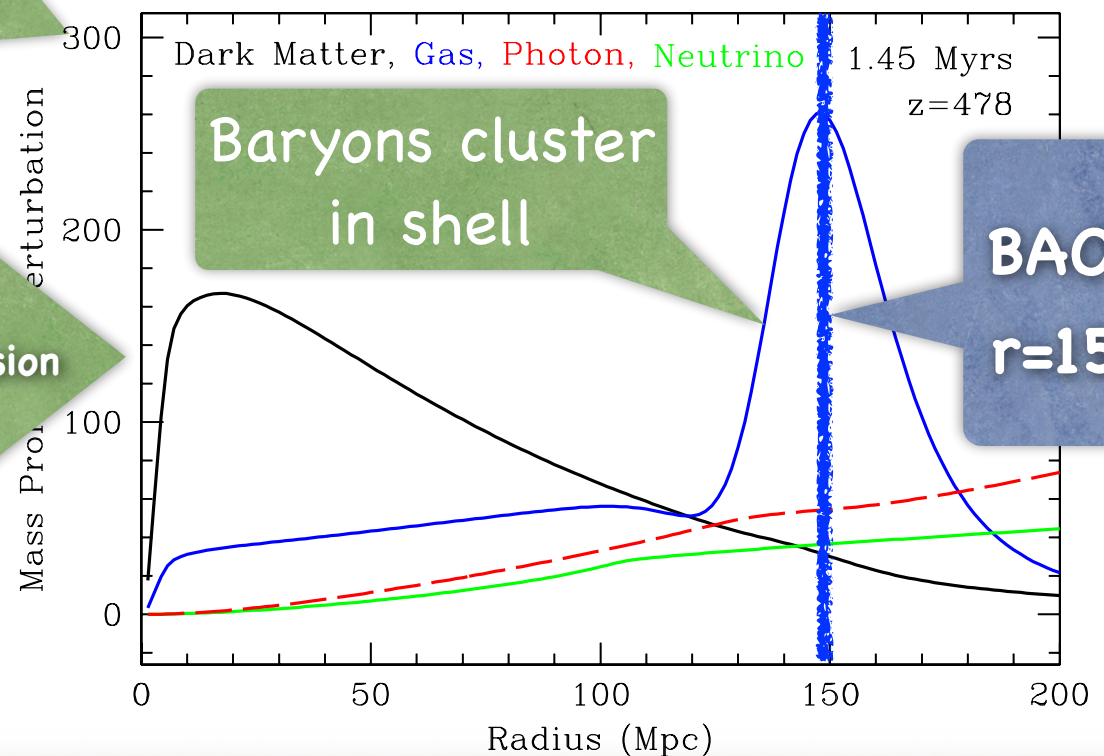
Expansion



Decoupling



Expansion

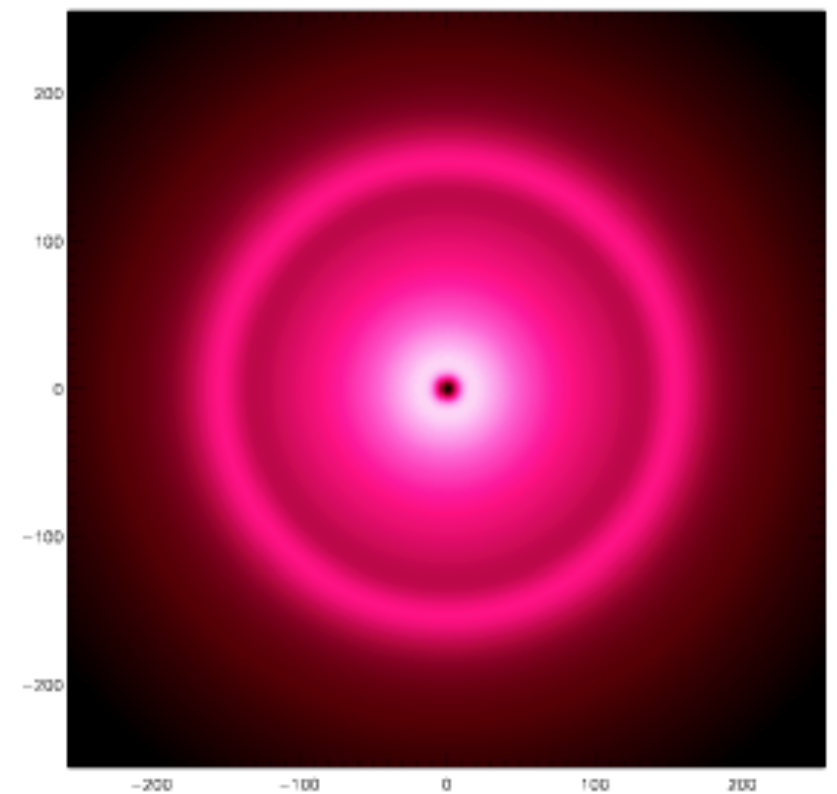
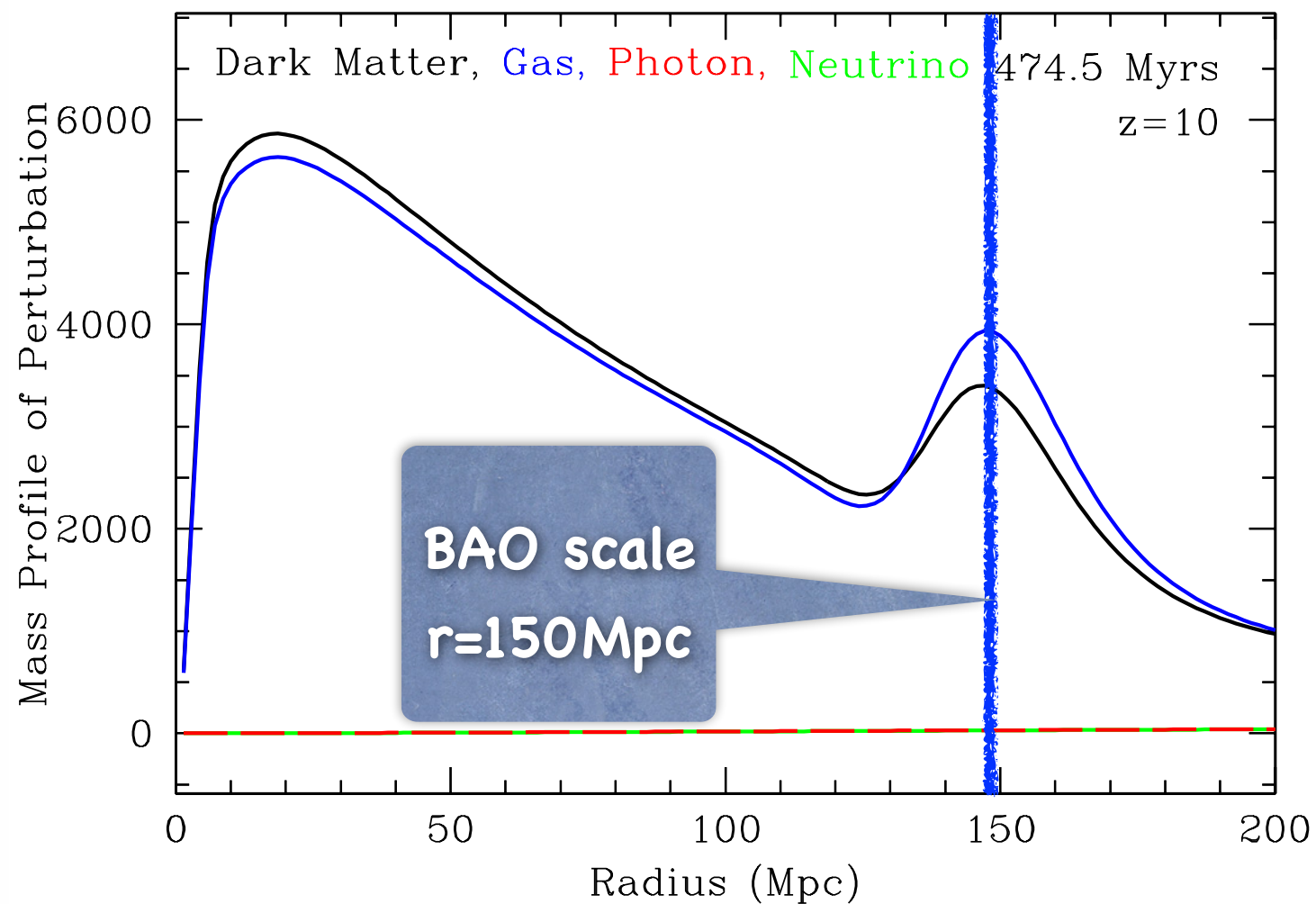




# BARYONIC ACOUSTIC OSCILLATIONS (BAO)

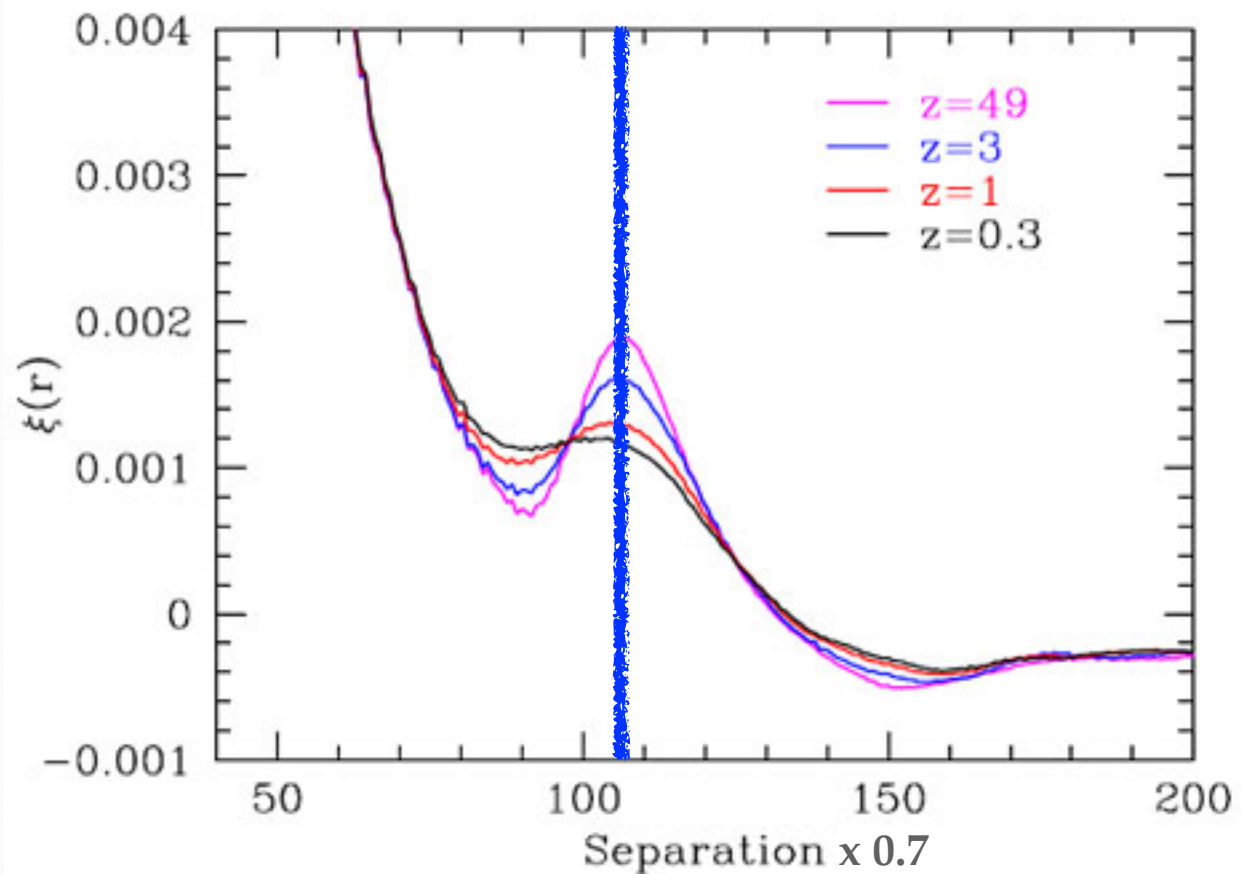
Eisenstein/Seo/White 2006

Expansion + clustering

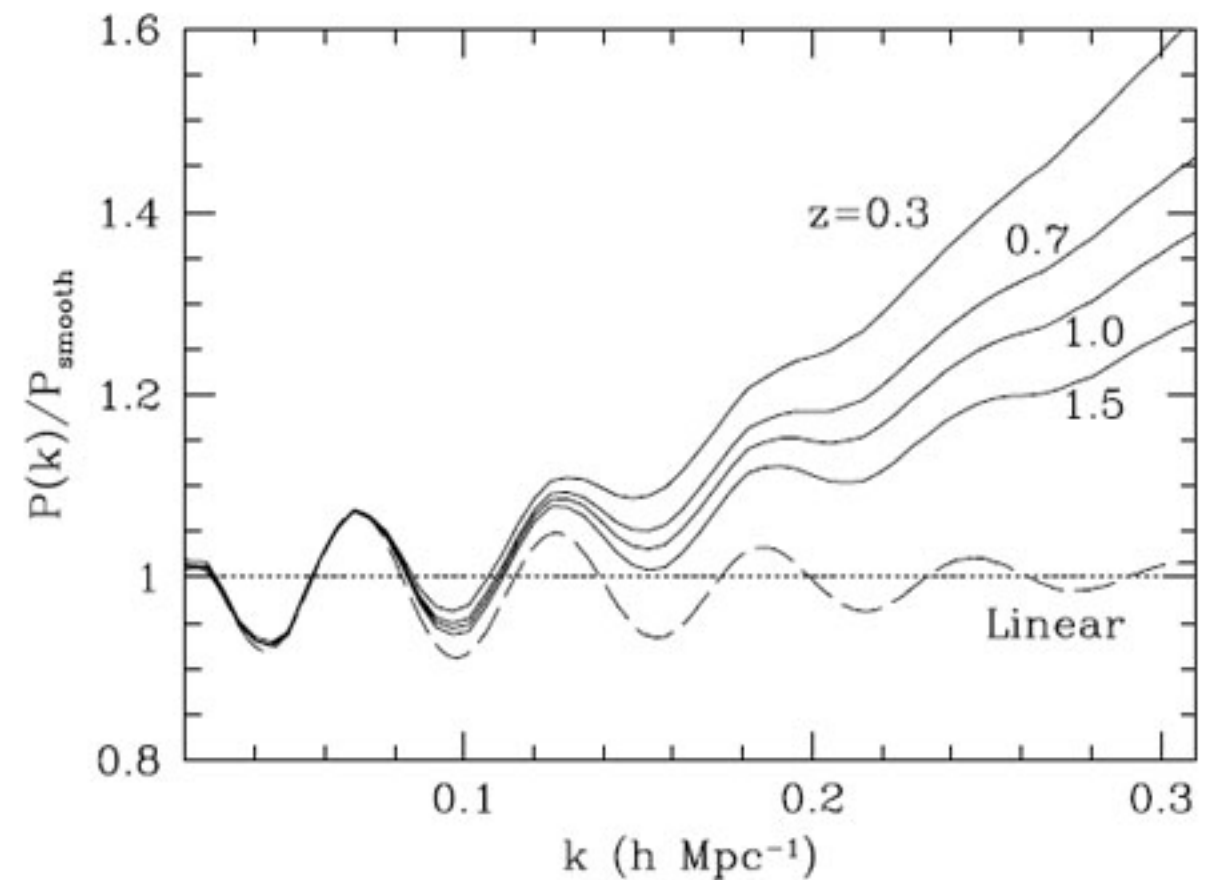


# BAO IMPRINT ON LSS

Correlation function  $\xi(r)$ : BAO bump

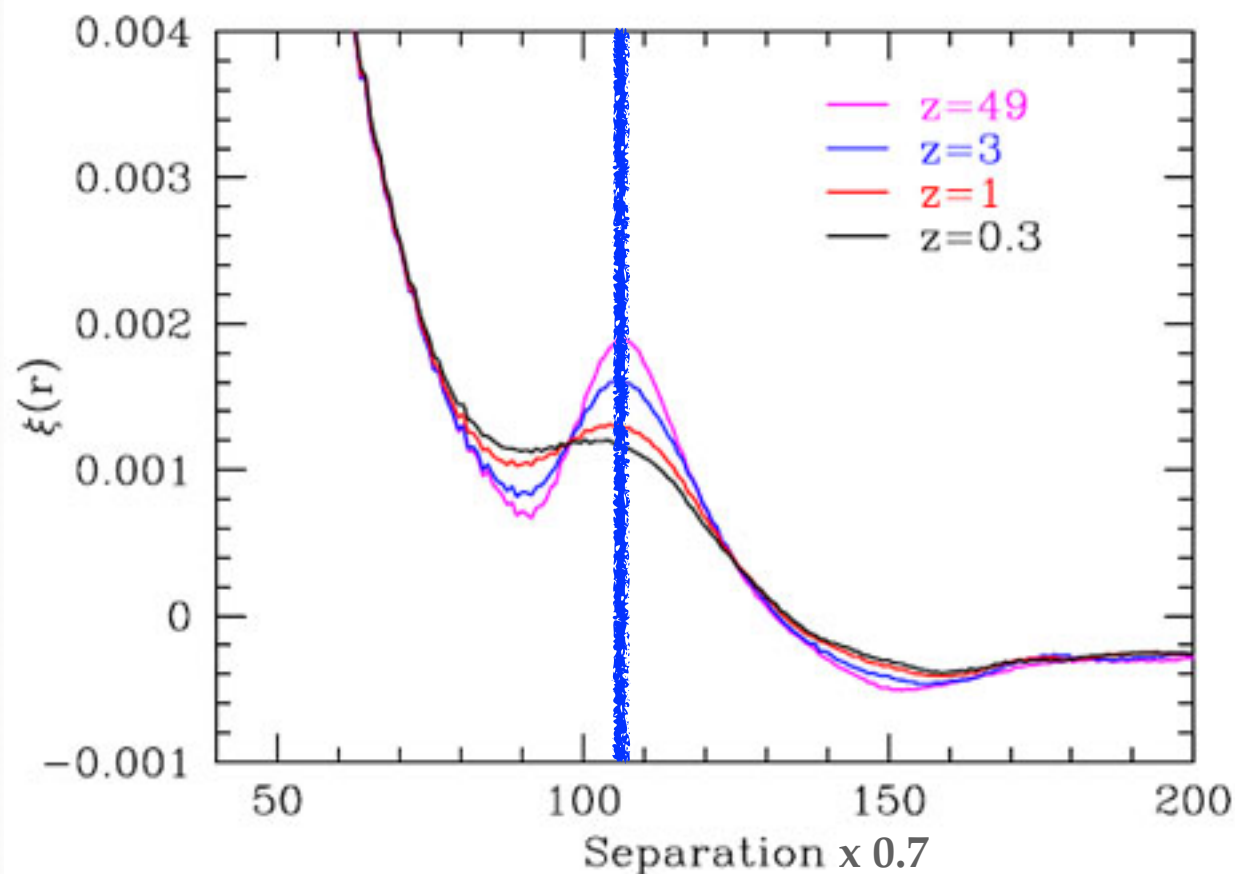


Power spectrum  $P(k)$ : BAO wiggles

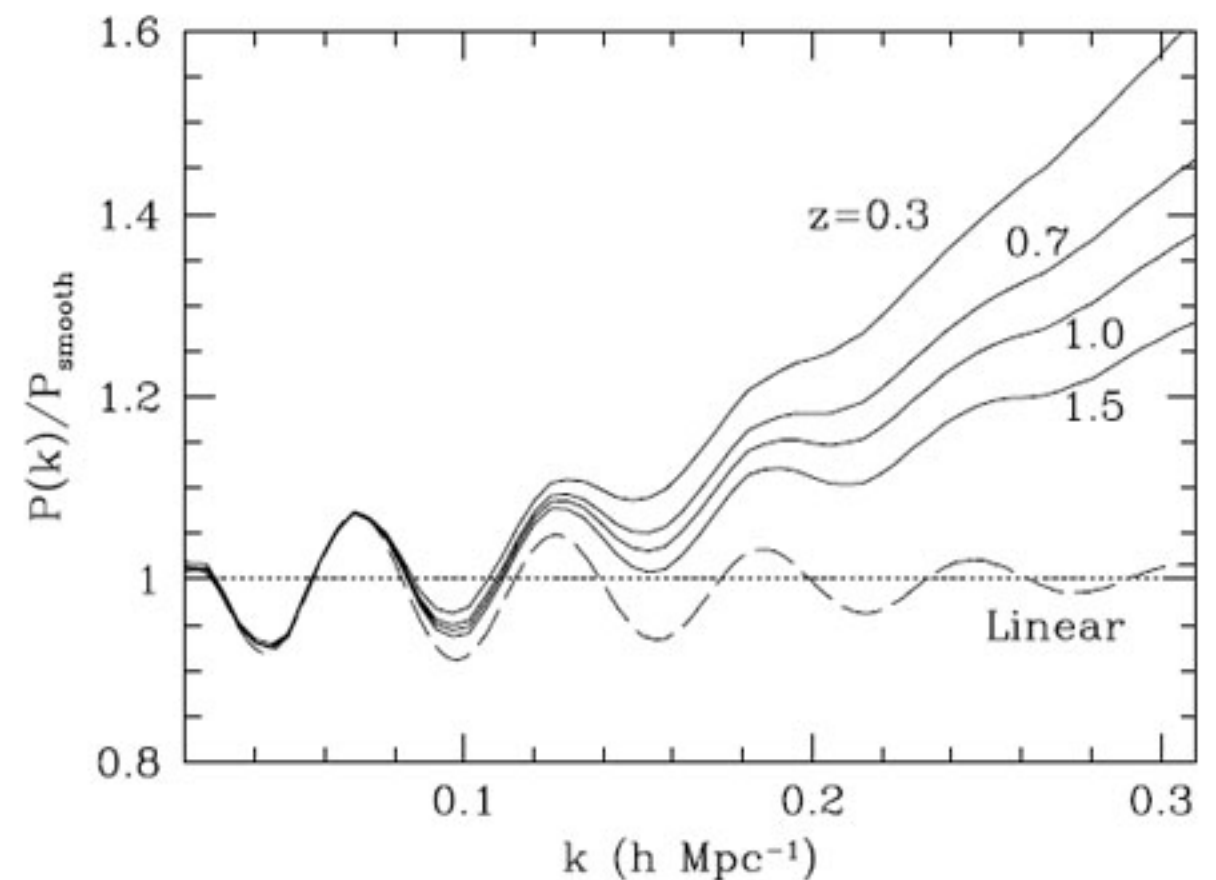


# BAO IMPRINT ON LSS

Correlation function  $\xi(r)$ : BAO bump



Power spectrum  $P(k)$ : BAO wiggles



## ► Non-linearities:

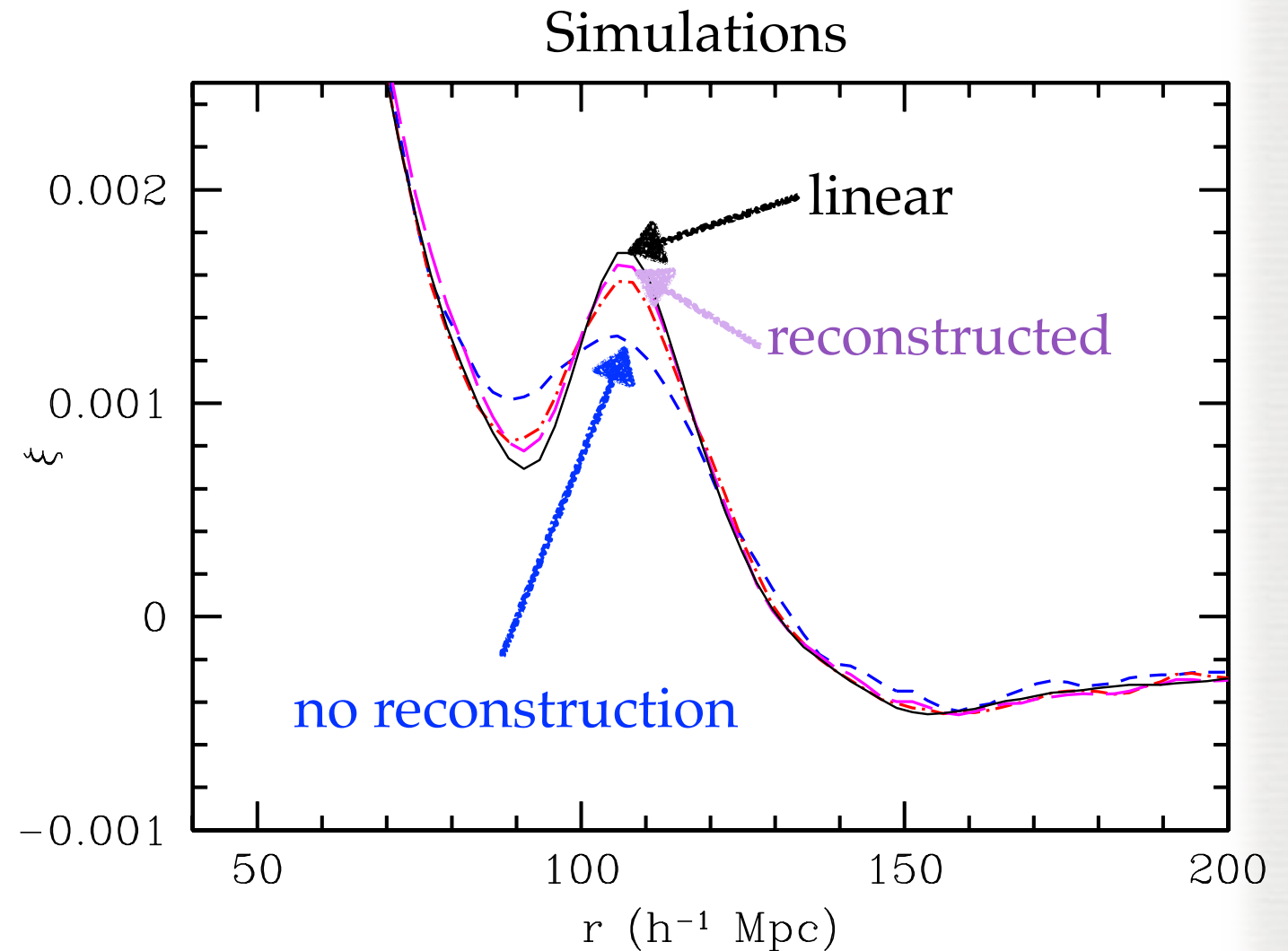
- ◆ Add small-scale power
- ◆ Smear out BAO peak, i.e. degrade BAO information
- ◆ Slightly shift BAO scale



# BAO RECONSTRUCTION

Eisenstein et al. 2006  
Padmanabhan et al. 2008

- **Goal:** Restore linear modes to increase BAO information
- **Method:** Undo large-scale flows that broaden the BAO peak:
  - ◆ Calculate large-scale displacement/velocity field with Zeldovich approximation
$$\mathbf{s}(\mathbf{k}) = -\frac{i\mathbf{k}}{k^2} W_R(k) \delta(\mathbf{k})$$
  - ◆ Displace clustered and random catalog by this
    - ➔ get 'displaced' and 'shifted' densities  $\delta_d$  and  $\delta_s$
  - ◆ Reconstructed density =  $\delta_d - \delta_s$

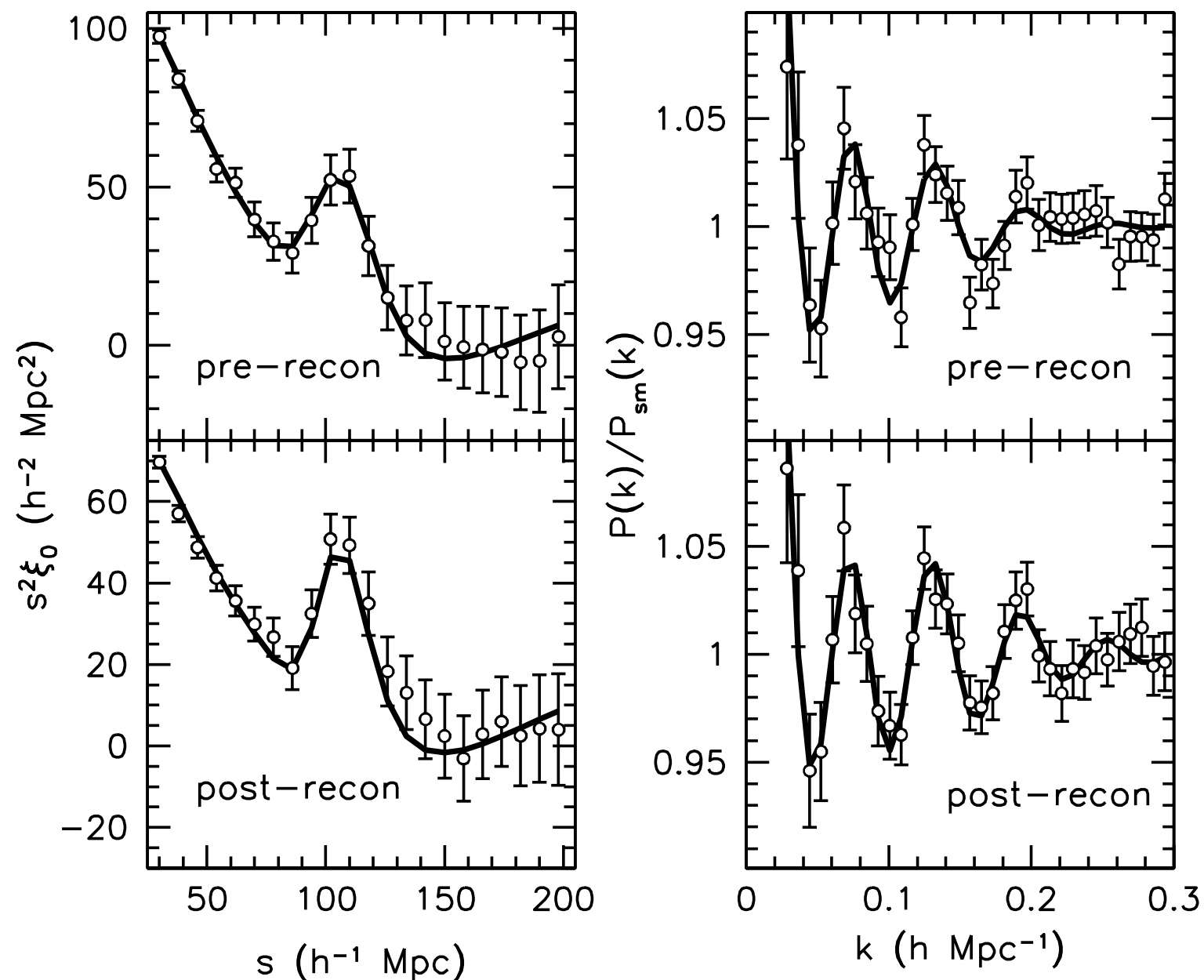


# BAO RECONSTRUCTION

Padmanabhan et al. 2012  
Anderson et al. 2013

► Works great in practice:

For BOSS DR11, BAO signal-to-noise improved by  $\sim 50\%$ ,  
achieving sub-percent BAO scale constraint



Anderson et al. 2013  
(BOSS DR11)

# NEW RECONSTRUCTION ALGORITHMS



# NEW ALGORITHMS: WHY?

- ▶ Motivations to dig deeper & explore new reconstruction algorithms:
  - ◆ Where does the new BAO information come from?
  - ◆ Can we derive reconstruction algorithm(s) better?
  - ◆ Can we do better in terms of BAO information?
  - ◆ Can we reduce intermixing of model and data when reconstructing?  
(e.g. standard reconstruction makes assumptions on  $f$ , galaxy bias, gravity when transforming data)
  
- ▶ Tried to address some of these points in recent paper (1508.06972)

# NEW ALGORITHMS: CATEGORIES

► Useful to consider two categories of reconstruction algorithms:

## Eulerian reconstructions

- \* Never displace any objects
- \* Work only with Eulerian density
- \* E.g.  $\delta_{\text{rec}} = \delta - \delta^2$

# NEW ALGORITHMS: CATEGORIES

► Useful to consider two categories of reconstruction algorithms:

## Eulerian reconstructions

- \* Never displace any objects
- \* Work only with Eulerian density
- \* E.g.  $\delta_{\text{rec}} = \delta - \delta^2$

## Lagrangian reconstructions

- \* Displace objects at some stage of the algorithm
- \* E.g. standard algorithm (Eisenstein et al. 2006)



# NEW EULERIAN ALGORITHM I

MS et al. 1508.06972

## ► Eulerian growth-shift (EGS) reconstruction

- ◆ Go back in time

$$\delta_{\text{rec}}(\mathbf{x}) = \delta(\mathbf{x}, \eta - \Delta\eta) \approx \delta(\mathbf{x}, \eta) - \Delta\eta \partial_{\eta} \delta(\mathbf{x}, \eta)$$

# NEW EULERIAN ALGORITHM I

MS et al. 1508.06972

## ► Eulerian growth-shift (EGS) reconstruction

- ◆ Go back in time

$$\delta_{\text{rec}}(\mathbf{x}) = \delta(\mathbf{x}, \eta - \Delta\eta) \approx \delta(\mathbf{x}, \eta) - \Delta\eta \partial_{\eta} \delta(\mathbf{x}, \eta)$$

- ◆ Get density time derivative nonperturbatively from nonlinear continuity equation

$$\partial_{\eta} \delta + \nabla \cdot [(1 + \delta) \mathbf{v}] = 0$$

$$\Rightarrow \partial_{\eta} \delta = -\nabla \cdot \mathbf{v} - \mathbf{v} \cdot \nabla \delta - \delta \nabla \cdot \mathbf{v}$$

# NEW EULERIAN ALGORITHM I

MS et al. 1508.06972

## ► Eulerian growth-shift (EGS) reconstruction

- ◆ Go back in time

$$\delta_{\text{rec}}(\mathbf{x}) = \delta(\mathbf{x}, \eta - \Delta\eta) \approx \delta(\mathbf{x}, \eta) - \Delta\eta \partial_{\eta} \delta(\mathbf{x}, \eta)$$

- ◆ Get density time derivative nonperturbatively from nonlinear continuity equation

$$\partial_{\eta} \delta + \nabla \cdot [(1 + \delta)\mathbf{v}] = 0$$

$$\Rightarrow \partial_{\eta} \delta = -\nabla \cdot \mathbf{v} - \mathbf{v} \cdot \nabla \delta - \delta \nabla \cdot \mathbf{v}$$

- ◆ Approximate velocity in terms of smoothed density  $\delta_R$  (using linear relation)

$$\mathbf{v}(\mathbf{k}) \approx -\mathbf{s}(\mathbf{k}) \equiv \frac{i\mathbf{k}}{k^2} \delta_R(\mathbf{k}) \quad \Rightarrow \quad \nabla \cdot \mathbf{v} = \delta_R$$

$$\Rightarrow \delta_{\text{EGS}}^{\text{rec}}(\mathbf{x}) = \delta(\mathbf{x}) - \underbrace{\mathbf{s}(\mathbf{x}) \cdot \nabla \delta(\mathbf{x})}_{\text{shift}} - \underbrace{\delta(\mathbf{x}) \delta_R(\mathbf{x})}_{\text{growth}}$$

- Not reverting linear time evolution
- Not displacing any objects, i.e. Eulerian
- Nonperturbative in  $\delta$ , linear in velocity



# NEW EULERIAN ALGORITHM I

MS et al. 1508.06972

## ► Eulerian growth-shift (EGS) reconstruction

### ◆ Reconstructed power spectrum:

$$\delta_{\text{EGS}}^{\text{rec}} = \delta - \delta^2 - \mathbf{s} \cdot \nabla \delta$$

$$\Rightarrow \langle \delta_{\text{EGS}}^{\text{rec}} | \delta_{\text{EGS}}^{\text{rec}} \rangle = \langle \delta | \delta \rangle \quad \text{2-point}$$

$$- 2 \langle \delta^2 | \delta \rangle - 2 \langle \mathbf{s} \cdot \nabla \delta | \delta \rangle \quad \text{3-point}$$

$$+ \langle \delta^2 | \delta^2 \rangle + \langle \mathbf{s} \cdot \nabla \delta | \mathbf{s} \cdot \nabla \delta \rangle + 2 \langle \delta^2 | \mathbf{s} \cdot \nabla \delta \rangle \quad \text{4-point}$$

- ➔ Automatically combines 2-, 3- and 4-point of the unreconstructed density
- ➔ Explicitly see how reconstruction exploits 3- and 4-point BAO information
- ➔ Cross-spectra are the same as in part I of the talk, i.e. nearly-optimal
- ➔ Get similar combinations for all our other Eulerian reconstructions

# NEW EULERIAN ALGORITHM II

MS et al. 1508.06972

## ► Eulerian F2 (EF2) reconstruction

- ◆ Second-order density

$$\delta^{(2)}(\mathbf{x}) = \underbrace{\frac{17}{21}\delta_0^2(\mathbf{x})}_{\text{growth}} - \underbrace{\Psi_0(\mathbf{x}) \cdot \nabla \delta_0(\mathbf{x})}_{\text{shift}} + \underbrace{\frac{4}{21}K_0^2(\mathbf{x})}_{\text{tidal}}$$

- ◆ Remove this from the full density

$$\delta_{\text{EF2}}^{\text{rec}}(\mathbf{x}) \equiv \delta(\mathbf{x}) - \underbrace{\frac{17}{21}\delta_R(\mathbf{x})\delta(\mathbf{x})}_{\text{growth}} - \underbrace{\mathbf{s}(\mathbf{x}) \cdot \nabla \delta(\mathbf{x})}_{\text{shift}} - \underbrace{\frac{4}{21}K_R^2(\mathbf{x})}_{\text{tidal}}$$

- ◆ More formal derivation using Newton-Raphson iteration:

Find linear density compatible with a given observed nonlinear density, i.e. solve

$$f[\delta_0] \equiv \delta_0 + F_2[\delta_0] - \delta_{\text{obs}} = 0 \quad \text{for } \delta_0$$

# NEW LAGRANGIAN ALGORITHMS

MS et al. 1508.06972

## ► Lagrangian Random-random (LRR) reconstruction

- ◆ 2LPT theory for **clustered** and **random** catalogs displaced by negative or positive Zeldovich displacement:  $\delta_d[\mathbf{s}]$ ,  $\delta_d[-\mathbf{s}]$ ,  $\delta_s[\mathbf{s}]$ ,  $\delta_s[-\mathbf{s}]$
- ◆ Only 2 of 6 possible combinations suppress 2nd order nonlinearities:

- \* Lagrangian growth-shift (LGS) reconstruction (= standard algorithm)

$$\delta_{\text{LGS}}^{\text{rec}} = \delta_d[\mathbf{s}] - \delta_s[\mathbf{s}]$$

- \* Lagrangian random-random (LRR) reconstruction:

$$\delta_{\text{LRR}}^{\text{rec}} = \delta - \frac{1}{2} \left\{ \delta_s[\mathbf{s}] + \delta_s[-\mathbf{s}] \right\}$$



# NEW LAGRANGIAN ALGORITHMS

MS et al. 1508.06972

## ► Lagrangian F2 (LF2) reconstruction

- ◆ Unique combination of LRR and standard LGS algorithms reverses full second-order density (up to smoothing)

$$\delta_{\text{LF2}}^{\text{rec}} = \frac{3}{7}\delta_{\text{LGS}}^{\text{rec}} + \frac{4}{7}\delta_{\text{LRR}}^{\text{rec}}$$

# OVERVIEW

MS et al. 1508.06972

► All reconstruction algorithms

## Eulerian

## Lagrangian

*Growth-Shift*

$$\delta_{\text{EGS}}^{\text{rec}}(\mathbf{x}) = \delta(\mathbf{x}) - \delta_R(\mathbf{x})\delta(\mathbf{x}) - \mathbf{s}(\mathbf{x}) \cdot \nabla \delta(\mathbf{x})$$

$$\delta_{\text{LGS}}^{\text{rec}} = \delta_d[\mathbf{s}] - \delta_s[\mathbf{s}]$$

*Full F2*

$$\delta_{\text{EF2}}^{\text{rec}}(\mathbf{x}) = \delta(\mathbf{x}) - \frac{17}{21}\delta_R(\mathbf{x})\delta(\mathbf{x}) - \mathbf{s}(\mathbf{x})\nabla\delta(\mathbf{x}) - \frac{4}{21}K_R^2(\mathbf{x})$$

$$\delta_{\text{LF2}}^{\text{rec}} = \frac{3}{7}\delta_{\text{LGS}}^{\text{rec}} + \frac{4}{7}\delta_{\text{LRR}}^{\text{rec}}$$

*Random-Random*

$$\delta_{\text{ERR}}^{\text{rec}} = \delta(\mathbf{x}) - \frac{2}{3}\delta_R^2(\mathbf{x}) - \mathbf{s}(\mathbf{x}) \cdot \nabla \delta_R(\mathbf{x}) - \frac{1}{3}K_{RR}^2(\mathbf{x})$$

$$\delta_{\text{LRR}}^{\text{rec}} = \delta - \frac{1}{2} \{ \delta_s[\mathbf{s}] + \delta_s[-\mathbf{s}] \}$$

Equivalent in 2LPT\*

\* If displaced clustered catalogs are modelled such that displacement field is evaluated at Eulerian, not Lagrangian position, i.e.  $\mathbf{s}[\mathbf{x}]$  instead of  $\mathbf{s}[\mathbf{q}]$ .

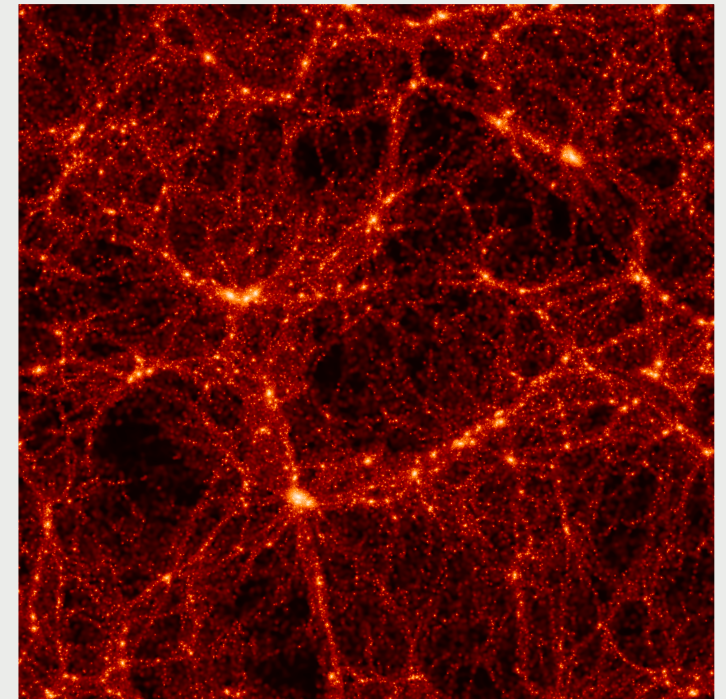
# SIMULATIONS



# SIMULATIONS

## ► FastPM code by Yu Feng

- ◆ Particle-mesh code, time-stepping linear in scale factor  $a$ , parallel COLA
- ◆ Ran wiggle and nowiggle simulations with same initial phases
- ◆  $2048^3$  DM particles,  $L=1380\text{Mpc}/h$ , 80 timesteps, 3 realizations, take 1% subsample at  $z=0.55$ ; use  $R=15\text{Mpc}/h$  smoothing



## ► RunPB simulations by Martin White

- ◆ Full TreePM (more accurate and expensive)
- ◆ Only wiggle simulations



# OVERVIEW

MS et al. 1508.06972

► All reconstruction algorithms

## Eulerian

## Lagrangian

*Growth-Shift*

$$\delta_{\text{EGS}}^{\text{rec}}(\mathbf{x}) = \delta(\mathbf{x}) - \delta_R(\mathbf{x})\delta(\mathbf{x}) - \mathbf{s}(\mathbf{x}) \cdot \nabla \delta(\mathbf{x})$$

$$\delta_{\text{LGS}}^{\text{rec}} = \delta_d[\mathbf{s}] - \delta_s[\mathbf{s}]$$

*Full F2*

$$\delta_{\text{EF2}}^{\text{rec}}(\mathbf{x}) = \delta(\mathbf{x}) - \frac{17}{21}\delta_R(\mathbf{x})\delta(\mathbf{x}) - \mathbf{s}(\mathbf{x})\nabla\delta(\mathbf{x}) - \frac{4}{21}K_R^2(\mathbf{x})$$

$$\delta_{\text{LF2}}^{\text{rec}} = \frac{3}{7}\delta_{\text{LGS}}^{\text{rec}} + \frac{4}{7}\delta_{\text{LRR}}^{\text{rec}}$$

*Random-Random*

$$\delta_{\text{ERR}}^{\text{rec}} = \delta(\mathbf{x}) - \frac{2}{3}\delta_R^2(\mathbf{x}) - \mathbf{s}(\mathbf{x}) \cdot \nabla \delta_R(\mathbf{x}) - \frac{1}{3}K_{RR}^2(\mathbf{x})$$

$$\delta_{\text{LRR}}^{\text{rec}} = \delta - \frac{1}{2} \{ \delta_s[\mathbf{s}] + \delta_s[-\mathbf{s}] \}$$

Equivalent in 2LPT\*

\* If displaced clustered catalogs are modelled such that displacement field is evaluated at Eulerian, not Lagrangian position, i.e.  $\mathbf{s}[\mathbf{x}]$  instead of  $\mathbf{s}[\mathbf{q}]$ .

# OVERVIEW

MS et al. 1508.06972

► All reconstruction algorithms

## Eulerian

## Lagrangian

*Growth-Shift*

$$\delta_{\text{EGS}}^{\text{rec}}(\mathbf{x}) = \delta(\mathbf{x}) - \delta_R(\mathbf{x})\delta(\mathbf{x}) - \mathbf{s}(\mathbf{x}) \cdot \nabla \delta(\mathbf{x})$$

$$\delta_{\text{LGS}}^{\text{rec}} = \delta_d[\mathbf{s}] - \delta_s[\mathbf{s}]$$

*Full F2*

$$\delta_{\text{EF2}}^{\text{rec}}(\mathbf{x}) = \delta(\mathbf{x}) - \frac{17}{21}\delta_R(\mathbf{x})\delta(\mathbf{x}) - \mathbf{s}(\mathbf{x})\nabla\delta(\mathbf{x}) - \frac{4}{21}K_R^2(\mathbf{x})$$

$$\delta_{\text{LF2}}^{\text{rec}} = \frac{3}{7}\delta_{\text{LGS}}^{\text{rec}} + \frac{4}{7}\delta_{\text{LRR}}^{\text{rec}}$$

*Random-Random*

$$\delta_{\text{ERR}}^{\text{rec}} = \delta(\mathbf{x}) - \frac{2}{3}\delta_R^2(\mathbf{x}) - \mathbf{s}(\mathbf{x}) \cdot \nabla \delta_R(\mathbf{x}) - \frac{1}{3}K_{RR}^2(\mathbf{x})$$

$$\delta_{\text{LRR}}^{\text{rec}} = \delta - \frac{1}{2} \{ \delta_s[\mathbf{s}] + \delta_s[-\mathbf{s}] \}$$

Equivalent in 2LPT\*

\* If displaced clustered catalogs are modelled such that displacement field is evaluated at Eulerian, not Lagrangian position, i.e.  $\mathbf{s}[\mathbf{x}]$  instead of  $\mathbf{s}[\mathbf{q}]$ .



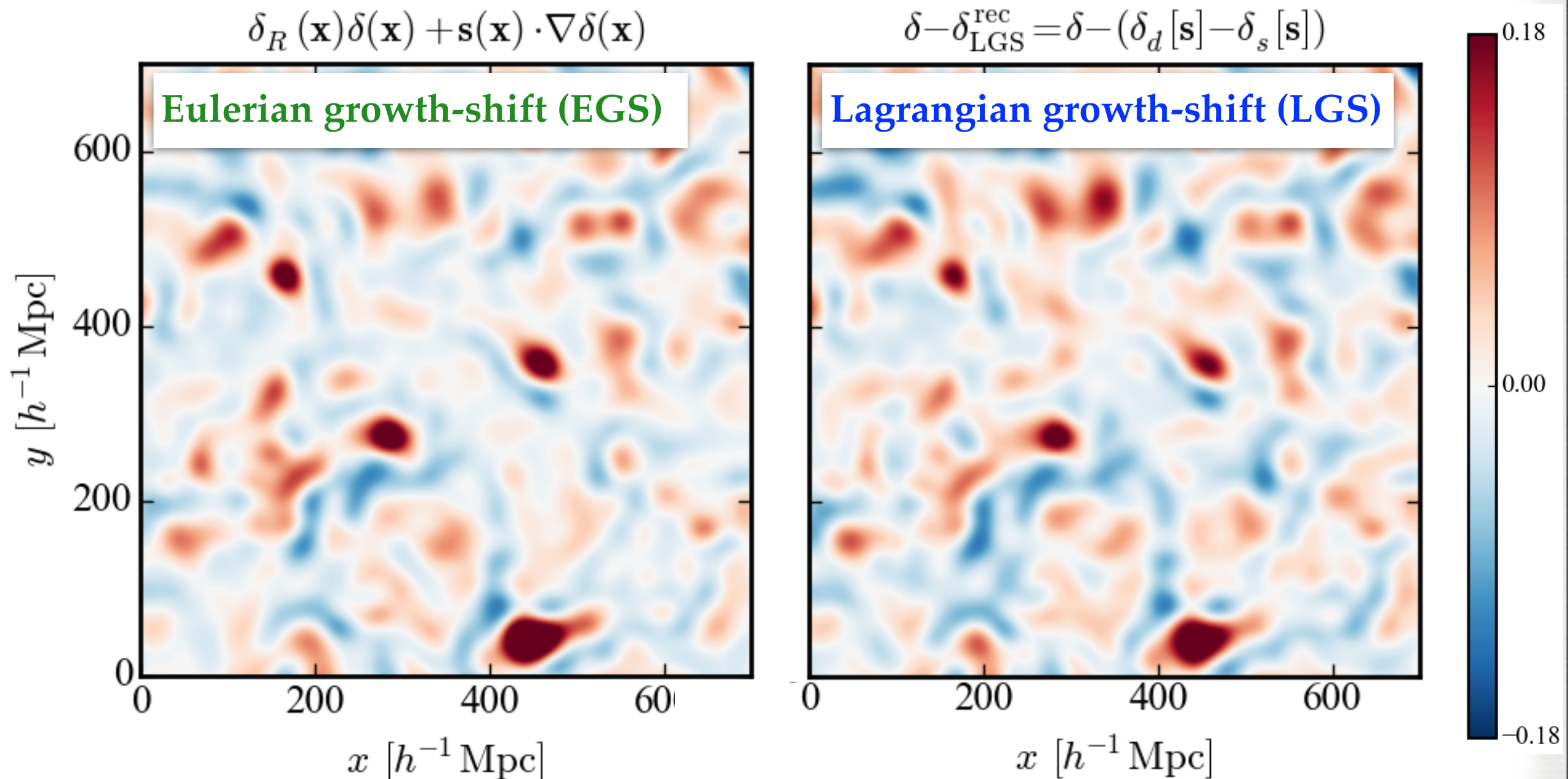
NUMERICAL RESULTS:  
GROWTH-SHIFT  
ALGORITHMS

# GROWTH-SHIFT ALGORITHMS

MS et al. 1508.06972

## ► 2D slice plots

Density change due to reconstruction,  $\delta - \delta_{\text{rec}}$

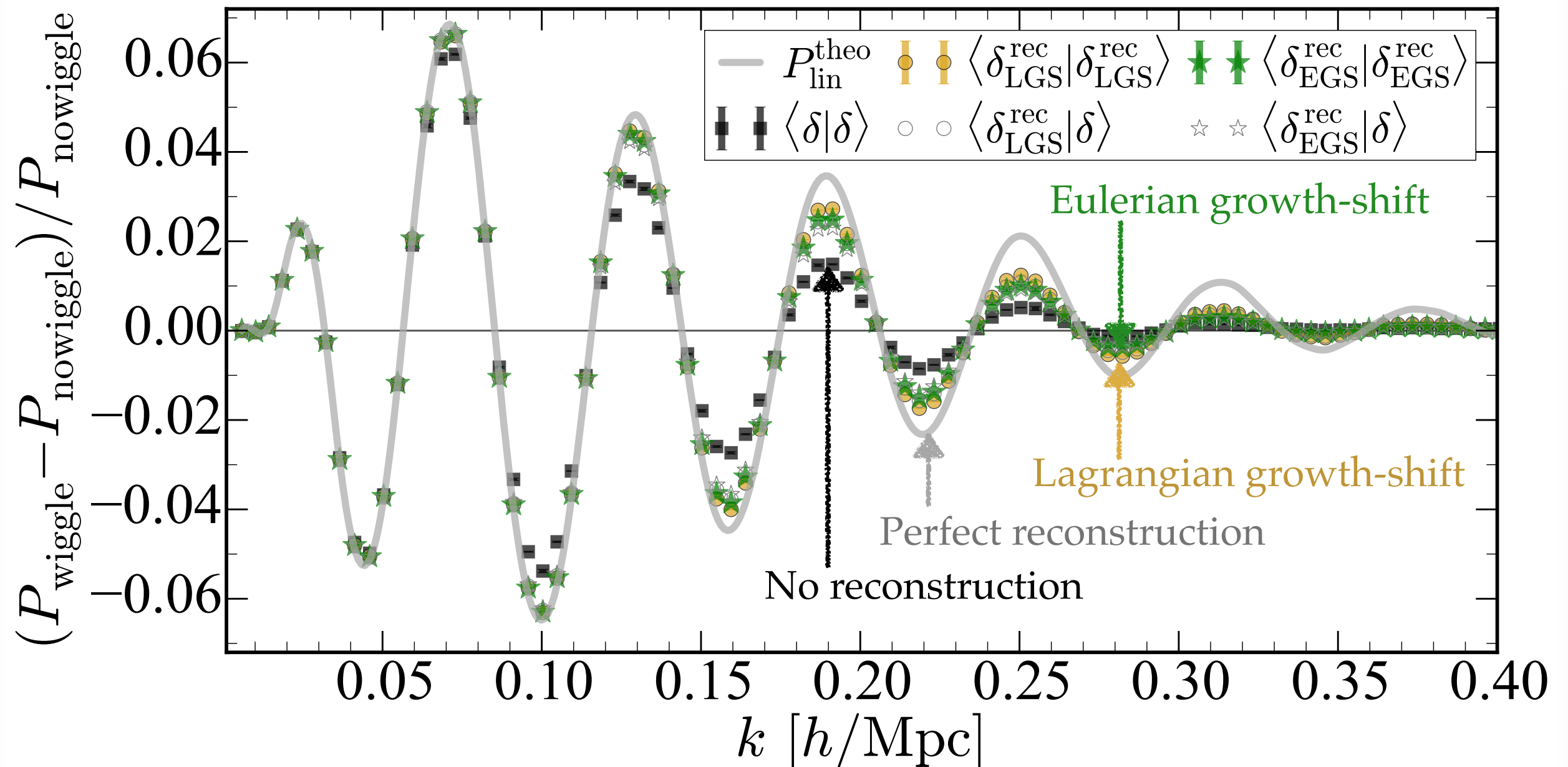




# GROWTH-SHIFT ALGORITHMS

MS et al. 1508.06972

- **BAO signal:** Fractional difference of power spectra between wiggle and nowiggle simulations, for **Lagrangian** and **Eulerian** growth-shift algorithms



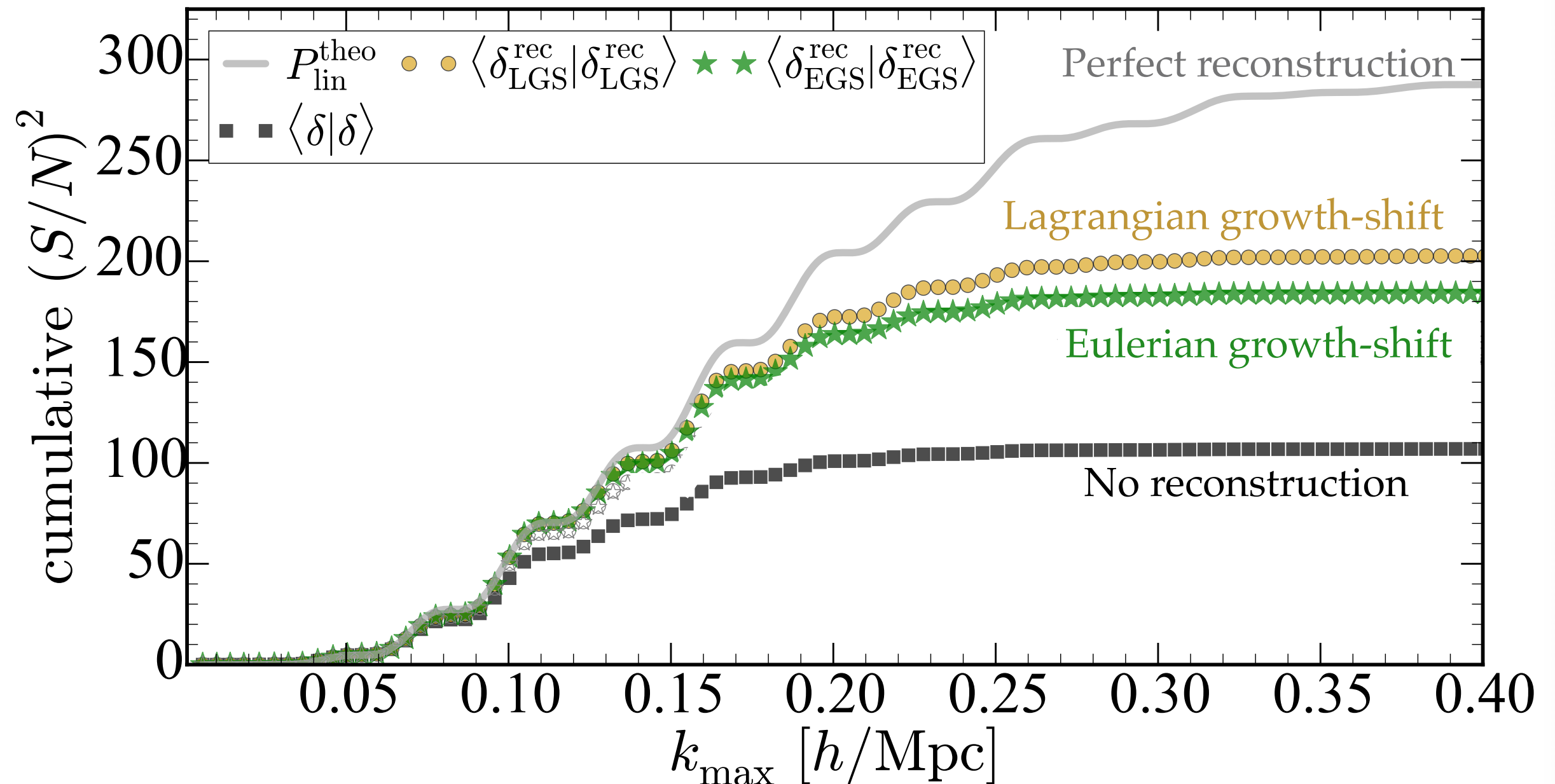


# GROWTH-SHIFT ALGORITHMS

MS et al. 1508.06972

## ► Cumulative BAO signal-to-noise-squared:

Eulerian algorithm yields 95% of BAO  $S/N$  of standard Lagrangian algorithm



WHERE DOES  
NEW BAO INFO  
COME FROM?

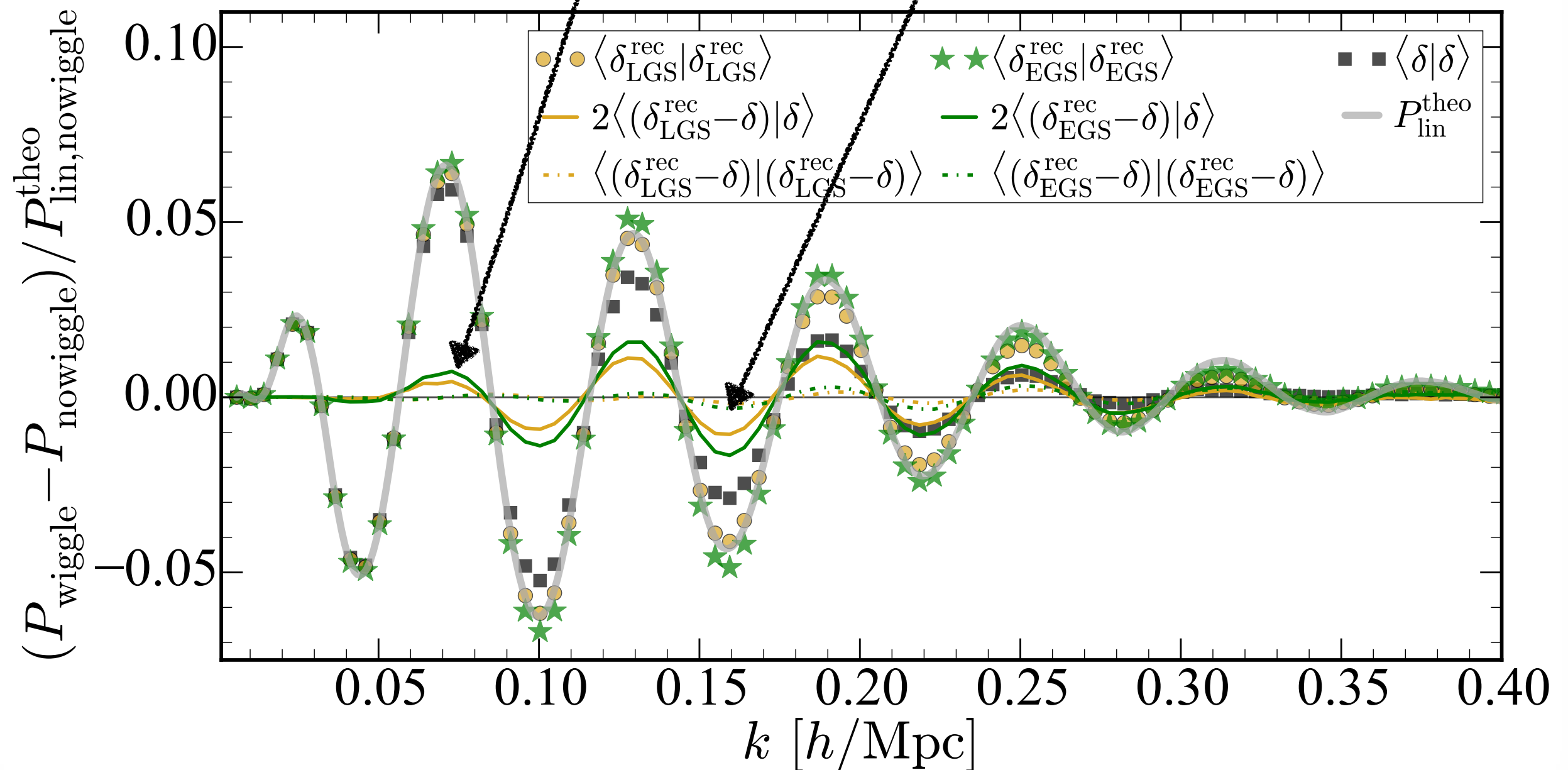


# GROWTH-SHIFT ALGORITHMS

MS et al. 1508.06972

► **3-point vs 4-point:** Split  $\delta_{\text{rec}} = \delta + (\delta_{\text{rec}} - \delta)$  in simulations

$$\Rightarrow \langle \delta^{\text{rec}} | \delta^{\text{rec}} \rangle = \underbrace{\langle \delta | \delta \rangle}_{2\text{pt}} + \underbrace{2 \langle (\delta^{\text{rec}} - \delta) | \delta \rangle}_{3\text{pt}} + \underbrace{\langle (\delta^{\text{rec}} - \delta) | (\delta^{\text{rec}} - \delta) \rangle}_{4\text{pt}}.$$



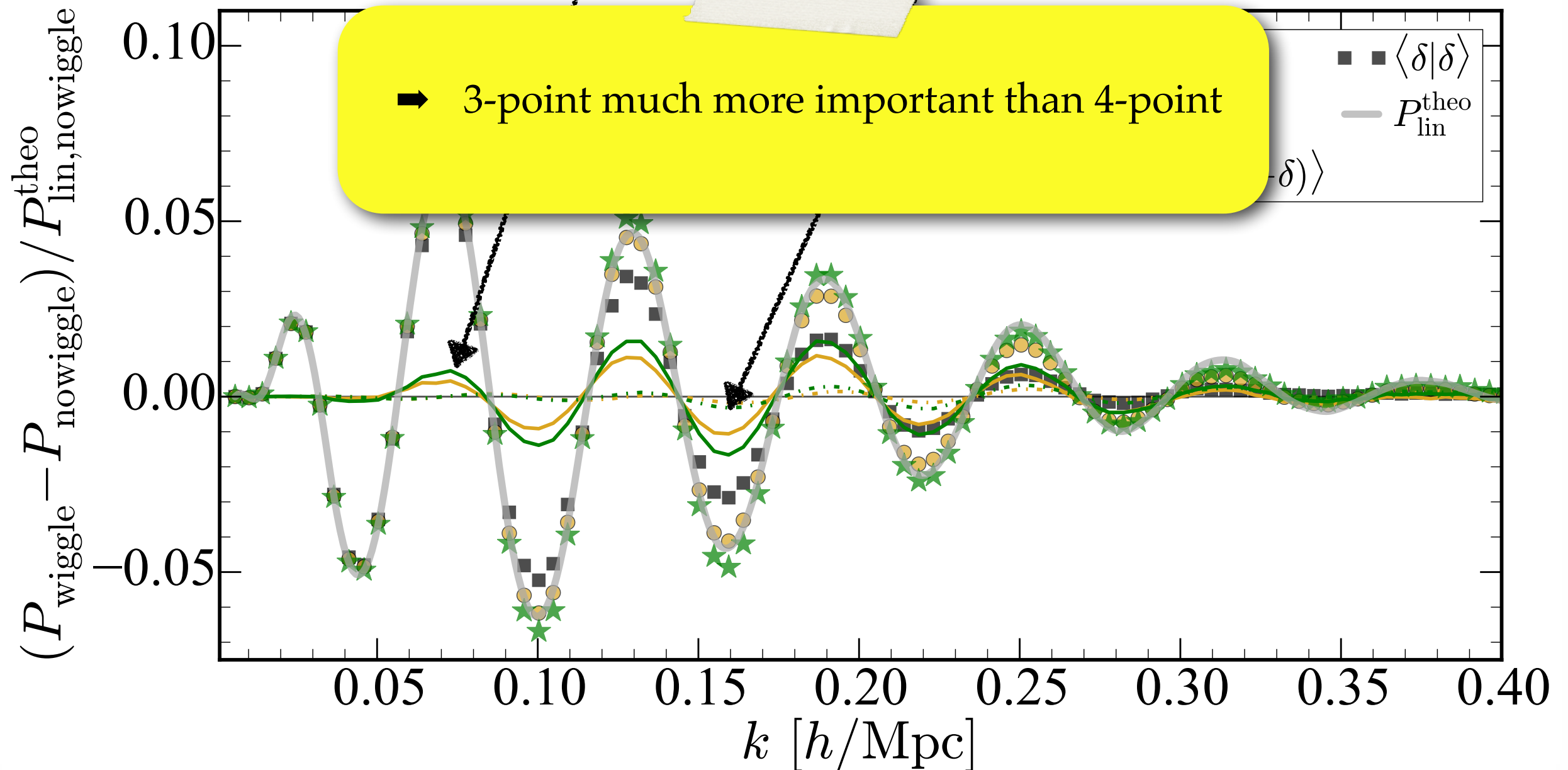


# GROWTH-SHIFT ALGORITHMS

MS et al. 1508.06972

► **3-point vs 4-point:** Split  $\delta_{\text{rec}} = \delta + (\delta_{\text{rec}} - \delta)$  in simulations

$$\Rightarrow \langle \delta^{\text{rec}} | \delta^{\text{rec}} \rangle = \underbrace{\langle \delta | \delta \rangle}_{2\text{pt}} + \underbrace{2 \langle (\delta^{\text{rec}} - \delta) | \delta \rangle}_{3\text{pt}} + \underbrace{\langle (\delta^{\text{rec}} - \delta) | (\delta^{\text{rec}} - \delta) \rangle}_{4\text{pt}}.$$

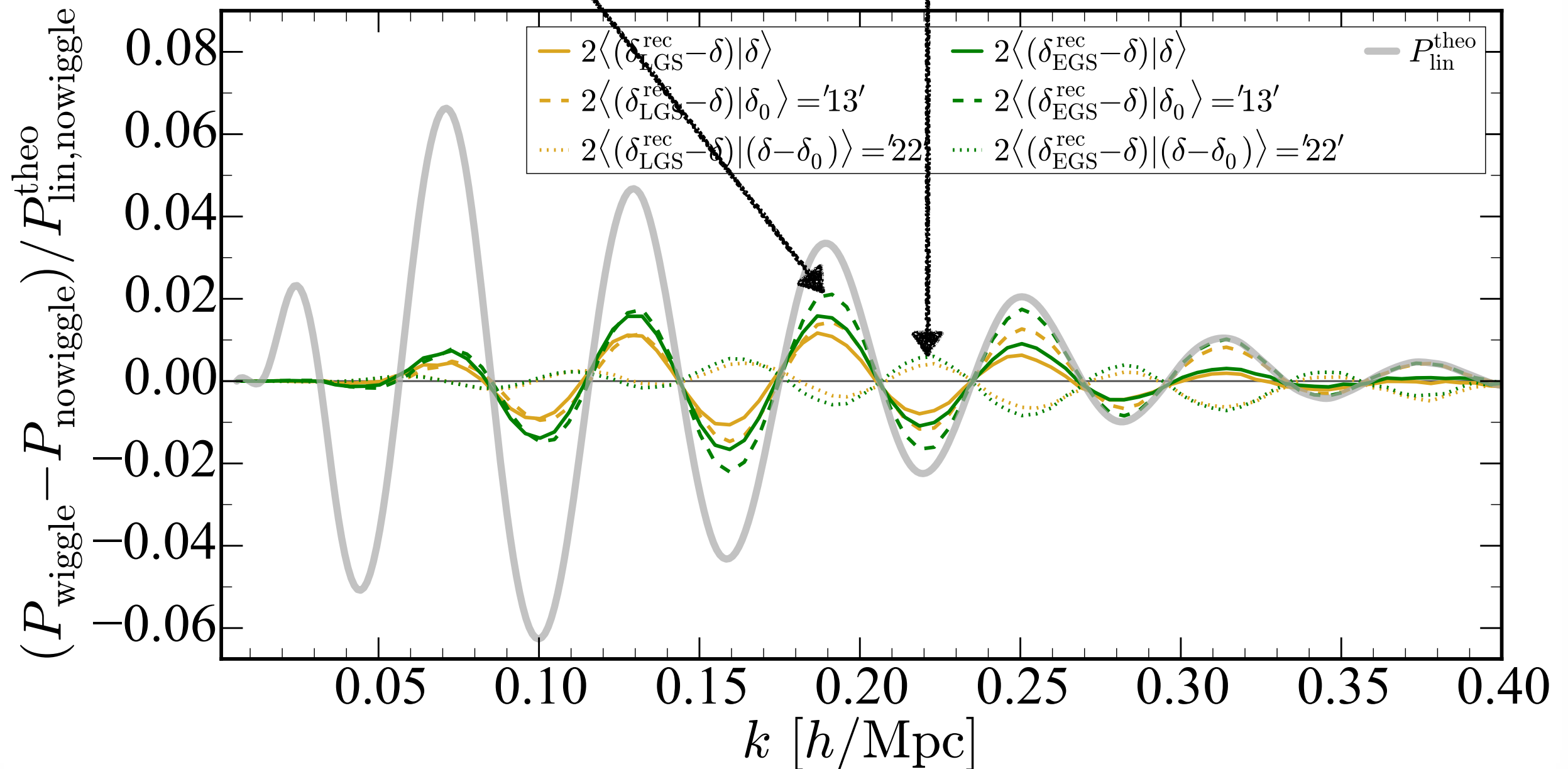


# GROWTH-SHIFT ALGORITHMS

MS et al. 1508.06972

► **13 vs 22 part (of 3-point):** Split  $\delta = \delta_0 + (\delta - \delta_0)$  in simulations, where  $\delta_0 =$  linear density

$$\Rightarrow \langle (\delta^{\text{rec}} - \delta) | \delta \rangle = \underbrace{\langle (\delta^{\text{rec}} - \delta) | \delta_0 \rangle}_{\sim \langle \Delta^{(3)} \delta_0 \rangle} + \underbrace{\langle (\delta^{\text{rec}} - \delta) | (\delta - \delta_0) \rangle}_{\sim \langle \Delta^{(2)} \delta^{(2)} \rangle}$$

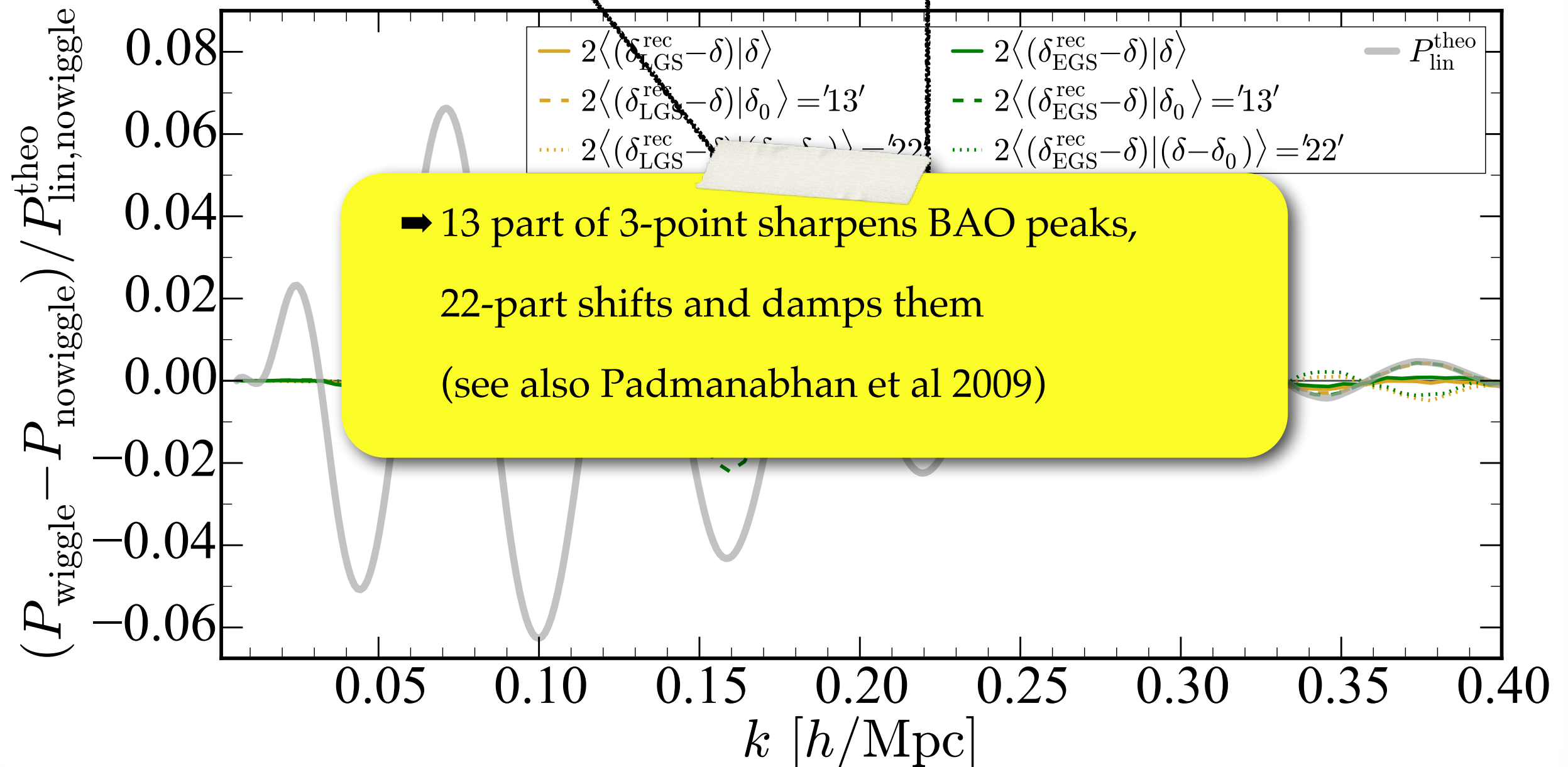


# GROWTH-SHIFT ALGORITHMS

MS et al. 1508.06972

► **13 vs 22 part (of 3-point):** Split  $\delta = \delta_0 + (\delta - \delta_0)$  in simulations, where  $\delta_0 =$  linear density

$$\Rightarrow \langle (\delta^{\text{rec}} - \delta) | \delta \rangle = \underbrace{\langle (\delta^{\text{rec}} - \delta) | \delta_0 \rangle}_{\sim \langle \Delta^{(3)} \delta_0 \rangle} + \underbrace{\langle (\delta^{\text{rec}} - \delta) | (\delta - \delta_0) \rangle}_{\sim \langle \Delta^{(2)} \delta^{(2)} \rangle}$$

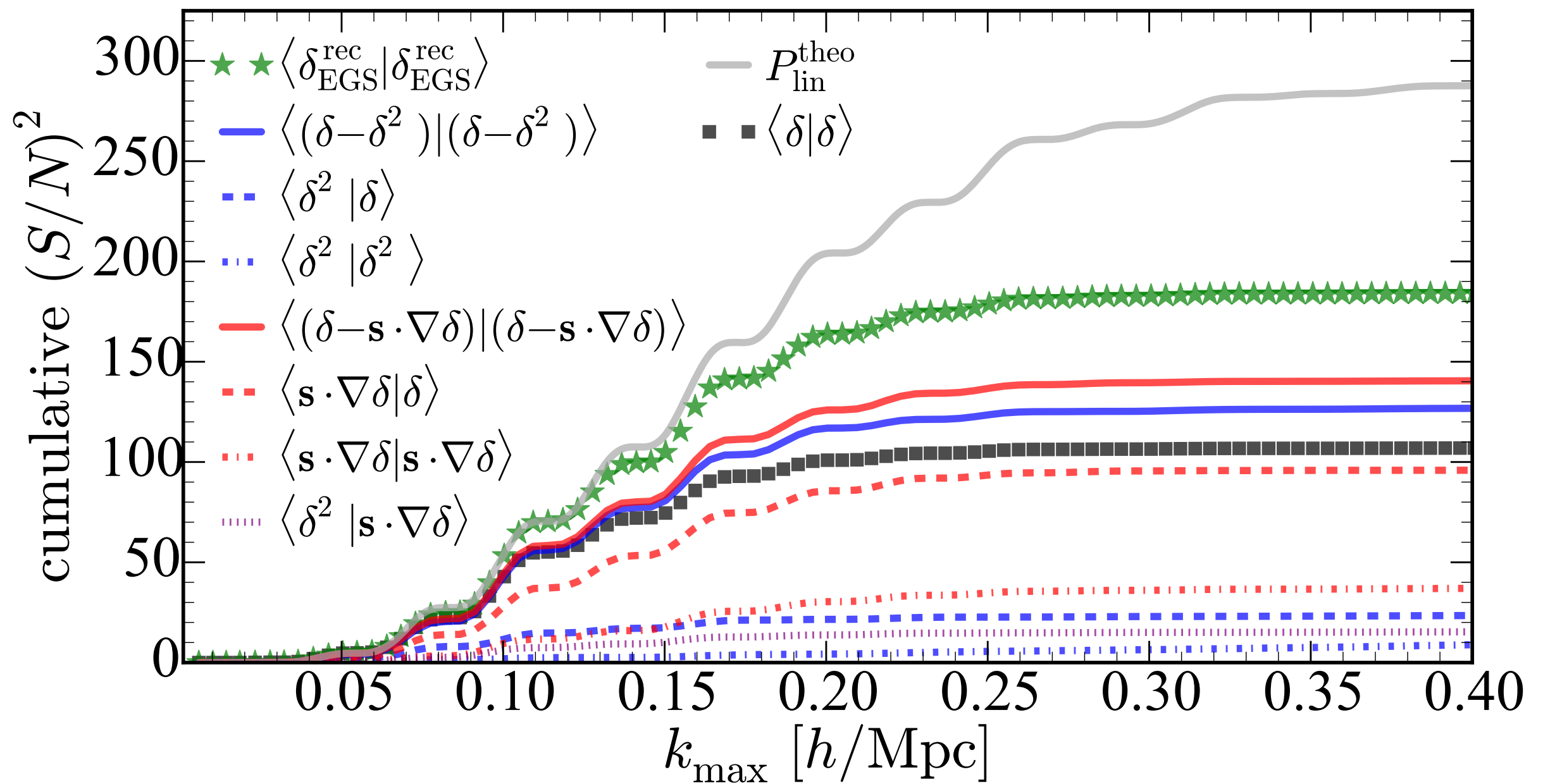




# GROWTH-SHIFT ALGORITHMS

MS et al. 1508.06972

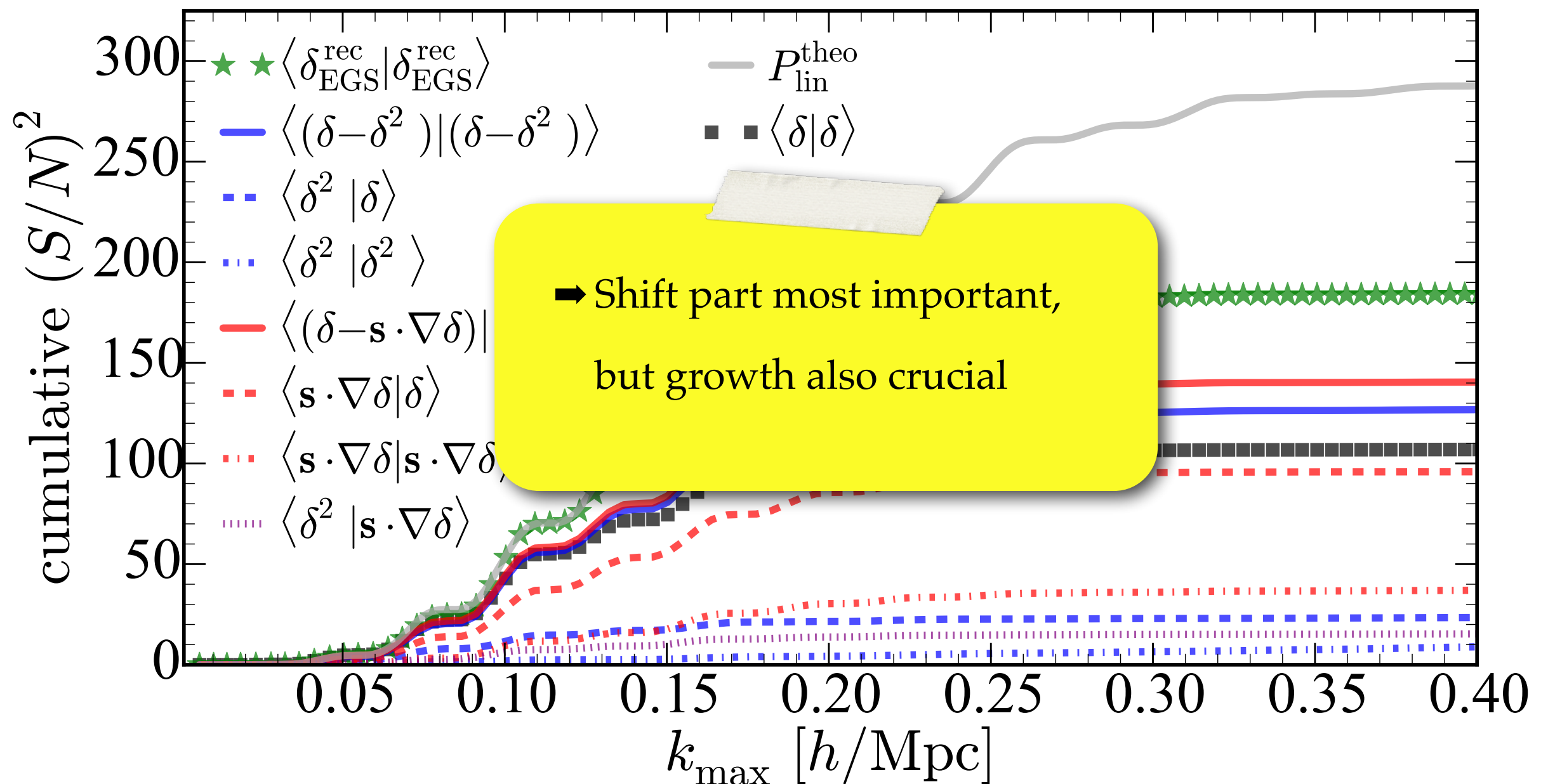
## ► Growth vs shift part



# GROWTH-SHIFT ALGORITHMS

MS et al. 1508.06972

## ► Growth vs shift part





NUMERICAL RESULTS:

ALL

ALGORITHMS

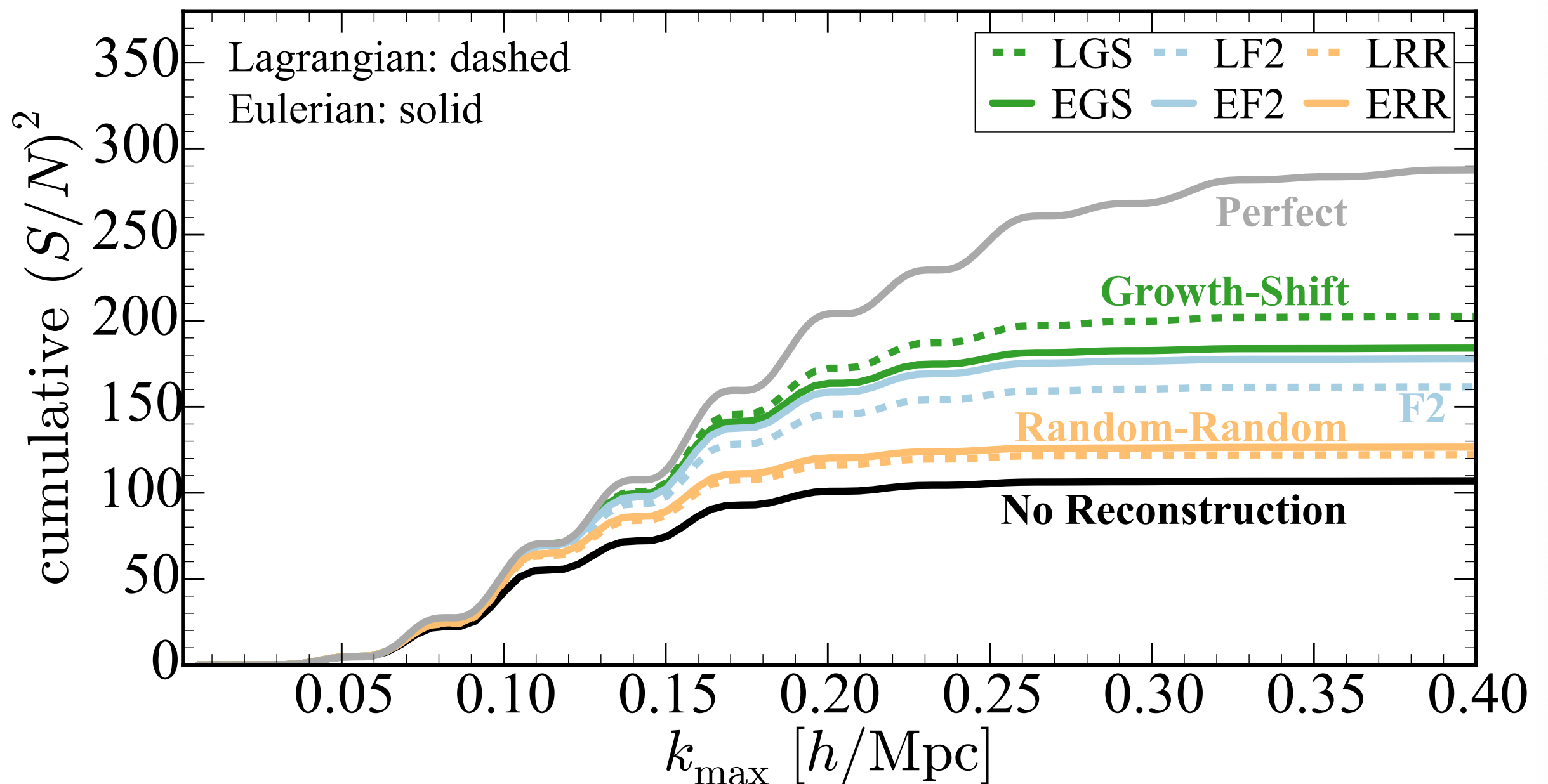


# ALL ALGORITHMS

MS et al. 1508.06972

## ► Performance comparison

- ◆ EGS algorithm yields 95% of BAO  $S/N$  of standard Lagrangian LGS algorithm
- ◆ EF2 algorithm similar, other algorithms significantly worse



# DISCUSSION

MS et al. 1508.06972

## ► Pros & Cons

### Eulerian reconstructions

- + BAO info comes from specific 3- & 4-point
- + Data transformations less dependent on fiducial model
- + Derived from nonperturbative continuity equation (EGS) or Newton-Raphson (EF2)
- Slightly worse performance
- Not worked out in redshift space

### Lagrangian reconstructions

- Less transparent where BAO info comes from
- Data transformation very dependent on fiducial model
- Justification of algorithm mostly a posteriori
- + Slightly better performance
- + Well established (10 yr old), applied to observations

# DISCUSSION

MS et al. 1508.06972

## ► Pros & Cons

### Euler reconstruction

- + BAO info comes from 4-point
- + Data transformation dependent on model
- + Derived from continuity equation
- Newton-Raphson (L12)
- Slightly worse performance
- Not worked out in redshift space

### Equivalent in 2LPT

- Reconstructions are connected
- New argument for success and robustness of standard reconstruction: implicitly includes 3- and 4-point
- Intuitively, expect little new BAO information in 3-point statistics, because rec. moves it into 2-point

### Angian reconstructions

- + BAO info comes from 2-point where BAO info is more prominent
- + Data transformation very simple
- + fiducial model
- + algorithm mostly a linear transform
- + Slightly better performance
- + Well established (10 yr old), applied to observations



# CONCLUSIONS

# CONCLUSIONS

## ► *Simple bispectrum estimators*

MS, Baldauf, Seljak  
1411.6595

- ◆ Three cross-spectra of quadratic fields with the density measure projection of full bispectrum on tree-level shape
- ◆ Simple, fast, nearly-optimal, simpler covariances
- ◆ Works well in simulations
- ◆ Extension to redshift space under development

## ► *Eulerian BAO reconstruction and higher N-point statistics*

MS et al. 1508.06972

- ◆ Presented 5 new BAO reconstruction algorithms
- ◆ Showed connection to 3- & 4-point of unreconstructed density
- ◆ Connected various algorithms to each other via 2LPT modelling
- ◆ Standard algorithm performs best, but two Eulerian algorithms are almost as well, achieving  $\sim 95\%$  BAO S/N of standard method

Thank you



# BISPECTRUM BONUS SLIDES

# THEORY CONTRIBUTIONS

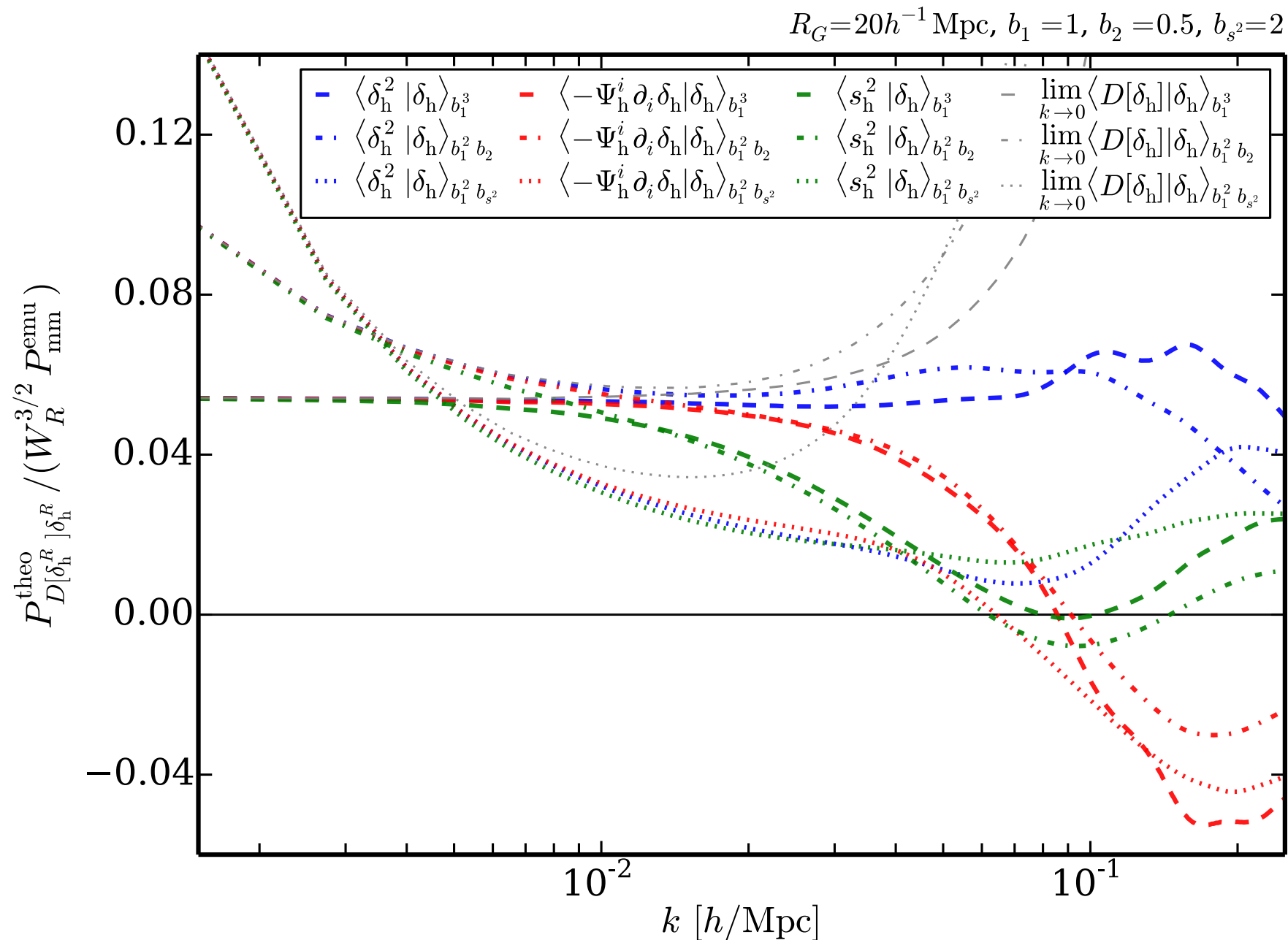


FIG. 1. Theory contributions (67) to halo-halo-halo cross-spectra scaling like  $b_1^3$  (dashed),  $b_1^2 b_2$  (dash-dotted) and  $b_1^2 b_{s^2}$  (dotted) for squared density  $\delta_h^2(\mathbf{x})$  (blue), shift term  $-\Psi_h^i(\mathbf{x}) \partial_i \delta_h(\mathbf{x})$  (red) and tidal term  $s_h^2(\mathbf{x})$  (green), evaluated for fixed bias parameters  $b_1 = 1$ ,  $b_2 = 0.5$  and  $b_{s^2} = 2$ , Gaussian smoothing with  $R_G = 20h^{-1} \text{Mpc}$ , at  $z = 0.55$ , with linear matter power spectra in integrands. Thin gray lines show the large-scale (low  $k$ ) limit given by Eq. (70). The cross-spectra are divided by the partially smoothed FrankenEmu emulator matter power spectrum  $W_R^{3/2} P_{\text{mm}}^{\text{emu}}$  [45–48] for plotting convenience.

# VERY LARGE SCALES

MS, Baldauf, Seljak, [1411.6595](#)

► Large scale limit ( $k \rightarrow 0$ ) of cross-spectrum expectation values:

$$\lim_{k \rightarrow 0} P_{D[\delta_h^R], \delta_h^R}(k) = W_R(k) \left[ b_1^3 P_{\text{mm}}^{\text{lin}}(k) \left( \frac{68}{21} \sigma_R^2 - \frac{1}{3} \sigma_{R,P'}^2 \right) + 2b_1^2 b_2 (\tau_R^4 + 2P_{\text{mm}}^{\text{lin}}(k) \sigma_R^2) + \frac{4}{3} b_1^2 b_{s^2} \tau_R^4 \right]$$

$$D \in \{P_0, -F_2^1 P_1, P_2\}$$

$$\sigma_R^2 \equiv \frac{1}{2\pi^2} \int dq q^2 W_R^2(q) P_{\text{mm}}(q)$$

$$\sigma_{R,P'}^2 \equiv \frac{1}{2\pi^2} \int dq q^2 W_R^2(q) P_{\text{mm}}(q) \frac{d \ln q^3 P_{\text{mm}}(q)}{d \ln q}$$

$$\tau_R^4 \equiv \frac{1}{2\pi^2} \int dq q^2 W_R^2(q) P_{\text{mm}}^2(q)$$

► Different from position-dependent power spectrum (Chiang *et al.* 2014):

$$\lim_{k \rightarrow 0} \int \frac{d^2 \Omega_{\hat{\mathbf{k}}}}{4\pi} B(\mathbf{k} - \mathbf{q}_1, -\mathbf{k} + \mathbf{q}_1 + \mathbf{q}_3, -\mathbf{q}_3) = \left[ \frac{68}{21} - \frac{1}{3} \frac{d \ln k^3 P(k)}{d \ln k} \right] P(k) P(q_3) + \mathcal{O} \left( \frac{q_{1,3}}{k} \right)^2$$



# RECONSTRUCTION BONUS SLIDES

# GROWTH-SHIFT ALGORITHMS

MS et al. 1508.06972

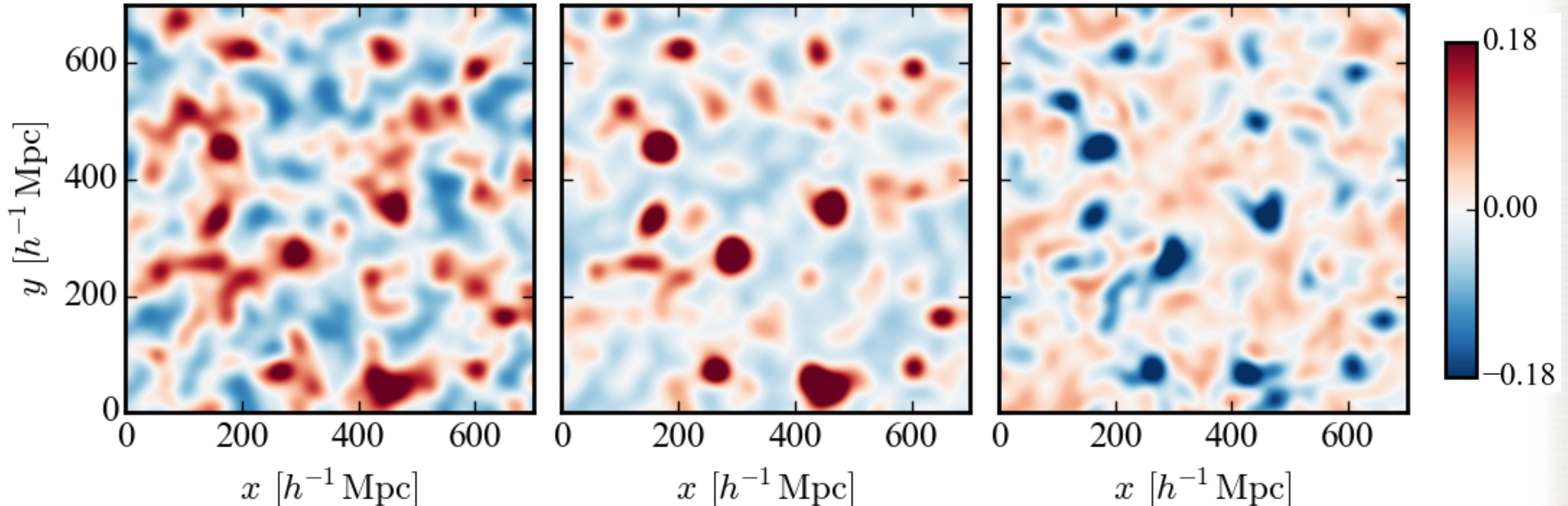
## ► 2D slice plots: Components of EGS reconstruction

$$\delta_{\text{EGS}}^{\text{rec}}(\mathbf{x}) = \delta(\mathbf{x}) - \underbrace{\delta(\mathbf{x})\delta_R(\mathbf{x})}_{\text{growth}} - \underbrace{\mathbf{s}(\mathbf{x}) \cdot \nabla \delta(\mathbf{x})}_{\text{shift}}$$

$\delta/3$

$\delta_R(\mathbf{x})\delta(\mathbf{x})$

$\mathbf{s}(\mathbf{x}) \cdot \nabla \delta(\mathbf{x})$





# ALL ALGORITHMS

MS et al. 1508.06972

## ► Performance comparison

- ◆ EGS algorithm yields 95% of BAO  $S/N$  of standard Lagrangian LGS algorithm
- ◆ EF2 algorithm similar, other algorithms significantly worse

Reconstruction method	Growth-Shift		F2 reconstruction		Random-Random		Perfect	NoRec
	LGS	EGS	LF2	EF2	LRR	ERR		
BAO signal-to-noise	14.2	13.6	12.7	13.3	11.1	11.3	17.0	10.3
Compared against LGS	$\pm 0\%$	$-4.7\%$	$-11\%$	$-6.3\%$	$-22\%$	$-21\%$	$+19\%$	$-27\%$
Compared against NoRec	$+38\%$	$+31\%$	$+23\%$	$+29\%$	$+6.9\%$	$+8.8\%$	$+64\%$	$\pm 0\%$

TABLE II. Total BAO signal-to-noise for  $k_{\max} = 0.4h/\text{Mpc}$  for various reconstruction algorithms (obtained from Fig. 9, based on simulations). ‘Perfect’ refers to the BAO signal-to-noise of the linear density and ‘NoRec’ to the BAO signal-to-noise of the measured nonlinear density without performing any reconstruction. The second-to-last row shows how much of the signal-to-noise is lost compared to performing the standard LGS reconstruction. The bottom row shows how much signal-to-noise is gained by reconstructions compared to performing no reconstruction.



# SMOOTHING SCALE

MS et al. 1508.06972

## ► Dependence on smoothing scale

